THERMAL PERFORMANCE ENHANCEMENT OF ALUMINUM CASTING PROCESSES IN FOUNDRY OPERATIONS: A CASE STUDY AT CEYLON ELECTRICITY BOARD

Pathiraja P.M.T.M.

199430X

Degree of Master of Engineering

Department of Mechanical Engineering

University of Moratuwa

Sri Lanka

January 2025

THERMAL PERFORMANCE ENHANCEMENT OF ALUMINUM CASTING PROCESSES IN FOUNDRY OPERATIONS: A CASE STUDY AT CEYLON ELECTRICITY BOARD

Pathiraja P.M.T.M.

199430X

Thesis/Dissertation submitted in partial fulfilment of the requirements for the degree Master of Engineering in Energy Technology

Department of Mechanical Engineering

University of Moratuwa
Sri Lanka

January 2025

DECLARATION

I declare that this is my own work and this thesis does not incorporate without acknowledgement any material previously submitted for a degree or diploma in any other University or institute of higher learning and to the best of my knowledge and belief it does not contain any material previously published or written by another person except where the acknowledgement is made in the text.

Also, I hereby grant to University of Moratuwa the non-exclusive right to reproduce and distribute my thesis, in whole or part in print, electronic or other medium. I retain the right to use this content in whole or part in future works (such as articles or books).

UOM Verified Signature

Signature: ..... Date: 7/20/25

Pathiraja P.M.T.M.

The above candidate has carried out research for the Masters Thesis under my supervision

UOM Verified Signature

Signature:..... Date: 7/21/25

Prof. Saliya Jayasekara

This work is lovingly dedicated to my dear wife, Manoja, and my two wonderful children, Sandamini and Sajan, whose unwavering love, support, and encouragement have been my constant source of strength and inspiration.

ABSTRACT

The Ceylon Electricity Board (CEB) foundry plays a vital role in Sri Lanka's energy sector by producing aluminum components for the national grid. However, reliance on outdated sand casting methods and inefficient oil-fired furnaces has led to low energy efficiency, high operational costs, and environmental concerns. This study addresses these challenges by designing and implementing a waste heat recovery system integrated with a welded plate heat exchanger to enhance energy efficiency and optimize foundry operations.

The research evaluated the performance of existing furnaces, revealing significantly low Specific Fuel Consumption (SFC) compared to the initial fuel consumption values , with the pit furnace operating performing at 0.681 *l/kg* and the tilting furnace operating at 0.294 *l/kg*. A welded plate heat exchanger was fabricated and integrated into the combustion system to preheat combustion air using exhaust gases. Computational Fluid Dynamics (CFD) simulations were employed to optimize the heat exchanger design and predict performance. Experimental results showed a 29.5% reduction in fuel consumption and a 32% decrease in melting time, with the heat exchanger achieving an energy recovery rate of 40%.

The findings demonstrate the feasibility of waste heat recovery in improving thermal efficiency and reducing emissions, providing a scalable solution for small and medium-scale foundries. This study recommends further modernization, including advanced monitoring systems and renewable energy integration, to enhance sustainability. By reducing reliance on imports and promoting local production, this research aligns with Sri Lanka's economic and environmental goals, offering a robust framework for energy-efficient aluminum casting practices.

ACKNOWLEDGMENT

I would like to extend my sincere gratitude and appreciation to Prof. Saliya Jayasekara, in the Department of Mechanical Engineering, University of Moratuwa, for his invaluable support and guidance throughout this research project. The contributions of Prof. Jayasekara have been paramount to the success of this research, I am deeply grateful for her assistance.

Furthermore, I would like to express my gratitude to Dr. Nissanka, Senior Lecturer and Course Coordinator of the M.Eng/PG Diploma on Energy Technology at the Department of Mechanical Engineering, University of Moratuwa, for his generous support and involvement at every stage of this research. The assistance of Dr. Nissanka has been essential to the successful completion of this study, and I am deeply grateful for his guidance.

The research was conducted under the supervision of Prof. Saliya Jayasekara, and I acknowledge my indebtedness to him for his invaluable guidance, kind-hearted cooperation, and encouragement throughout the project. My gratitude extends to my colleagues in the post-graduate programme, who provided unwavering support and assistance, allowing for the successful completion of this research.

Finally, I would like to express my appreciation to all those who contributed to the success of this study in various ways, as their support was of utmost importance in bringing this effort to fruition.

TABLE OF CONTENTS

DECLARATION ..... **i**

ABSTRACT ..... **iii**

ACKNOWLEDGEMENT ..... **iv**

TABLE OF CONTENTS ..... **v**

LIST OF FIGURES ..... **ix**

LIST OF TABLES ..... **xi**

LIST OF APPENDICESS ..... **xi**

LIST OF NOMENCLATURE ..... **xii**

LIST OF ABBREVIATIONS ..... **xiii**

TABLE OF CONTENTS

CHAPTER 1: INTRODUCTION AND OUTLINE OF THE RESEARCH 15

1.1. Background 15

1.2. Problem Identification 16

1.3. Aim 16

1.4. Objectives 17

1.5. Methodology 17

CHAPTER 2: LITERATURE REVIEW 18

2.1. Global Aluminum Foundry Industry 18

2.1.1. Overview of the Global Aluminum Foundry Industry 18

2.1.2. Key Consumer Industries 18

2.1.3. Leading Producers and Growth Dynamics 19

2.1.4. Recycling and Sustainability 19

2.2. Foundry Industry in Sri Lanka 19

2.2.1. Overview of the Foundry Industry in Sri Lanka 19

2.2.2. Current Challenges 20

2.3. Aluminum Casting Processes 21
2.3.1. Sand Casting: 21
2.3.2. Permanent Mold Casting: 23
2.3.3. Die Casting: 25
2.4. Furnace Types and Combustion Processes 26
2.4.1. Types of Melting Furnaces 27
2.5. Energy Efficiency in Foundry Operations 30
2.5.1. Energy Sources 30
2.5.2. Energy Requirements and Thermal Efficiency 30
2.5.3. Operational Parameters 31
2.6. Waste Heat Recovery TechnologiesFor Foundry Applications 32
2.6.1. Plate Heat Exchangers (PHEs) 32
2.6.2. Shell-and-Tube Heat Exchangers (S&T) 34
2.6.3. Plate-Fin Heat Exchangers (PFHE) 35
2.6.4. Plate-and-Shell Heat Exchangers 35
2.6.5. Welded Plate Heat Exchanger Technology 36
2.6.6. High Temperature Heat Exchangers (HTHEs): 37
2.6.7. Heat Pipe Heat Exchangers (HPHEs) 38
2.6.8. Comparison of Prominent Heat Recovery Technologies 40
2.7. Combustion Techniques Used in the Foundry Industry 40
2.7.1. Mechanical Atomizing Burners 41
2.7.2. Pressure Atomizing Burners 42
2.7.3. Air Atomizing Burners 43
2.7.4. Dual-Fuel Burners 43
2.7.5. Waste Oil Burners 44
2.7.6. Considerations for Using Waste Oil or Diesel Fuel 44
CHAPTER 3: INTRODUCTION TO THE CEB FOUNDRY 45
3.1. Overview of the CEB Foundry 45

3.2. Location of the CEB Foundry 45

3.3. Products Manufactured at the CEB Foundry 46

3.4. Summary of Production Data 48

3.5. Casting Methods and Equipment 49

3.6. Initial Foundry Layout 53

3.7. Foundry Layout After Modifications 53

CHAPTER 4: PERFORMANCE EVALUATION AND METHODOLOGY FOR COMBUSTION AIR PREHEATING AND ENERGY OPTIMIZATION 57

4.1. Introduction 57

4.2. Efficiency Analysis of Existing Furnaces 57

4.2.1. Pit Furnace Efficiency Analysis 57

4.2.2. Tilting Furnace Efficiency Analysis 60

4.3. Review of Combustion System Designs 63

4.3.1. Combustion Principles and Their Applications 63

4.3.1.1. Crucible Shape and Size 63

4.3.1.2. Airflow and Combustion Dynamics 64

4.3.1.3. Chimney and Ventilation Design 65

4.4. Modelling of Crucible Furnace and Study of Combustion Mechanism Using Ansys Fluent 65

4.4.1. Simulation Simplifications Applied 65

4.4.2. Computational Model Setup 66

4.4.3. Boundary Conditions and Inputs 67

4.4.4. Mesh and Geometry 68

4.4.5. Solution and Solution Controls 69

4.4.6. Key Findings from the Simulation 69

4.5. Development of the Combustion Air Preheating Methodology 75

4.5.1. Rationale for Combustion Air Preheating 75

4.5.2. Proposed Methodology 75

4.5.3. Design Objectives 77

4.6. Design of the Heat Exchanger 78

4.6.1. Design Calculations 78

4.7. Modeling of Heat Exchanger and Study of Heat Transfer using ANSYS Fluent Simulations 83

4.7.1. 3D Modeling 83

4.7.2. Simplified Simulation Approach for Welded Plate Heat Exchanger 84

4.7.3. Simulation Setup for Welded Plate Heat Exchanger: 85

4.7.4. Boundary Conditions 86

4.7.5. Mesh and Geometry of the Welded Plate Heat Exchanger 86

4.7.6. Solution and Solution Controls 89

4.7.7. Key Findings from the Simulation 90

CHAPTER 5: FABRICATION AND EXPERIMENTAL SETUP 94

5.1. Fabrication of the Welded Plate Heat Exchanger 94

5.1.1. Material Selection and Construction Details 94

5.1.2. Assembly Techniques and Equipment Used 94

5.2. Experimental Setup 96

5.3. Measurement and Instruments 97

5.4. Procedure for Evaluating Heat Exchanger Performance 103

CHAPTER 6: RESULTS AND DISCUSSION 106

6.1. Overview 106

6.2. Experimental Challenges and Setup 106

6.3. Experimental Results before the integration of combustion air preheating system. 106

6.4. Experimental results after integration of combustion air preheating system 107

6.5. Comparative Analysis: Experimental Results Before and After Heat Exchanger Integration. 110

6.6. Simulation Results Intepretation 114

6.7. Correlation Between Simulation and Experimental Findings 115
6.8. Economic Analysis of the welded plate heat exchanger 115
6.8.1. Payback Associated with the Fuel Saving 115
6.8.2. Time Saving and Associated Labor Cost Benefit 116
6.9. Deviations, Limitations and Future Scope 117
CHAPTER 7: CONCLUSIONS AND RECOMMENDATIONS 119
7.1. Conclusion 119

LIST OF FIGURES

Figure 1-Global Aluminum Production, Production of Aluminum Castings and Aluminum Annal Price..... 18
Figure 2-Sand Casting Process 22
Figure 3-Mould Section and casting nomenclature 22
Figure 4-Pattern attached with gating and risering system 23
Figure 5-Schematic of permanent mould casting process..... 24
Figure 6-Steel moulds left unused at the Foundry 24
Figure 7-Schematic of a hot chamber horizontal die casting setup..... 26
Figure 8-Cold chamber horizontal die casting process. 26
Figure 9-Plate-and-frame PHE (construction scheme): 1—stack of plates with gaskets; 2—fixed frame plate; 3—moving plate of frame; 4—carrying bar; 5—tightening bolts (courtesy of OAO Alfa Laval Potok, Korolev, Moscow region, Russian Federation [19]..... 33
Figure 10-Geometrical features of a single pass WPHE. Crossflow arrangement [22]..... 37
Figure 11-High Temperature Heat Exchanger (HTHE) and heat recovery system [23]..... 38
Figure 12-Schematic of a Heat Pipe [24]..... 39
Figure 13-Heat Pipe Heat Exchanger Used in the Steel Industry 39
Figure 14-Schematic of a Rotary Cup Burner (courtesy of AATRAL ENGINEERING) [26] 41
Figure 15-Schematic of a pressure jet burner (Courtesy Lennox Industries Inc.) 42
Figure 16-Schematic of an air atomizing burner [29]..... 43
Figure 17-Aluminum clamps manufactured at the CEB foundry 46
Figure 18-A bronze casting pump end cover produced by CEB foundry..... 47
Figure 19-Aluminium anodes each 70kg produced by CEB foundry..... 48
Figure 20-Sand cast mould ready for pouring..... 49
Figure 21-Starting the ignition using a burning piece of cloth 50
Figure 22-Flame spreading inside the furnace..... 50
Figure 23-Improper construction of the pit furnace..... 50
Figure 24-Measuring aluminum..... 50
Figure 25-Loading aluminum into the crucible 51
Figure 26-Furnace covered by a lid 51
Figure 27-Pouring, Cooling and knocked out castings 51
Figure 28: Tilting furnace covered with various materials due to non-use..... 52
Figure 29-Foundry layout modification..... 54
Figure 30-Desired position for the burner flame entry into the furnace 61
Figure 31-Rounded and Conical bottom crucibles 63

Figure 32-Fig. 1: Schematic diagram of a fuel-fired and tiltable crucible furnace. 1) Crucible, 2) Furnace lining (permanent lining), 3) Firing compartment, 4) Gas or oil burner, 5) Emergency tap (leading towards the emergency accumulation pit), 6) Refractory base, 7) Exhaust port, 8) Stack 64
Figure 33-Temperature contour across the X-Y plane of the burner. 70
Figure 34-Velocity streamline of the flow inside the air body of crucible furnace in a burner designed for high air velocity 72
Figure 35-Study of the effects of burner angle for temperature distribution 73
Figure 36-Designated path for flame travel around the crucible 74
Figure 37-3D model of the Welded plate heat exchanger 79
Figure 38-Effectiveness for Heat Exchangers [36] 82
Figure 39-3D Wireframe model of welded plate heat exchanger assembly 84
Figure 40-Temperature volume rendering diagram for plate heat exchanger 91
Figure 41- Temperature contours across the hot gas inlet to hot gas outlet 91
Figure 42-Temperature contour across the cold air inlet to hot air outlet 92
Figure 43-Heat exchanger and Furnace air-body considered for CFD study ..... **Error! Bookmark not defined.**
Figure 44-Fabricaiton of the welded plate heat exchanger 95
Figure 45-Integrated assembly of welded plate heat exchanger and the tilted crucible furnace consisting all the instrumentation for testing 96
Figure 46-Molten aluminum temperature measurement using a K-type thermocouple 98
Figure 47-Digital temperature controller for temperature measurement, 1) T1-Cold air inlet, 2) Hot air outlet, 3) T3-Hot gas inlet, 4) T4-Hot gas outlet, 5) For temperature measurements inside the liquid aluminum 99
Figure 48-Gauge for fuel temperature measurement 100
Figure 49-Fuel temperature adjustment 100
Figure 50-Fuel pressure gauge 101
Figure 51-Fuel tank dipstick 101
Figure 52-Blower damper position indicator 102
Figure 53-Burner characteristic curve 103

LIST OF TABLES

Table 1:Comparison of Heat Exchanger Types 40
Table 2-Summary of Production Data 48
- Table 3: Operational Data Summary for Pit Furnace Aluminum Casting Test 58
Table 4: Operational Data Summary for Tilting Furnace Aluminum Casting Tests 62
Table 5-Combustion air preheater performance evaluation test data..... 107
Table 6-Operating Conditions and System Parameters for the Combustion Air Preheating Test..... 107
Table 7-Temperature Variation at Measuring Points on the Plate Heat Exchanger 108
Table 8- Performance Analysis of Tilting Furnace with Combustion Air Preheating System 109

LIST OF APPENDICESS

Appendix 1-Production Data of Manufactured Components at CEB Foundry 122
Appendix 2-Waste oil calorific value test report 127
Appendix 3- Weishaupt burner data sheet 128

LIST OF NOMENCLATURE

As	Area	m^2
c_p	Specific heat capacity	J/kg·K
E	Energy	J (Joules)
h	Specific enthalpy	kJ/kg
h_c	Convective heat transfer coefficient	W/m²·K
k	Thermal conductivity	W/m·K
m	Mass	kg
$\dot{m}$	Mass flowrate	kg/s
NTU	Number of Transfer Units	--
Nu	Nusselt Number	--
P	Pressure	Pa (Pascals)
Q	Thermal Energy	J
Re	Renold Number	--
t	Time	s (seconds)
T	Temperature	K
U	Overall heat transfer coefficient	W/m²·K
v	Velocity	m/s
$\dot{\boldsymbol{V}}$	Volume flowrate	m^3/s
ΔT	Temperature difference	K
ε	Heat exchanger Effectiveness	--
η	Efficiency	--
ρ	Density	kg/m³

LIST OF ABBREVIATIONS

AFR	Air to fuel ratio
AL	Aluminum
CAD	Computer aided design
CAM	Computer aided manufacturing
CEB	Ceylon Electricity Board
CFD	Computational Fluid Dynamics
HE	Heat Exchanger
FDSI	Foundry Development and Services Institute
GCV	Gross Calorific Value
HPHE	High Pressure Heat Exchanger
HTHE	High Temperature Heat Exchanger
IDB	Industrial Development Board
KCCP	Kelanitissa Combined Cycle Power Plant
kWh	Kilowatt hour
NTU	Number of Transfer Units
ORC	Organic Rankine Cycle
PHE	Plate Heat Exchanger
WHR	Waste Heat Recovery
WPHE	Welded Plate Heat Exchanger

CHAPTER 1: INTRODUCTION AND OUTLINE OF THE RESEARCH

1.1. Background

The aluminum casting process plays a crucial role in the production of components for the transmission and distribution networks of the national grid of Sri Lanka. At the Ceylon Electricity Board (CEB) foundry, sand casting is employed to produce aluminum parts essential for maintaining and expanding the national electricity grid. However, despite the in-house production capabilities, it represents only a small fraction of the total demand, leading to a heavy reliance on imports. The exact import quantities, however, are not centrally documented, making it challenging to quantify. This situation underscores a significant opportunity for optimizing the aluminum casting process to improve productivity and energy efficiency.

The underground furnace at the CEB foundry operates with a crucible surrounded by refractory bricks and uses a gravity-fed, used lubrication oil-based burner without pressure pumps. This setup results in inefficient combustion and high energy consumption. This furnace is manually ignited by a conventional pilot flame method, which is neither time-efficient nor environmentally friendly. Given the higher temperature and heat requirement of melting aluminum at uniform temperature, enhancing the combustion process and optimizing heat utilization is paramount.

The tilting furnace, equipped with a burner featuring a blower, pressure pump, and injection nozzle for atomization of waste oil, is left idle due to improper installation. This improper setup has resulted in operational difficulties stemming from ergonomic issues for the operators, leading to inefficiencies and underutilization. The system also generates heavy emissions, including excessive heat and smoke, underscoring the need for proper installation, ergonomic improvements, and optimization to minimize waste and environmental impact.

This research proposes an integrated approach to enhance the aluminum casting process at the CEB foundry by focusing on improving efficiency as well as the specific

fuel consumption through waste heat recovery from exhaust gases. By developing and implementing waste heat recovery systems, such as preheating setups for combustion air, the study aims to reduce energy consumption and optimize operational performance. Computational simulations using tools like ANSYS will be utilized to analyze heat transfer and refine the recovery process.

By addressing these aspects, the study seeks to provide actionable insights into enhancing foundry efficiency and increasing local production capacity. These improvements will help reduce dependency on imported components while promoting energy efficiency and supporting sustainable practices within Sri Lanka's electricity sector.

1.2. Problem Identification

The Ceylon Electricity Board (CEB) foundry relies on outdated sand-casting methods and oil-fired furnaces, leading to low energy efficiencies and high operational costs. The absence of heat recovery systems contributes to significant fuel consumption and wasted energy through flue gas which has temperature well above the aluminum melting point. This waste is unavoidable as a single unit. This study aims to develop a combustion air preheating system that recovers exhaust gas energy to improve combustion efficiency and reduce fuel costs. The objective is to create a sustainable, energy-efficient model that modernizes CEB’s foundry operations, reduces dependency on imports, and aligns with Sri Lanka's environmental and economic goals.

1.3. Aim

The aim of this research is to investigate the feasibility of improving the specific fuel consumption of Aluminum melting process at the Ceylon Electricity Board (CEB) foundry.

1.4. Objectives

1. To evaluate the potential of developing a combustion air preheating system by recovering exhaust gas energy, focusing on its impact on combustion efficiency and fuel consumption.
2. To investigate benchmark specific fuel consumption of advanced combustion techniques used in similar industry.
3. To apply computational fluid dynamics (CFD) studies to model heat transfer and refine the waste heat recovery process for preheating combustion air.
4. To improve the waste heat recovery on the operation, productivity and reduce melting time,

1.5. Methodology

1. Conduct a literature review of existing research and best practices in aluminum casting processes, waste heat recovery, and combustion optimization
2. Analyze the current aluminum casting process at the CEB foundry by gathering historical data on fuel consumption, melting time, and production outputs. Measure energy efficiency to establish a performance baseline.
3. Design and implement a waste heat recovery system to preheat combustion air. Monitor its impact on energy consumption, melting time, and furnace performance to optimize operational efficiency.
4. Perform a cost-benefit analysis to evaluate the economic feasibility of the optimizations. Assess the environmental impact, including potential reductions in greenhouse gas emissions and other pollutants, to ensure sustainability.

CHAPTER 2: LITERATURE REVIEW

2.1. Global Aluminum Foundry Industry

2.1.1. Overview of the Global Aluminum Foundry Industry

The aluminum foundry industry has experienced remarkable growth in the 21st century, with global production increasing by 2.4 times from 2000 to 2017, reaching 19.1 million tons in 2017[1]. This growth as shown in figure1 reflects aluminum's rising demand due to its versatile applications and inherent material advantages.

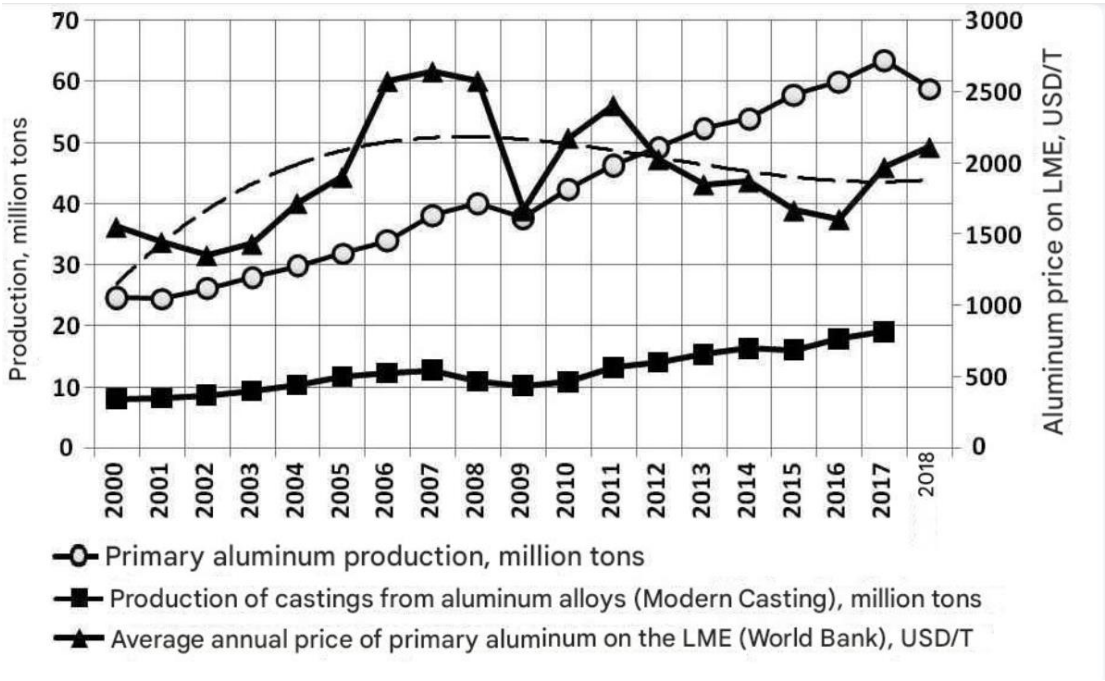

Figure 1-Global Aluminum Production, Production of Aluminum Castings and Aluminum Annal Price

2.1.2. Key Consumer Industries

The transport sector remains the dominant consumer of aluminum castings, accounting for 75% of global demand in 2011, with the automotive industry alone representing 57%. Aluminum's lightweight properties and strength make it indispensable for manufacturing engine blocks, cylinder heads, pistons, and structural components. Advanced casting techniques allow for high-strength, heat-resistant components necessary for modern transportation[1].

2.1.3. Leading Producers and Growth Dynamics

The top aluminum casting producers in 2017 were[1]:

- China: 38.3% of global production
- USA: 8.8%
- Japan: 7.8%

Countries like Turkey (+40.7%), China (+40.4%), and Mexico (+36.2%) showed the highest production growth from 2013 to 2017. These figures highlight aluminum casting's expanding role in global manufacturing.

2.1.4. Recycling and Sustainability

Aluminum is highly sustainable due to its excellent recyclability. Recycling aluminum uses just 5% of the energy required for primary production. This makes it ideal for closed-loop manufacturing, supporting environmental goals while remaining cost-effective.

The aluminum foundry industry's continuous evolution underscores its critical role in modern manufacturing. Advanced technologies, alloy innovations, and an emphasis on sustainability will shape its trajectory, making aluminum an indispensable material for global industrial and environmental needs.

2.2. Foundry Industry in Sri Lanka

2.2.1. Overview of the Foundry Industry in Sri Lanka

The foundry industry in Sri Lanka has a rich history, dating back to the second century BC, when ancient iron-making foundries highlighted the region's long-standing tradition of metalworking [2], [3], [4] . Despite this heritage, the industry remains underdeveloped today, facing challenges that limit its global competitiveness. As a vital part of the country’s economy, the foundry sector supports industries such as tea, rubber, oil, and fiber processing by supplying essential components. It also plays a key role in marine engineering, turbine bearing production, and the creation of various exportable metal products [2], [3]

2.2.2. Current Challenges

The foundry industry faces several critical challenges:

1. **Quality Issues:**

The quality of foundry products in Sri Lanka is not competitive with international standards. Inferior quality of cast products stems from inadequate foundry equipment and poor work planning[2].

2. **Traditional Practices:**

The reliance on sand casting and manual operations leads to inefficiencies in energy use and limits productivity. Manual mold preparation and unregulated sand recycling degrade mold quality over time, causing higher rejection rates and increased energy consumption[2].

3. **Combustion Inefficiency:**

Many foundries use oil-fired furnaces fueled by low-grade waste oils. These result in incomplete combustion, excessive emissions, and high energy losses. The lack of automation and proper air-fuel mixing systems exacerbates these problems. Additionally, furnace designs often lack insulation, causing further heat loss[2].

4. **Raw Material Challenges:**

The high cost of raw materials, particularly pure copper and zinc for brass production, has forced many foundries to rely on lower-quality scrap metal. This reduces product quality and hinders international competitiveness[2].

5. **Technological Stagnation:**

The industry heavily relies on traditional and outdated methods, struggling to keep up with global advancements in manufacturing technology[2].

6. **Efforts to Modernize the Industry**

Efforts to modernize the industry are gradually emerging. The Foundry Development & Services Institute (FDSI) is working to improve productivity and quality while aligning local practices with international standards. Initiatives include[2], [5]:

- Training programs on safety, environmental compliance, and modern technologies like CNC machining and CAD/CAM software.
- Promoting research, facilitating investment, and improving access to high-quality raw materials at affordable prices.
- Introducing new processes, such as the cupola process, to refine the quality of iron and steel products.
- Exploring waste heat recovery systems, efficient burner designs, and automated casting techniques to enhance energy efficiency and reduce waste.

In Sri Lanka, comprehensive research to accurately assess the number of foundries, production volumes of materials like aluminum, steel and detailed export and import data remains absent. These crucial datasets are not available through online sources or institutions such as the Foundry Development and Services Institute (FDSI), Industrial Development Board (IDB), or Export Development Board (EDB). This lack of readily accessible information underscores the underdeveloped and primitive state of the foundry industry in Sri Lanka. The absence of such data not only hinders strategic planning but also limits the industry's ability to compete effectively on both local and global scales. Addressing this gap through systematic research and data collection is essential for the growth and modernization of the sector.

2.3. Aluminum Casting Processes

Aluminum casting is a versatile manufacturing process that allows for the production of complex shapes and high-quality components. It is widely used across various industries due to aluminum's favorable properties, such as its strength-to-weight ratio and corrosion resistance. This section explores the different aluminum casting processes which can be easily adopted at the Ceylon Electricity Board Foundry, and which are applicable to common casted products manufactured in Sri Lanka.

2.3.1. Sand Casting:

Both green sand and dry sand casting are used for aluminum. This method is flexible and cost-effective for low-volume production but generally results in lower

dimensional accuracy and surface finish compared to die casting[6], [7]. The foundry industry in Sri Lanka predominantly employs sand casting[2]. Sand casting's cost-effectiveness and adaptability make it the preferred method, especially for non-ferrous metals like aluminum. Key challenges in aluminum sand casting include ensuring mold quality and preventing defects such as shrinkage, porosity, and inclusions. Effective mold preparation involves selecting appropriate sand-clay mixtures, achieving optimal compaction, and ensuring permeability to avoid gas entrapment. Foundries in Sri Lanka often rely on locally available silica sand, but its properties vary, influencing casting quality[2]. Figure 2 below shows the sand-casting process. The figure 3 and 4 below shows the parts of a typical sand-casting mold and pattern.

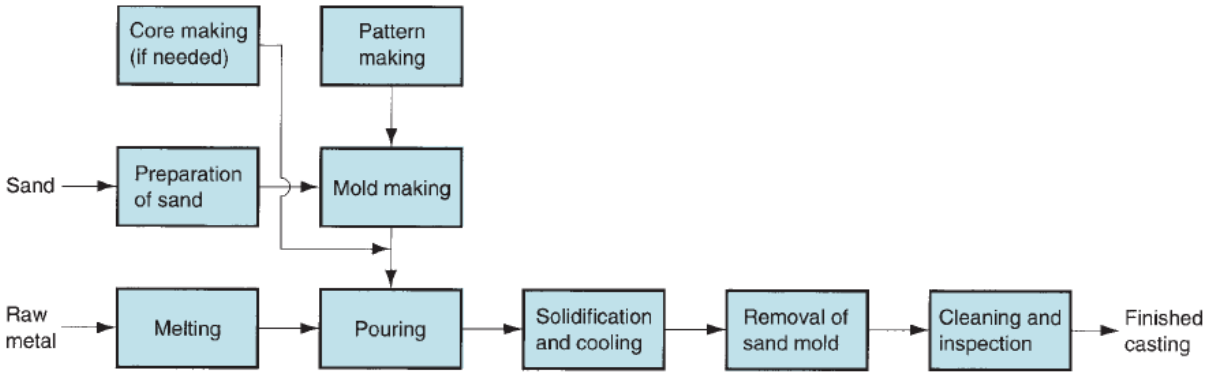

Figure 2-Sand Casting Process

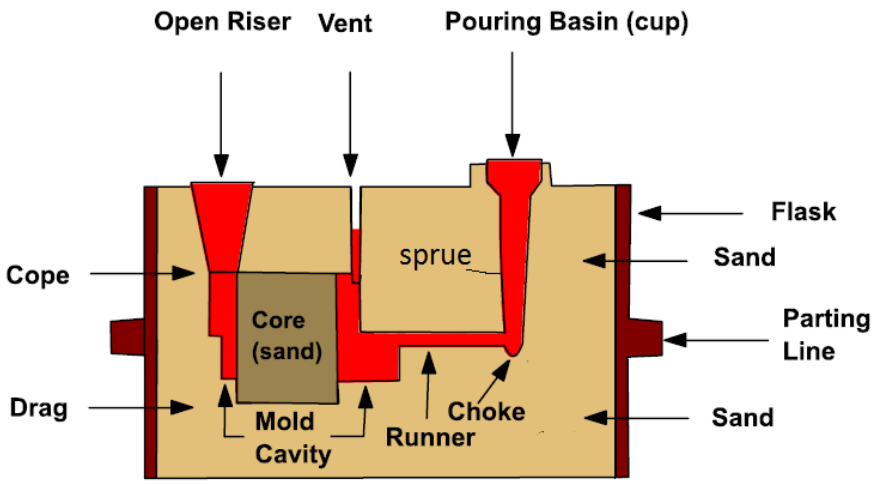

Figure 3-Mould Section and casting nomenclature

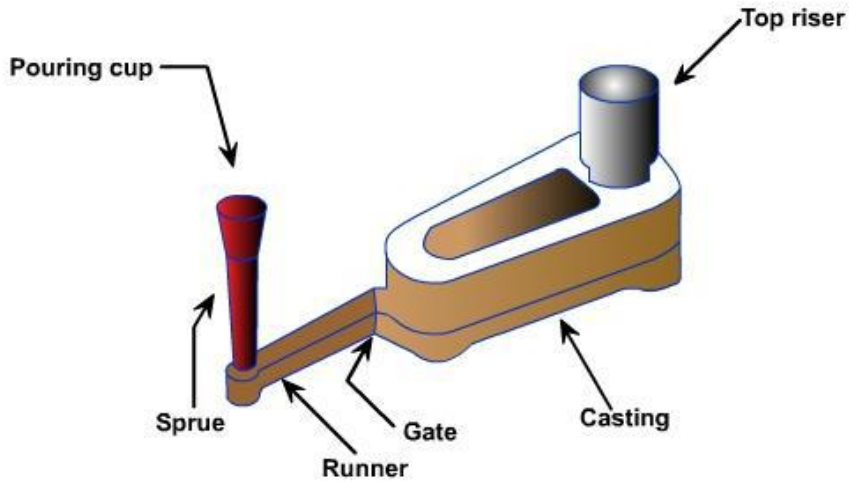

Figure 4-Pattern attached with gating and risering system

At the CEB foundry, molding sand is prepared using a mixture of silica sand sourced from the Naththandiya area and bentonite. Wooden flasks are employed during the sand casting process, while patterns made from either wood or aluminum are utilized specifically for manufacturing bolted clamps.

2.3.2. Permanent Mold Casting:

This process uses reusable molds and is suitable for medium to high-volume production. It offers better mechanical properties than sand casting due to faster cooling rates[6] . Figure 5 below shows various steps in permanent mould casting.

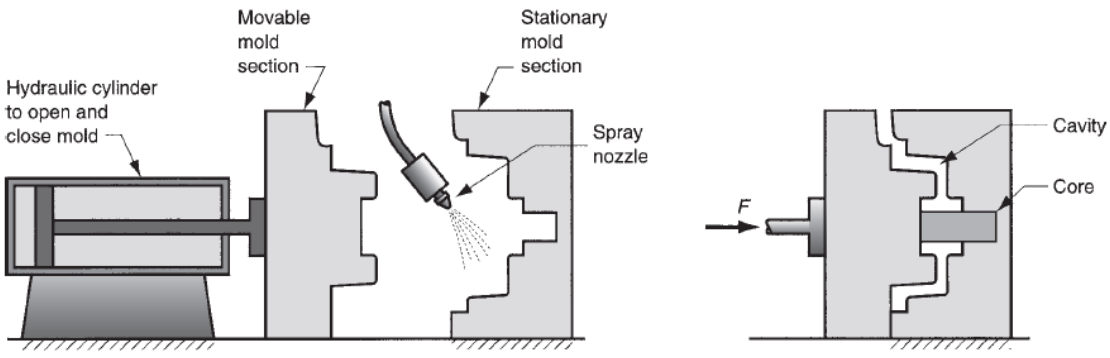

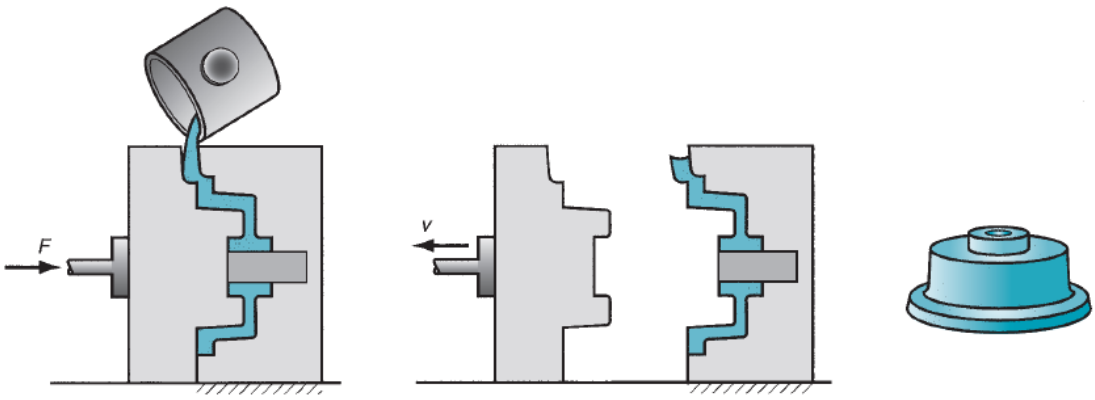

Figure 5-Schematic of permanent mould casting process

Permanent mold casting process has been previously attempted at the Central Workshop and Garage Unit. Although there are a few unused dies as shown in the figure 6 below, remaining in the unit, the exact reason for the discontinuation of this process is unclear. These dies have not been utilized for the past ten to fifteen years. It is possible that the process was abandoned due to the lack of proper mechanical systems, such as hydraulic mechanisms, necessary for opening and closing the dies. Recently, an experiment was conducted using the die casting process using these dies, demonstrating that it is still feasible within the unit. This area warrants further investigation and improvement in the future.

Figure 6-Steel moulds left unused at the Foundry

2.3.3. Die Casting:

This is the most prevalent method for aluminum casting, known for its ability to produce high-volume, high-precision components. It involves forcing molten aluminum into a mold cavity under high pressure[6].

Figure 7 below shows a schematic representation of a typical horizontal die casting setup. The system includes a fixed die half and a movable die half that form the mold cavity. The molten metal is injected into the cavity under high velocity (denoted by **V**) and pressure, ensuring proper filling and formation of the desired shape.

Figure 8 illustrates the cold chamber die casting process. In this process, the molten metal is poured into a shot chamber using a ladle. A ram then forces the metal into the cavity under high pressure. This method is commonly used for materials like aluminum. The use of ejector pins helps release the casting from the mold after solidification.

On the other hand, Figure 7 demonstrates the hot chamber die casting process. Unlike the cold chamber method, here the molten metal is maintained in a heated reservoir and fed into the cavity through a gooseneck mechanism. A plunger applies the necessary pressure for injection. This technique is faster but is generally limited to metals with lower melting points, such as zinc or lead.

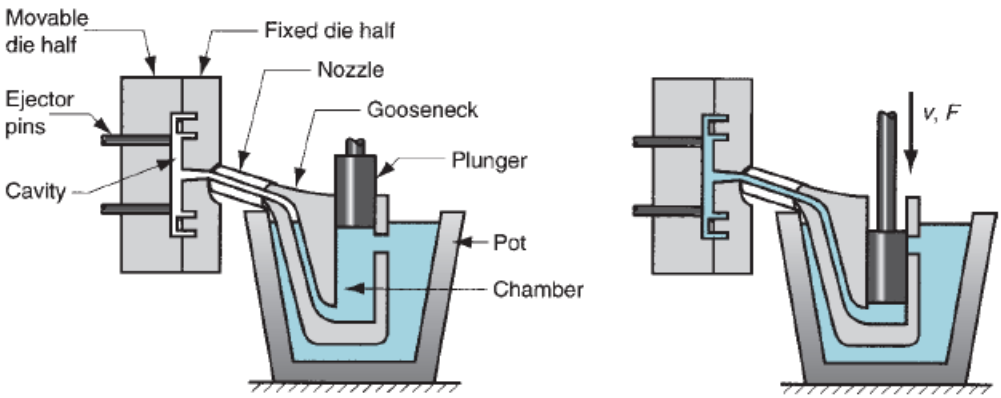

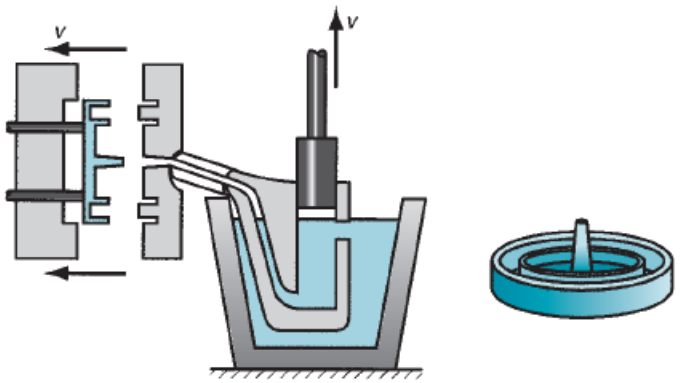

Figure 7-Schematic of a hot chamber horizontal die casting setup.

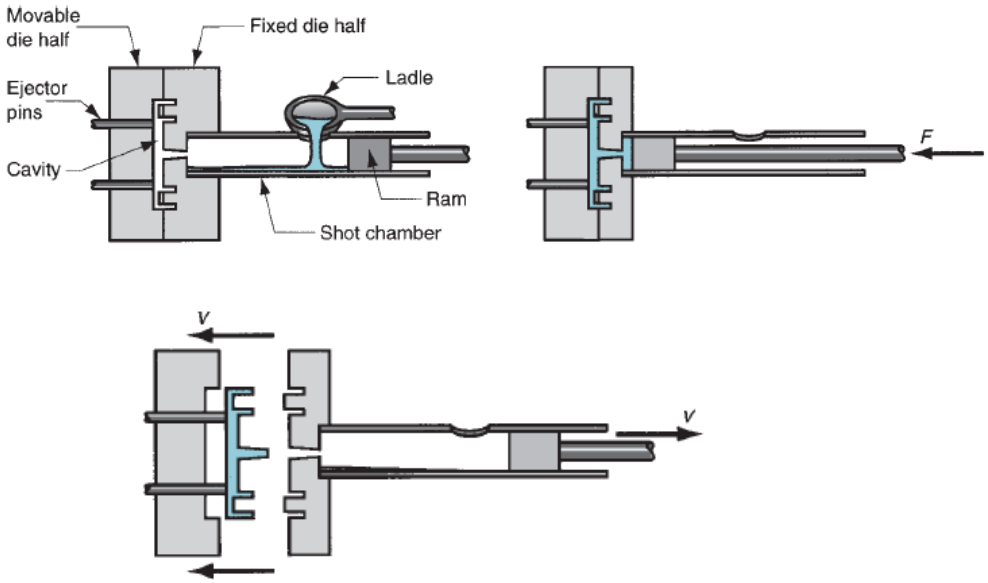

Figure 8-Cold chamber horizontal die casting process.

In conclusion, aluminum casting processes are diverse and continually evolving, with innovations aimed at improving efficiency, sustainability, and the mechanical properties of cast components. These advancements are crucial for meeting the growing demands depending on the industrial application of the aluminum components.

2.4. Furnace Types and Combustion Processes

Melting furnaces play a critical role in the metal casting process, with their economical and efficient performance hinging on several factors. These include the

design, shape, and dimensions of the melting chamber, as well as the rate of heat input [8]. Additional factors contributing to efficiency include:

1. Monitoring and managing parameters such as temperature and fuel consumption can optimize furnace performance[8].
2. Maintaining a relatively small temperature gradient between the flame and fuel ensures effective combustion[8].
3. Using preheated air for combustion improves efficiency significantly[8].

To achieve optimal operation, process monitoring instruments such as thermocouples, radiation and optical pyrometers for temperature measurement, fuel measuring devices, and pressure or draft gauges are used[8].

2.4.1. Types of Melting Furnaces

1. **Major Types of Melting Furnaces**

    a. **Open Hearth Furnaces**: Widely used for large-scale metal production[8].

    b. **Electric Arc Furnaces**: Suitable for high-purity metal production[8].

    c. **Shaft-Type Furnaces**: Used primarily for continuous melting operations[8].

    d. **Crucible Furnaces**: These are versatile and widely used in non-ferrous metal industries. Crucible furnaces can be coke or oil-fired and are capable of achieving high combustion intensity and temperatures[8].

    e. **Electric Induction Furnaces**: Highly efficient and suitable for precise control of melting conditions[8].

2. **Classification based on Energy Use**

Melting furnaces can be broadly classified based on their energy source:

a. **Fuel-Fired Furnaces**:

- **Indirect Flame Furnaces**: Here, the flame and combustion products do not come into direct contact with the metal. Examples include pot furnaces and crucible furnaces[8].
- **Direct Flame Furnaces**: In these furnaces, the flame and combustion products are in direct contact with the metal. Examples include reverberatory furnaces and certain types of pot furnaces.

b. **Induction Furnaces**: These are further divided into low-frequency and high-frequency types, which utilize electromagnetic induction for heating.

3. **Specific Furnace Types**

a. **Reverberatory Furnaces**

Reverberatory furnaces are used mainly for large-scale production, capable of handling up to 50,000 kilograms of charge. These are direct flame furnaces where the flame and combustion products come into contact with the metal being melted. Reverberatory furnaces are primarily applied for bulk melting of ingots and scrap. Once the metal is melted or held, it is transferred to a smaller furnace, such as one used at a die casting machine[8].

The furnace is constructed with a steel shell lined with refractory bricks or a monolithic lining. A burner is positioned at one end, while the exhaust stack is located at the opposite end. Charging is performed through a separate door or the exhaust stack. Metal removal is done either by tilting the furnace or using a tap hole[8].

b. Pot Furnaces

Pot furnaces are further classified into:

- **Stationary Pot Furnaces**: Ideal for low melting capacities[8].
- **Tilting Pot Furnaces**: Used for higher melting capacities. In both cases, molten metal is transferred to ladles for distribution to molds[8].

c. Crucible Furnaces

Oil-fired crucible furnaces are widely used in small-scale non-ferrous industries in Sri Lanka. These furnaces are capable of high combustion intensity and temperatures[9]. The burner is a critical component, as it atomizes the fuel and ensures complete combustion. The performance of an oil-fired crucible furnace depends on three key factors[8]:

1. A suitable burner.
2. A combustion chamber with the right shape and size.
3. Correct overall design.

d. Induction Furnaces

Induction furnaces are known for their high efficiency and ability to produce high-quality metal melting. They operate based on simple electrical principles: a high-frequency current passes through a copper coil, which surrounds a crucible containing the metal charge. The metal heats up due to secondary current losses, eddy current losses, and hysteresis losses[8].

The choice of a melting furnace depends on various operational needs such as the type of metal being processed, desired efficiency, and scale of operation. Understanding the classification, functionality, and design considerations of melting furnaces can help optimize performance and reduce energy consumption in metal casting processes.

2.5. Energy Efficiency in Foundry Operations

The process of melting aluminum is highly energy-intensive, posing a significant challenge for foundries, especially in regions like Sri Lanka, where traditional oil-fired systems dominate. These systems are often characterized by low thermal efficiency and high operational costs, primarily due to suboptimal design, inadequate construction, and poor maintenance. The lack of heat recovery systems further exacerbates these issues. Additionally, the inefficiency of these systems contributes to elevated ambient temperatures within the foundry, creating an uncomfortable working environment[8].

This report examines the various energy sources utilized in the aluminum casting industry, assesses their energy demands, and evaluates the associated thermal efficiencies and operational parameters, providing insights into potential improvements and innovations.

2.5.1. Energy Sources

a. **Liquid Fuels:** Waste oil is commonly used in traditional furnaces. This fuel is known for their high energy content but also contribute to significant greenhouse gas emissions. The energy requirement for liquid fuel is typically measured in liters per kilogram of aluminum melted[10], [11]**.**

b. **Electricity:** Electricity is increasingly used in modern foundries due to its cleaner energy profile and ease of control. The energy requirement is often measured in kWh per kilogram of aluminum

c. **Gas:** Natural gas is another alternative, offering a cleaner combustion process compared to oil. It is measured in kJ per kilogram of aluminum melted

2.5.2. Energy Requirements and Thermal Efficiency

Energy Requirements: The foundry process for aluminum production is highly energy-intensive, with melting being the most demanding stage, consuming 12.39 GJ per tonne of material. The energy requirement for manufacturing aluminum ingots is

approximately 33.3 GJ/t, and a total energy of 98 GJ is needed to produce 1 tonne of aluminum[12].

Thermal Efficiency: Improvements in thermal efficiency can be achieved through better furnace design and operation. The thermal efficiency of a pit furnace, calculated at 13.72% during the melting of 2 kg of aluminum in 75 minutes, falls within the typical efficiency range of 4-19% for such furnaces, as reported in prior studies [13].

2.5.3. Operational Parameters

Melting and Pouring Temperatures: The melting temperature for aluminum is typically around 660°C, while pouring temperatures can vary depending on the specific alloy and casting process. However, the general range is between 700°C - 750°C[14].

Air-Fuel Ratio and Ignition Temperature: Proper control of the air-fuel ratio and ignition temperature is essential for efficient combustion and energy use[15]. For used oil-based crucible furnaces, specific air-to-fuel ratios are not directly provided in the available data, but insights can be drawn from similar systems. In the design of a 30 kg aluminum crucible furnace and a 50 kg cast iron crucible furnace, both using diesel fuel, an air-to-fuel ratio of 400:1 is employed[9], [16]. This ratio is used to ensure efficient combustion and melting of metals within the specified time and temperature ranges. Lean air-fuel mixtures, which have a higher air-to-fuel ratio, can lead to complete combustion and reduced emissions of unburnt species. However, near-stoichiometric mixtures (where the air-to-fuel ratio is close to the ideal for complete combustion) can achieve higher heating outputs [17]

Improving energy efficiency in foundry operations is crucial for reducing operational costs and environmental impact. By exploring alternative energy sources and optimizing operational parameters, foundries can achieve significant energy savings and enhance their competitive advantage. Implementing advanced technologies and practices, such as heat recovery systems and optimized furnace operations, can lead to substantial improvements in thermal efficiency and overall sustainability.

2.6. Waste Heat Recovery TechnologiesFor Foundry Applications

Waste heat recovery (WHR) plays a crucial role in enhancing energy efficiency, reducing emissions, and lowering operational costs in foundry operations. For small to medium-scale foundries, adopting WHR systems can lead to significant savings and sustainability improvements.

Exhaust gases leaving from a melting furnaces are typically at temperatures between 600°C to 900°C, containing substantial thermal energy. By using a heat exchanger, this waste heat can be transferred to incoming air before it is introduced into the furnace. Preheating combustion air reduces the need for additional fuel to reach the desired furnace temperature. In addition to this, the furnace charge can be preheated.

Several waste heat recovery technologies are available for application in foundries, ranging from heat exchangers to complex systems such as organic Rankine cycles (ORC). The selection of an appropriate technique depends on factors like the temperature of the exhaust gases, the size of the foundry, the available budget, and the specific requirements of the foundry process.

The following section presents some of the most promising waste heat recovery (WHR) techniques suitable for small- to medium-scale foundries. The selection of these techniques depends on several factors, including operational parameters, space availability, fouling tendency, pressure and temperature conditions, and cost considerations. Four prominent WHR types are evaluated, and the proposed welded plate heat exchanger (WPHE) is positioned within this comparative framework.

2.6.1. Plate Heat Exchangers (PHEs)

Plate Heat Exchangers (PHEs) as shown in figure 9 are widely recognized for their high efficiency in heat transfer and compact design, making them integral to industries such as processing, air-conditioning, refrigeration, and manufacturing[18], [19]. Their ability to recover low-grade heat in a practical and cost-effective manner enhances their appeal for industrial applications[20]. PHEs exhibit high heat transfer coefficients

and minimal end-temperature differences, which are essential for efficient energy recovery [18].

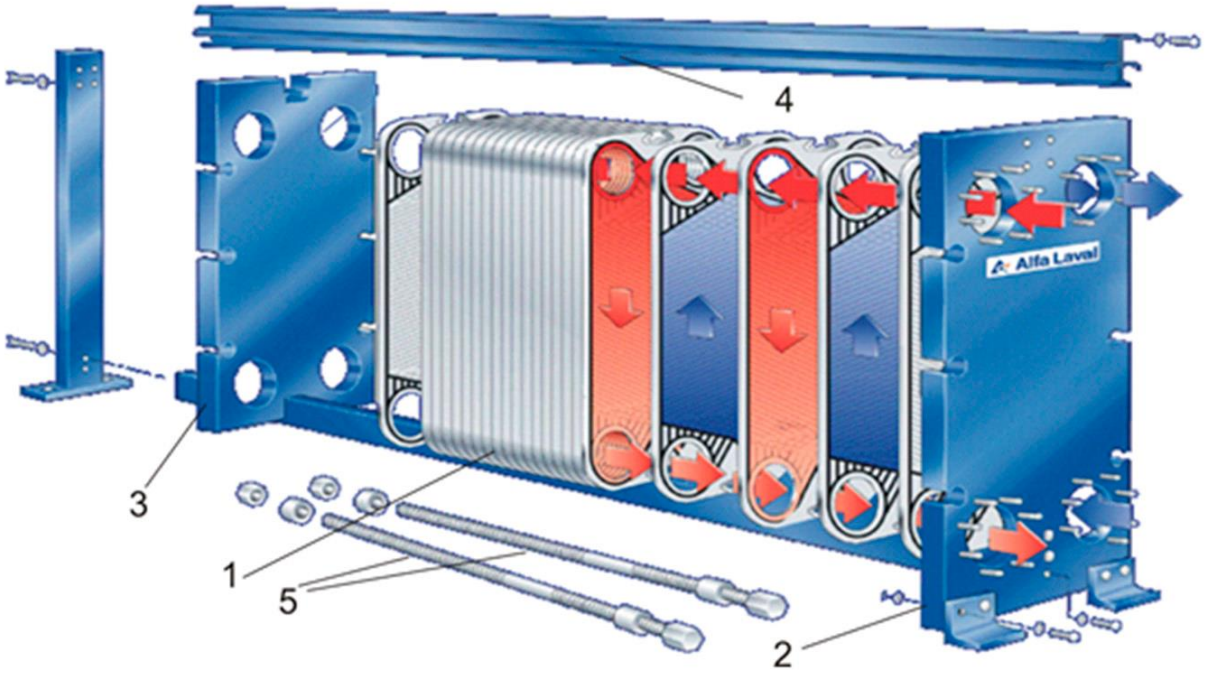

Figure 9-Plate-and-frame PHE (construction scheme): 1—stack of plates with gaskets; 2—fixed frame plate; 3—moving plate of frame; 4—carrying bar; 5—tightening bolts (courtesy of OAO Alfa Laval Potok, Korolev, Moscow region, Russian Federation [19]

PHEs are employed in air-to-air heat recovery systems to improve energy efficiency by recovering heat from exhaust air. A notable innovation in this domain is the heat pipe inserted plate (HPIP) exchanger, which effectively transfers heat between air streams of differing temperatures. With temperature effectiveness reaching up to 70%, these systems demonstrate considerable performance in both winter and summer conditions[21].

Plate Heat Exchangers (PHEs) offer high thermal performance due to the intense turbulence created by their corrugated plate design. Their modular and compact construction makes them ideal for applications where space is limited, and they are particularly effective for recovering low- to medium-grade heat. However, PHEs are limited by the risk of gasket failure at elevated temperatures and are unsuitable for

handling dirty flue gases without proper preprocessing, as contaminants can clog the narrow flow channels.

2.6.2. Shell-and-Tube Heat Exchangers (S&T)

Shell-and-tube heat exchangers (S&T) are widely used in heavy industrial applications due to their robust design and ability to handle high temperatures and pressures[22]. These exchangers consist of a bundle of tubes enclosed within a pressure-resistant shell. Figure 10 illustrates a typical shell-and-tube heat exchanger, showing the arrangement of the shell, tube bundle, and fluid paths. One fluid flows through the tubes, while the other flows around them within the shell. This configuration enables efficient heat transfer between the two fluids, even under demanding operating conditions.

A major strength of shell-and-tube heat exchangers is their broad operating range. They can function effectively at temperatures up to around 500 °C and pressures as high as 150 bars[22]. In addition, the design often incorporates floating tube bundles, which makes the equipment easier to inspect, maintain, and clean.

Moreover, shell-and-tube systems require a large physical footprint and use a considerable amount of material, resulting in higher costs and greater space requirements. They are also prone to fouling, especially on the shell side, which can reduce performance and require periodic shutdowns for cleaning and maintenance.

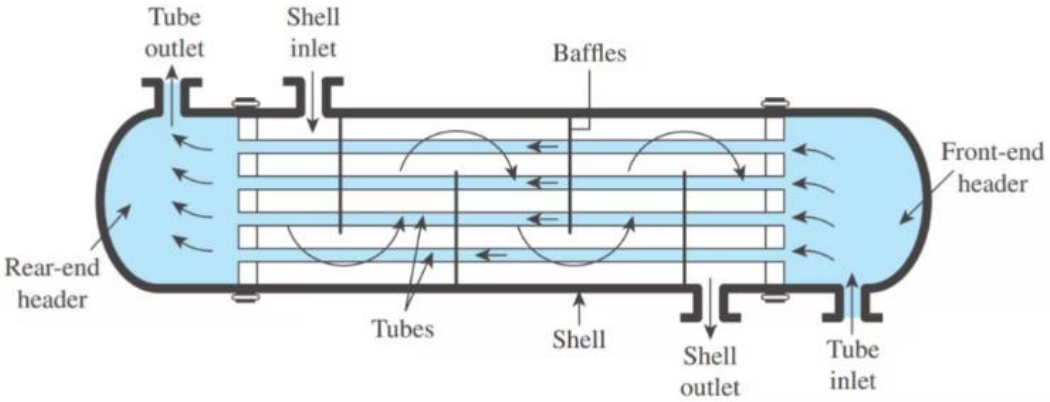

Figure 10: Typical shell-and-tube heat exchanger

2.6.3. Plate-Fin Heat Exchangers (PFHE)

Plate-Fin Heat Exchangers (PFHE) consist of a series of finned passages sandwiched between plates, making them ideal for compact, high-efficiency applications. Figure 11 shows a typical plate-fin heat exchanger, highlighting the layered structure of fins and plates that form multiple parallel flow channels. Their design offers an extremely high surface area per unit volume, resulting in exceptional thermal performance and compactness. PFHEs are especially effective in handling multi-stream flows and phase-change processes. However, their narrow channels are prone to fouling, and cleaning can be challenging. Due to their complexity and cost, PFHEs are typically reserved for specialized industries rather than foundry-scale operations

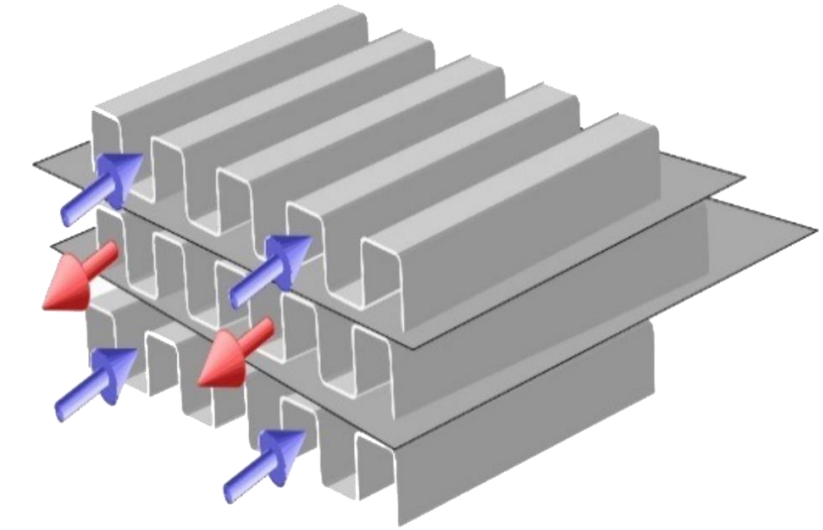

Figure 11: Typical plate-fin heat exchanger arrangement

2.6.4. Plate-and-Shell Heat Exchangers

Plate-and-shell heat exchangers are designed to optimize thermal exchange by incorporating a plate pack inside a fully welded shell, thereby creating two distinct flow zones for fluids. Figure 12 illustrates a typical plate-and-shell heat exchanger, showing the internal arrangement of the plate pack within the pressure-resistant shell. This configuration allows them to function similarly to welded plate heat exchangers while ensuring that the components are securely encapsulated within the shell. One of the main advantages of plate-and-shell heat exchangers is their ability to withstand high pressures and temperatures, capable of operating up to 400 bar and 550 °C. This high-performance rating makes them suitable for demanding industrial

applications where space is at a premium, as their compact design and the reliance on the shell for pressure containment minimize the dependence on welds in the plate, enhancing overall durability and reliability.

However, the manufacturing of plate-and-shell heat exchangers presents certain challenges. The complexity of production increases significantly, particularly when employing laser-welded plates, which require advanced technology and precision. This complexity can lead to longer manufacturing times and higher costs**.**

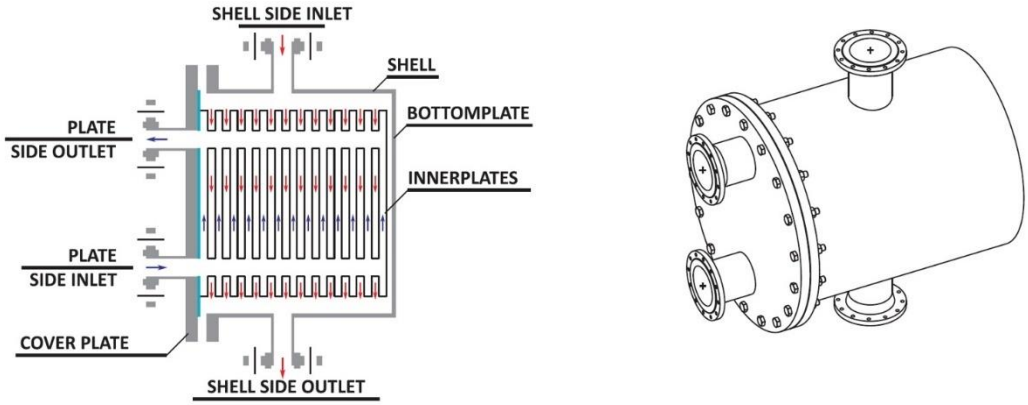

Figure 12: Typical plate-and-shell heat exchanger internal arrangement

2.6.5. Welded Plate Heat Exchanger Technology

Welded Plate Heat Exchanger (WPHE) technology as shown in figure 10, in particular, offers significant advantages in heat exchanger networks by reducing the number of units required and optimizing energy recovery. For instance, a previous study shows potential reduction in the number of heat exchangers in crude oil preheat trains from 12 to as few as 3, with a corresponding reduction in total heat exchanger area from 9350.96 m² to 3598 m². This innovative approach results in potential energy reductions of up to 25%, with a payback period of just 1.6 years. Such efficiency enhancements make WPHEs effective for reducing energy consumption in foundries[23].

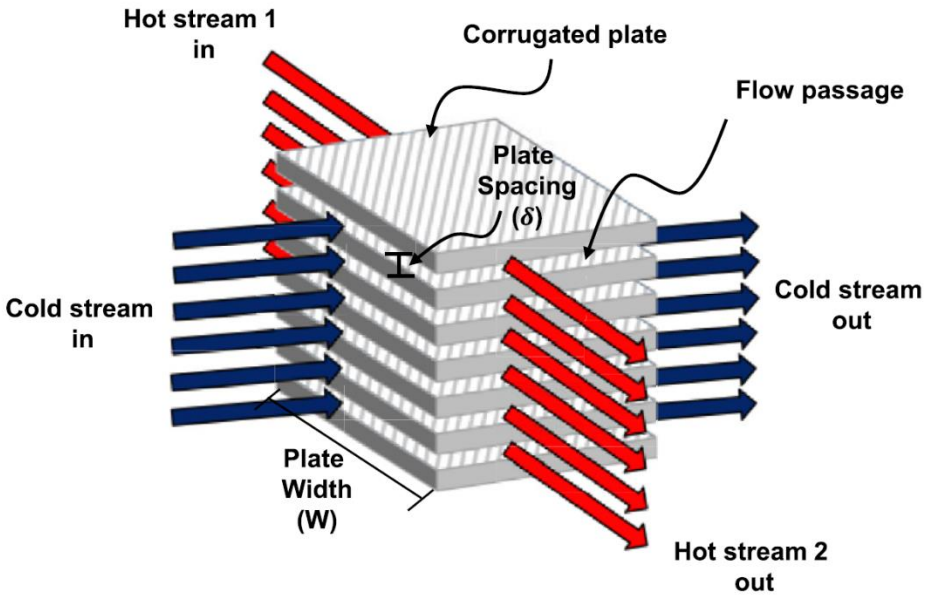

Figure 13-Geometrical features of a single pass WPHE. Crossflow arrangement [22]

2.6.6. High Temperature Heat Exchangers (HTHEs):

Research has been conducted on high-temperature heat exchangers (HTHEs) as shown in figure 11 for efficient waste heat recovery from exhaust gases. These devices can operate at gas temperature above 600ºC[24]. Novel designs incorporating twisted inserts, H-type fins, and wave-like fins, have been proposed to improve heat transfer efficiency and reduce pressure drops. Studies show that the effectiveness of these HTHEs can be increased by up to 12.5%, with heat transfer units (NTU) improving by 53% compared to traditional designs. Despite a 70% and 22% increase in pressure drop on air and gas sides respectively, the optimized designs achieve 12.6% greater effectiveness without further increasing pressure drop, highlighting their potential for high-temperature applications. [24].

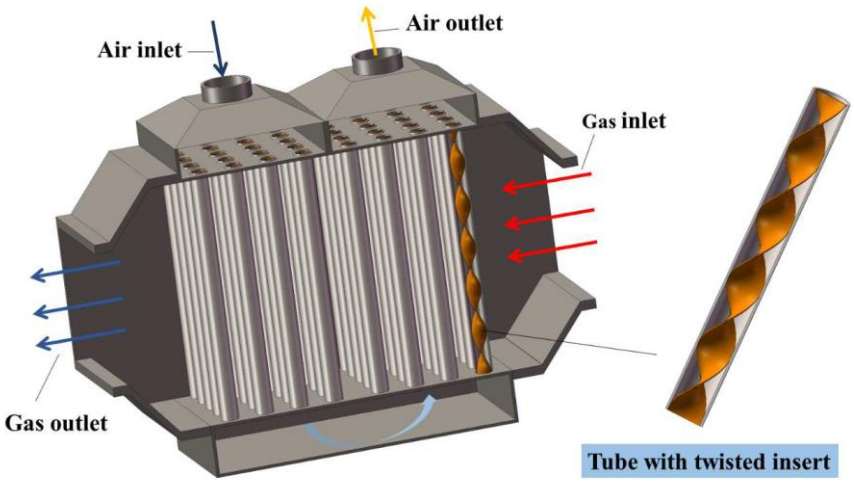

Figure 14-High Temperature Heat Exchanger (HTHE) and heat recovery system [23]

2.6.7. Heat Pipe Heat Exchangers (HPHEs)

Heat Pipe Heat Exchanger (HPHE) technology is emerging as one of the most efficient passive systems for waste heat recovery in industrial processes, especially in energy-intensive industries such as foundries, steel, and ceramics[25]. The general thermal efficiency of HPHE is around 50% [26].

The **HPHE** is a device that utilizes the two-phase heat transfer process, which is particularly effective in transferring waste heat from one location to another. A typical HPHE as shown in the figure 12 consists of a sealed container, often incorporating a wick structure, and a working fluid (such as water, acetone, or ammonia). When heat is applied to one end of the heat pipe (the evaporator), the working fluid boils, vaporizes, and travels to the other end (the condenser), where it releases the absorbed heat. The condensate then flows back to the evaporator through capillary action in the wick or by gravity in wickless heat pipes (thermosyphons)[25].

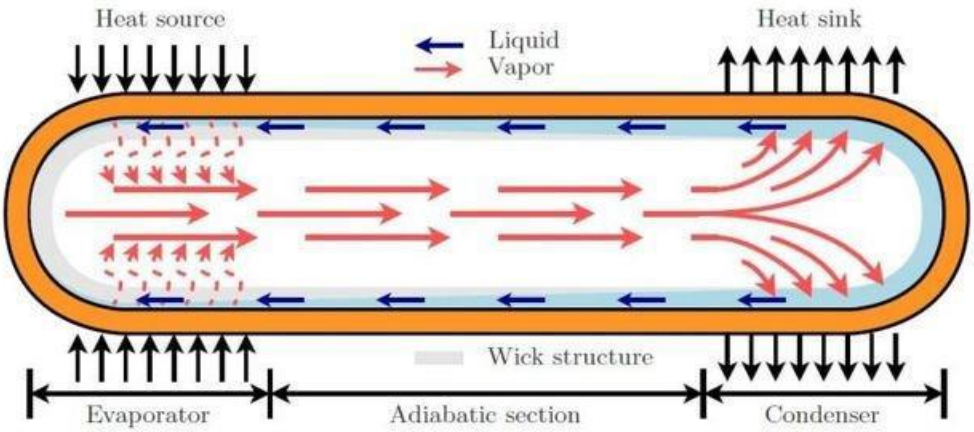

Figure 15-Schematic of a Heat Pipe [24]

They are advantageous due to their maintenance-free nature and ability to handle high temperatures and corrosive environments, with a payback period of less than three years[25]. A study of a flat heat pipe in a steel plant as shown in figure 13 has shown a heat recovery rate of 17kW[25].

Figure 16-Heat Pipe Heat Exchanger Used in the Steel Industry

Despite its promising performance, the technology has certain limitations. One key challenge is the scaling of HPHE systems; although HPHEs can be upsized to recover more heat, there is a diminishing return on investment as the system size increases. Beyond a certain point, any further expansion results in only marginal increases in heat recovery, while the cost of the system escalates significantly[25]. The general

operating temperature of the heat pipe systems is ranging from 293K to 393K and it is largely depending on the type of working fluid[27].

2.6.8. Comparison of Prominent Heat Recovery Technologies

To identify the most suitable WHR solution for the CEB foundry, Table 1 below compares prominent heat exchanger types, focusing on their suitability for aluminum foundry applications.

Table 1:Comparison of Heat Exchanger Types

Feature / Type	S&T (Shell & Tube)	PFHE (Plate-Fin)	HPHE (Heat Pipe)	HTHE (Twisted Fin)	WPHE (Proposed)
Temp. Capability (°C)	Up to 500	150–300	20–120	600+	600+
Pressure Capability	Very High	Moderate	Low	High	Low
Fouling Resistance	Moderate	Low	High	Moderate	Moderate–High
Footprint	Large	Compact	Compact	Medium	Compact
Maintenance	Complex	Difficult	Minimal	Moderate	Accessible
Suitability for Foundries	Fair	Low	Low	Good	High

2.7. Combustion Techniques Used in the Foundry Industry

Crucible furnaces are essential in the foundry industry for melting metals such as aluminum, with oil-fired burners providing the high temperatures needed for efficient melting. In the CEB foundry, waste engine oil is used as the primary fuel, offering

potential cost savings but also challenges in achieving optimal combustion. Efficient combustion relies on proper atomization, breaking fuel into fine droplets for complete burning. This section examines various burner designs and their atomization techniques, exploring their suitability for crucible furnaces. Different burner types, including mechanical, pressure, air atomizing, dual-fuel, and waste oil burners, play a key role in enhancing combustion efficiency, emissions, and operational costs in the foundry industry.

2.7.1. Mechanical Atomizing Burners

Mechanical atomizing burners employ a mechanical mechanism, such as a rotating disk or cup as shown in the figure 14, to atomize the fuel. The finely atomized droplets promote efficient combustion by increasing the surface area of the fuel, allowing for more complete mixing with the air. This type of burner is ideal for burning higher viscosity fuels, such as waste oils or thicker petroleum products. The fuel is generally introduced into the combustion chamber through a rotating component that breaks it up into smaller droplets, promoting better combustion efficiency[28].

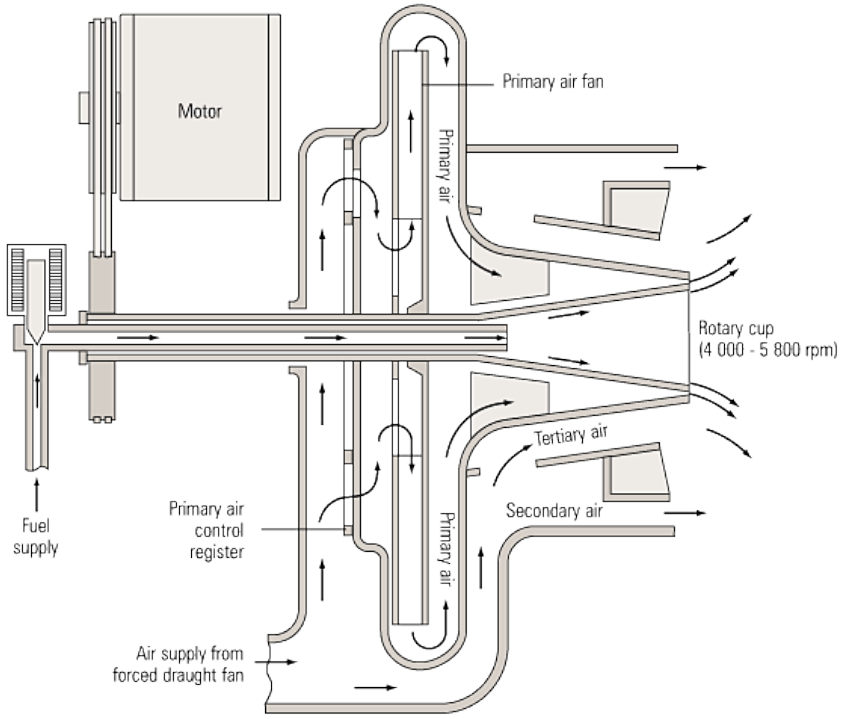

Figure 17-Schematic of a Rotary Cup Burner (courtesy of AATRAL ENGINEERING) [26]

Applications: These burners are commonly used in industrial heating systems and waste oil heaters. Their ability to handle thick fuels makes them suitable for situations where waste oils, including used engine oils and hydraulic fluids, are the primary fuel source[28], [29].

2.7.2. Pressure Atomizing Burners

Pressure atomizing burners use high-pressure pumps to force the liquid fuel through a nozzle, creating fine sprays. These sprays ensure the fuel is mixed thoroughly with the combustion air for more efficient combustion. This type of burner is ideal for lower viscosity fuels such as diesel or kerosene, which atomize more easily under pressure. The figure 15 below shows a schematic diagram, detailing components such as the FB head, nozzle adapter, and electronic ignition transformer.

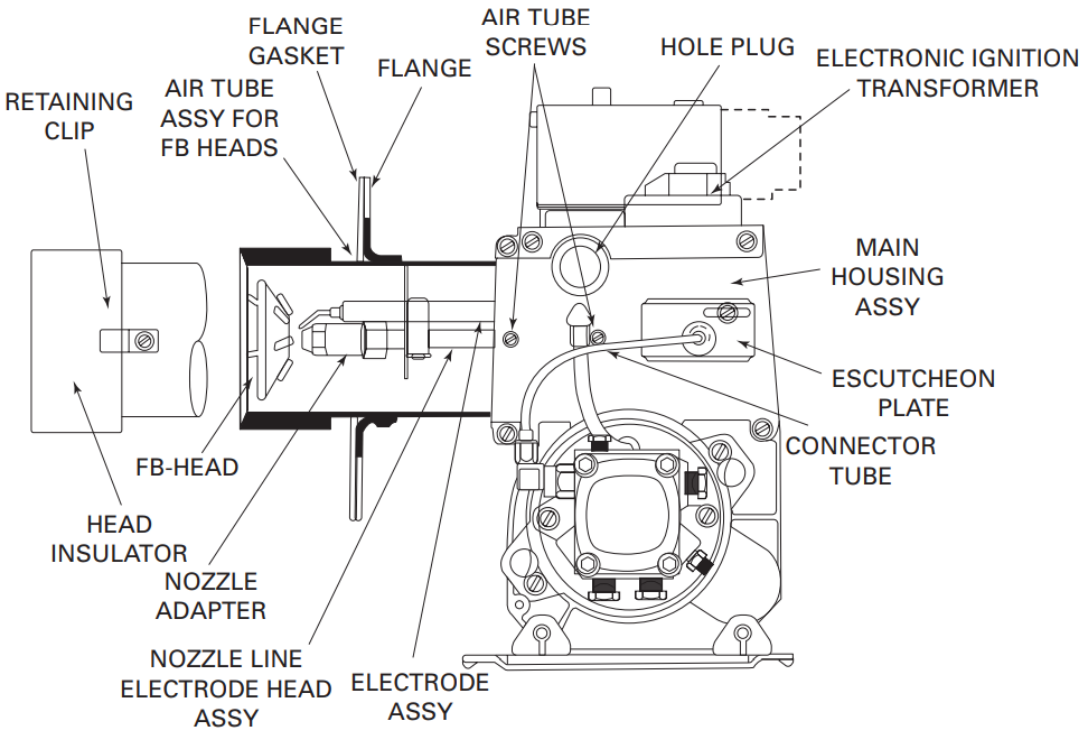

Figure 18-Schematic of a pressure jet burner (Courtesy Lennox Industries Inc.)

Applications: Pressure atomizing burners are widely used in residential and commercial heating systems, particularly for smaller scale applications where fine atomization is crucial to achieve optimal efficiency[29], [30].

2.7.3. Air Atomizing Burners

Air atomizing burners as shown in figure 16 mix fuel with compressed air before combustion, with the velocity of the air helping to atomize the fuel into smaller droplets. This method is particularly effective for burning low viscosity fuels like kerosene and diesel.

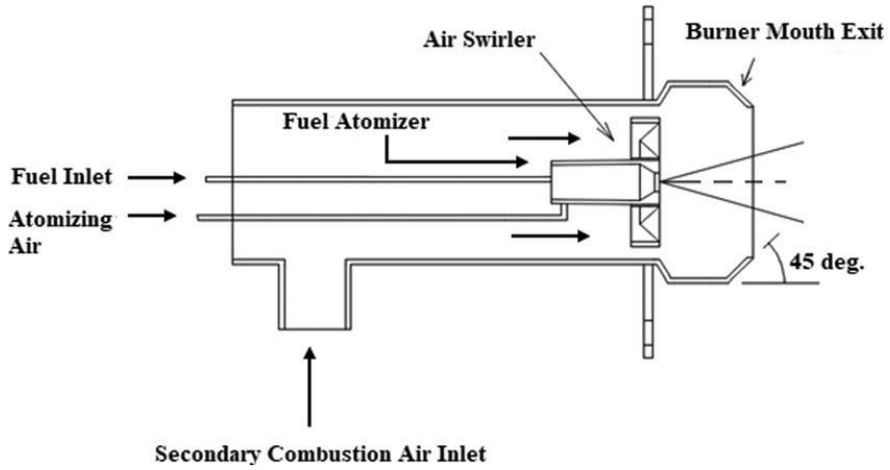

Figure 19-Schematic of an air atomizing burner [29]

Applications: These burners are commonly used in industrial furnaces and boilers where air is readily available. The fine spray created by the air helps improve combustion efficiency and reduces emissions[29], [31].

2.7.4. Dual-Fuel Burners

Dual-fuel burners are designed to operate on two different fuels, such as waste oil and diesel. These burners provide flexibility and are especially useful in environments where fuel supply may vary, or where operational cost optimization is a concern.

Applications: Used in foundries and other industrial settings where fuel availability may change, dual-fuel burners allow operations to continue smoothly regardless of the fuel source, while also ensuring efficient combustion[32], [33].

2.7.5. Waste Oil Burners

Waste oil burners are specifically designed to handle used oils, which often have higher viscosities and contain contaminants. These burners include specialized components, such as preheating systems or filtration units, to handle the higher viscosity and impurities found in waste oils.

Applications: Waste oil burners are frequently used in automotive repair shops, manufacturing facilities, and other industries that generate used oils. They are often integrated into systems designed to recycle waste oil for use in furnaces or heating systems[28], [32].

2.7.6. Considerations for Using Waste Oil or Diesel Fuel

When selecting a burner for either waste oil or diesel fuel, several factors must be considered:

- **Viscosity**: Waste oils generally have higher viscosities than diesel. Specialized burners may be required to preheat the oil or to ensure the fuel is atomized properly for efficient combustion[28].
- **Contaminants**: Waste oils can contain impurities, including water, metals, and other chemicals. Burners used for waste oil typically incorporate filtration or separation systems to prevent contaminants from affecting combustion efficiency.[28], [32]
- **Maintenance**: Waste oil burners require more frequent maintenance, primarily due to soot buildup and the potential for clogging from contaminants[28], [29].

By choosing the appropriate burner and considering these factors, foundries can optimize their fuel consumption, reduce emissions, and maintain efficient operations while managing the challenges posed by different fuel types.

CHAPTER 3: INTRODUCTION TO THE CEB FOUNDRY

3.1. Overview of the CEB Foundry

The Ceylon Electricity Board (CEB) Foundry is a vital component of Sri Lanka's industrial landscape, providing essential casting services to meet the demands of the Ceylon Electricity Board. Located within the Central Workshop & Garage Unit, the foundry ensures the production of high-quality components for various applications. Over the past 35 years, the CEB Foundry has reliably supplied cast aluminum products, serving sectors including power generation, transmission, and distribution.

However, the foundry has not yet adopted modern casting techniques such as die casting and permanent mold casting, which are crucial for producing high-quality components for electrical and mechanical products. Instead, the primary focus of the foundry remains on aluminum casting through sand casting methods, a technique that has been employed for many decades. These methods are well-suited for producing a wide range of components, from small and medium-sized castings to larger, more complex parts for industrial machines and power plants.

3.2. Location of the CEB Foundry

The CEB Foundry is strategically located on a nine-acre plot within the Central Workshop & Garage Unit in Aniyakanda, Kandana, near Colombo. This location offers easy access to raw materials from CEB's distribution division stores and an efficient transportation network. The positioning ensures an ideal environment for the production and distribution of its products, providing direct access to critical materials such as silica sand and other foundry supplies.

Despite the high emissions from the foundry, no complaints have been reported by neighboring residents, largely due to the ample land space available, which allows for the dilution of emissions. However, the foundry faces challenges in attracting skilled labor. Staff transfers to the Central Workshop & Garage Unit have made it difficult to maintain a workforce with the necessary expertise. Currently, the foundry operates with just one skilled worker and a few semi-skilled workers.

3.3. Products Manufactured at the CEB Foundry

The CEB Foundry specializes in the production of a wide range of castings, primarily focusing on aluminum. These products cater to various sectors, including power generation, transmission, and distribution networks. Some key products manufactured include:

- **Aluminum Clamps**: These clamps are critical for electrical infrastructure, particularly for connecting aluminum bare conductors. As shown in Figure 17, the clamps come in various sizes and designs, depending on the application.

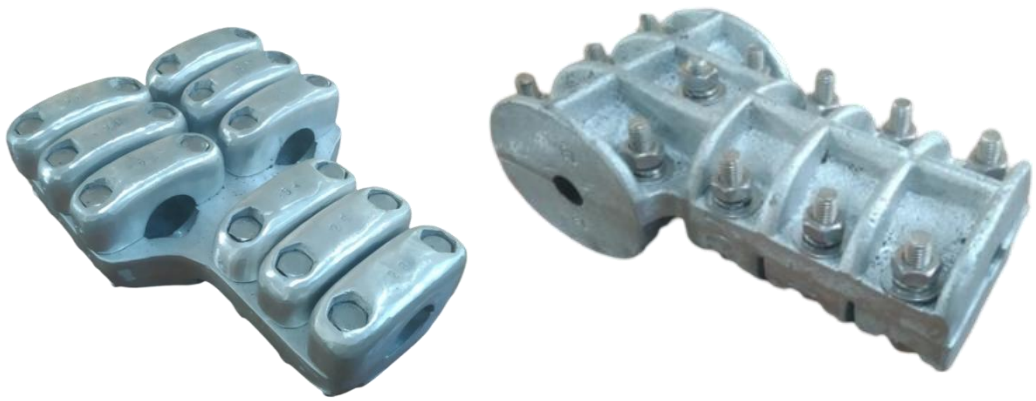

Figure 20-Aluminum clamps manufactured at the CEB foundry

- Bronze Castings for Industrial Machinery: The foundry manufactures parts for pumps, seals, and brackets, which are integral components in industrial machinery. The figure shows a bronze casting of a pump end cover at the Colombo Barge Power station manufactured by the CEB foundry.

Figure 21-A bronze casting pump end cover produced by CEB foundry

- Industrial Castings: The foundry also produces industrial castings such as zinc anodes and aluminum anodes, which play vital roles in various industrial processes. The figure 19 below shows aluminum anodes manufactured for the Colombo Barge Mounted Power Station.

Figure 22-Aluminium anodes each 70kg produced by CEB foundry

3.4. Summary of Production Data

Table 2 below summarizes the yearly production data of the foundry activities. Complete details of this data are available under Appendix 1.

Table 2-Summary of Production Data

Year	Aluminum Raw material Quantity (kg)	Nos. of Items	Estimated Cost of Production
2017	610	122	1,287,920.00
2018	2180	436	2,476,197.00
2019	3300	660	8,602,955.00
2020	1505	301	2,780,648.00
2021	5015	1003	9,224,603.00
2022	3115	623	3,587,100.00
2023	3070	614	6,879,645.00
2024	4250	850	7,134,052.00

The increasing quantity of aluminum processed annually and the diversity of products demonstrates the foundry's importance in Sri Lanka's energy sector and its ability to meet the growing demand for quality castings.

3.5. Casting Methods and Equipment

The CEB Foundry predominantly uses sand casting methods for aluminum components. Sand casting is an ideal method for producing complex shapes and large parts, especially when the requirements for dimensional accuracy and surface finish are not as stringent as those for other casting processes like die casting or investment casting. The key steps involved in the sand-casting process at CEB include:

1. **Pattern Making**: Patterns are created using aluminum or wood, depending on the complexity and size of the casting. These patterns are designed to be easily removable from the mold without damaging the final casting.
2. **Molding**: The molds are made from a mixture of silica sand, bentonite clay, and water. The sand mold is formed by packing the sand around the pattern as shown in the figure 20, and the mold cavity is shaped according to the design specifications.

Figure 23-Sand cast mould ready for pouring

3. **Melting and Pouring**: Aluminum scrap or ingots are melted in a furnace, and the molten metal is poured into the prepared sand molds. The pit furnace used in the foundry is ignited manually as shown in Figure 21. The flame travel around the periphery is important for equal heating of the crucible. The figure 22 shows the flame travel inside the furnace. However, due to the improper construction of the pit furnace as shown in Figure 23, most of the heat escapes to the surroundings, creating an uncomfortable working environment.

Measuring Aluminum: Aluminum is measured using a scale as shown in Figure 24 and loaded into the furnace as shown in Figure 25.

Furnace Covering: The furnace is covered with a metal plate as shown in Figure 26 but much of the heat still escapes, making the work environment highly uncomfortable.

Figure 24-Starting the ignition using a burning piece of cloth

Figure 25-Flame spreading inside the furnace

Figure 26-Improper construction of the pit furnace

Figure 27-Measuring aluminum

Figure 28-Loading aluminum into the crucible

Figure 29-Furnace covered by a lid

4. **Cooling and Finishing**: After the mold has been filled, the metal is allowed to cool and solidify. Once cooled, the mold is broken open, and the casting is removed as shown in figure 27. Finishing processes such as cleaning, machining, and inspection are performed to meet the final product specifications.

Figure 30-Pouring, Cooling and knocked out castings

Currently, the CEB Foundry has not yet upgraded its equipment with modern technologies such as induction furnaces, shot blasting machines, and sand mixing machines, which are crucial for improving productivity and product quality. The foundry continues to rely on traditional sand-casting methods, and the equipment used is not regularly maintained or upgraded to improve the overall efficiency of the casting process.

The foundry's reliance on manual labor is another limiting factor. The tilted furnace as shown in Figure 28 is rarely used due to difficulties in removing molten metal. Additionally, working on the elevated platform near the furnace is challenging due to the heat that escapes from the top of the furnace, further complicating operations.

Figure 31: Tilting furnace covered with various materials due to non-use

3.6. Initial Foundry Layout

The existing atmosphere inside the foundry is no longer suitable for research and development activities due to an improper layout and significant heat leakage. It is evident that thermal efficiency could be greatly improved simply by controlling the heat that escapes from the furnace without being utilized. An initial thermal efficiency test on the pit furnace revealed that its performance was well below the accepted standards. This highlighted the urgent need to modify both the foundry building and the equipment layout.

The initial layout of the CEB Foundry was designed without sufficient consideration for maximizing available space or optimizing the flow of materials throughout the production process. Both the tilting furnace and the pit furnace were constructed in the middle of the building, leaving little space for other activities. As product demand grew, it became clear that the original layout was inefficient. Key issues included inadequate storage for raw materials, production line bottlenecks, and poor material flow management.

3.7. Foundry Layout After Modifications

The layout was urgently redesigned to address key challenges such as material handling, space utilization, and worker ergonomics as shown in the figure 29.

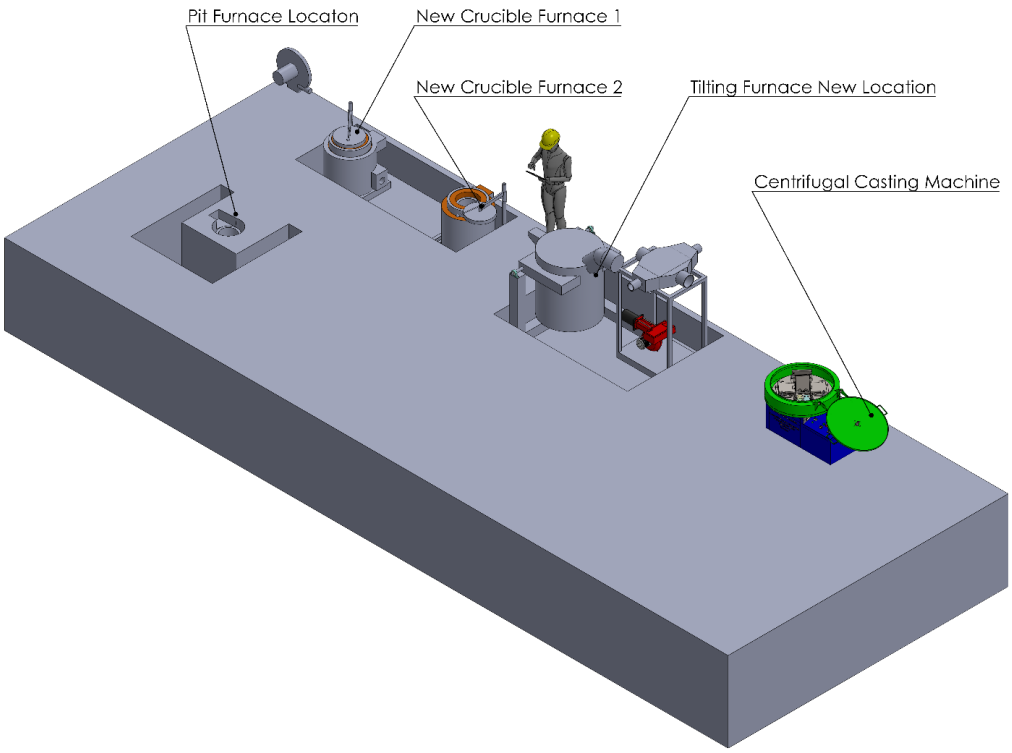

Figure 32-Foundry layout modification

The final layout included the following improvements:

1. Relocation of the Tilting Furnace: The tilting furnace was originally located on the ground at the center of the building. To improve ergonomics, the furnace was relocated near the wall and lowered by constructing a pit. This new position also facilitates the construction of the exhaust gas duct, optimizing the overall layout.

2. Relocation of the Pit Furnace: The pit furnace was no longer viable for further development due to its poor construction. As a result, it was decommissioned. A new pit, adjacent to the wall, was constructed to house two crucible furnaces. The new crucibles are currently under construction. This relocation not only enhances operational efficiency but also supports the installation of exhaust gas ducts and the development of a heat recovery system integrating all three furnaces.

These layout modifications have significantly improved the efficiency of the foundry and increasing overall productivity. The figure 30 below shows the foundry inside after the modifications.

Figure 33: Foundry Layout after the Modifications

The improvements made to the CEB Foundry's layout and equipment have been crucial in addressing the operational challenges that previously hindered its efficiency. The original layout, which was not designed with optimal space utilization or material flow in mind, led to various inefficiencies, such as insufficient storage for raw materials, production line bottlenecks, and poor ergonomics. These issues were particularly evident with the improper placement of both the tilting furnace and pit furnace, which created unnecessary constraints in the foundry's operations.

The redesign of the foundry layout addressed these challenges by relocating the furnaces, improving the ergonomics of worker operations, and optimizing the flow of materials. The tilting furnace was relocated and lowered to a more efficient position, and the pit furnace was decommissioned and replaced with two new crucible furnaces.

These changes not only increased the operational efficiency but also provided the necessary space for the installation of exhaust gas ducts and a heat recovery system, which will contribute to significant improvements in thermal efficiency.

While the CEB Foundry continues to rely on traditional sand-casting methods, these layout modifications have provided a foundation for future upgrades. As the foundry continues to meet the growing demands of Sri Lanka's energy sector, further technological upgrades, such as the introduction of induction furnaces and automated equipment, will likely drive even greater improvements in productivity, product quality, and energy efficiency.

CHAPTER 4: PERFORMANCE EVALUATION AND METHODOLOGY FOR COMBUSTION AIR PREHEATING AND ENERGY OPTIMIZATION

4.1. Introduction

This chapter evaluates the performance of existing furnaces at the CEB Foundry, including pit and tilting furnaces, and explores methods to improve energy efficiency. Key strategies involve optimizing furnace operations, enhancing combustion systems, and implementing heat recovery methods such as preheating combustion air with a heat exchanger. The focus is on reducing inefficiencies, improving energy utilization, and minimizing emissions

4.2. Efficiency Analysis of Existing Furnaces

4.2.1. Pit Furnace Efficiency Analysis

The pit furnace at the CEB Foundry exhibits significant heat losses due to its poor design and construction. A thermal efficiency test was conducted to assess the performance, measuring variables such as fuel consumption, heat input, and heat utilized for melting aluminum. The following observations were made:

- Heat Input: The total heat supplied by the furnace was calculated based on the calorific value of the fuel.
- Heat Utilized: The energy absorbed by the molten aluminum was determined using the specific heat capacity and the melting temperature range.
- Heat Losses: Significant heat was found to escape through the furnace walls and exhaust gases.

The Table 3 below shows the summary of operational data for the pit furnace test.

Item produced - casting of 12 bolt type aluminum clamps

Charge - 24kg of aluminum, 1.2kg of Zinc

Fuel- Waste oil (used engine oil)

Date: 09.09.2024 Time: 9 a.m.

- Table 3: Operational Data Summary for Pit Furnace Aluminum Casting Test

Date	Furnace Started at	Furnace Stopped at	time hr	time (min)	Weight of Charge	Volume of Fuel (liters)	Specific Fuel Consumption (*l/kg*)
2024.09.09	09:05 AM	10:30 AM	1:55	115	25.2kg	18	0.714
2024.09.09	10:37 AM	11:00 AM	0:23	23	10.0kg	6	0.600

- Fuel consumption for the first cycle of melting 24 kg of aluminum was 18 liters of waste lube oil.
- Fuel flow rate = 0.00168 kg/s
- Fuel consumption for the second cycle of melting 10 kg aluminum was 6 liters of waste lube oil.
- A total of 2.24 kg of slag was removed from the molds.
- The temperature of molten aluminum was raised up to 720 ºC. Afte reaching this temperature, burner was stopped.

$The\ density\ of\ the\ used\ lube\ oil,\quad \boldsymbol{\rho_{oil}} = 0.870\ kg\ /L$

A waste oil sample was tested at the Industrial Technology Institute-Colombo for the testing of calorific value. The report is attached as Appendix 2.

$Gross\ Calorific\ value\ of\ lube\ oil,\ \ GCV = 42.92\text{MJ/kg}$

$\underline{Average\ specific\ oil\ consumption\ = 0.681\ l/kg\ of\ aluminum}$

$Average\ energy\ consumption$

$$= 0.681 \frac{l\ oil}{kg\ of\ aluminum}\ x\ 42.92 \frac{MJ}{kg\ of\ oil}\ \text{x}\ 0.87 \frac{\text{kg oil}}{l\ oil}$$

$\underline{= 25.42\ MJ/kg}$

$Specific\ heat\ capacity\ of\ aluminum\ at\ 300K\ [34], Cp = 0.902\ kJ/kg.K$

$Specific\ enthalpy\ of\ aluminum\ at\ room\ temperature, h_{Al@300K} = C_p.T$
$= 270\ kJ/kg$

$Specific\ enthalpy\ of\ aluminum\ at\ 720^oC\ temperature\ [35], h_{Al@1000K} = 1075\ kJ/kg$

$Weight\ of\ aluminum, \quad m_{Al} = 25.2kg$

$Energy\ required\ for\ melting\ and\ to\ raise\ the\ temperature\ upto\ 720\ C$

$E = m_{Al}.(h_{Al@1000K} - h_{Al@300K})$

$= 25.2\ x\ (1075 - 270)kJ$

$= 20{,}286kJ$

$Required\ mass\ of\ fuel = \frac{20{,}286kJ}{42{,}920\ kJ/kg} = 0.472kg$

$Required\ volume\ of\ waste\ oil = \frac{0.472}{870} x1000\ l = 0.542\ l$

$Actual\ volume\ of\ waste\ oil\ consumed = 24\ l$

$Efficiency\ of\ the\ furnace = \frac{0.542\ l}{24} = 2.2\ \%$

The amount of energy consumed for melting one tonne of metal is in the range of 600 kWh/tonne to 680 kWh/tonne as per the available literature[36]. If this value was taken as baseline value, the efficiency if metal melting furnaces are in the range,

680kWh/tonne = 2.448MJ/kg

$The\ efficiency\ of\ a\ general\ industrial\ furnace = \frac{Energy\ consumed}{Energy\ Input}$

$= \frac{2.448}{42.92} = 5.9\%.$

The efficiency of pit furnaces has been recorded in the range of 4% to 19%, with some literature indicating efficiencies as high as 13% under optimized conditions[13]. However, the analysis of the pit furnace at the CEB Foundry reveals an efficiency of only 2.2%, which is significantly below even the lowest reported values. When compared to baseline energy consumption values for metal melting furnaces, which typically achieve efficiencies of 5.9%, the CEB Foundry's pit furnace is clearly operating at a highly inefficient level.

This inefficiency is attributed to several factors, including excessive heat losses, improper combustion practices, and outdated furnace design. The high fuel consumption and poor energy utilization underscore the need for immediate intervention to improve the furnace's thermal performance. Optimizing the combustion process, reducing heat losses, and integrating modern heat recovery technologies such as combustion air preheating systems are critical steps toward enhancing furnace efficiency. Without such measures, the continued operation of the pit furnace will result in excessive fuel consumption, increased operational costs, and environmental impacts. Addressing these inefficiencies is crucial to achieving sustainable and cost-effective foundry operations.

4.2.2. Tilting Furnace Efficiency Analysis

The tilting furnace's efficiency was similarly analyzed. While it exhibited a better insulation compared to the pit furnace, inefficiencies were observed in its heat transfer mechanism and fuel utilization. Key findings include:

- Non-uniform Heat Distribution: Due to the burner's placement, heat distribution within the furnace was not efficient. The figure 30 below show the desired location for the flame entry into the furnace and the current location of the flame entry of the tilted furnace due to improper construction.

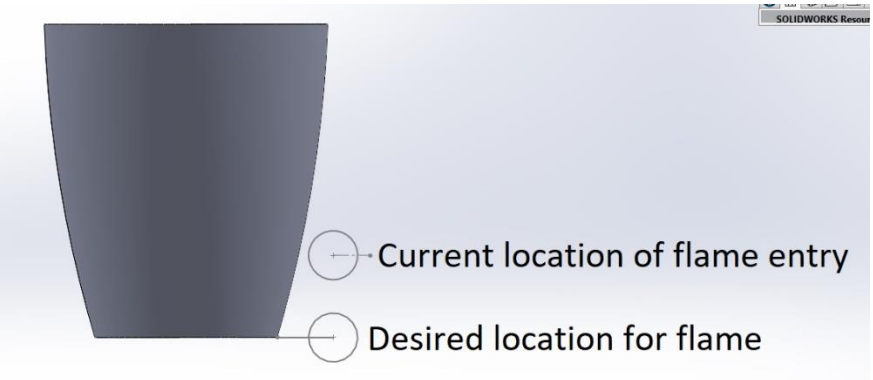

Figure 34-Desired position for the burner flame entry into the furnace

- Heat Losses: Substantial losses occurred through top area of the furnace due to unavailability of insulation and unavailability of a lid.

As the flame characteristics adjustment required extensive modification, only the fabrication and installation of a lid was completed before starting the tests.

The Table 4 below shows the summary of operational data for the tilted furnace test.

Metal Charge: Aluminum

Fuel: Used Engine Oil

Item Produced: Aluminum Anodes

Client: Colombo Barge Power Station

Table 4: Operational Data Summary for Tilting Furnace Aluminum Casting Tests

Date	Furnace Started at	Furnace Stopped at	time hr	time (min)	Weight of Charge	Volume of Fuel (liters)	Specific Fuel Consumption (l/kg)
2024.11.08	8:45 AM	10:50 AM	2:05	125	83	21.5	0.259
2024.11.11	1:30 PM	4:00 PM	2:30	150	83	24.4	0.294
2024.11.19	8:45 AM	11:10 AM	2:25	145	83	23.5	0.283
2024.11.20	8:40 AM	11:20 AM	2:40	160	83	26.4	0.318
2024.11.21	8:40 AM	11:15 AM	2:35	155	83	26.0	0.313
2024.11.27	1:30 PM	4:05 PM	2:35	155	83	24.8	0.298
2024.11.28	1:20 PM	3:30 PM	2:10	130	83	22.5	0.271
2024.11.29	1:45 PM	3:55 PM	2:10	130	83	23.1	0.278

$Average\ fuel\ consumption\ per\ one\ cycle\ of\ operation\ =\ 24.4\ l$

$Average\ specific\ fuel\ consumption\ =\ 0.294\ l/kg$

$Specific\ heat\ capacity\ of\ aluminum\ at\ 300K\ [34], Cp =\ 0.902\ kJ/kg.K$

$Specific\ enthalpy\ of\ aluminum\ at\ room\ temperature, h_{Al@300K} = C_p.T = 270\ kJ/K$

$Specific\ enthalpy\ of\ aluminum\ at\ 720oC\ temperature\ [35], h_{Al@1000K} = 1075\ kJ/kg$

$Weight\ of\ aluminum\ =\ 80kg$

$Energy\ input\ required\ to\ raise\ the\ temperature\ to\ 720\ C,$

$$E = m.(h_{Al@1000K} - h_{Al@300K}) =\ 80\ x\ (1075 - 270)kJ$$

$=\ 64{,}400kJ$

$GCV_{oil}\ =\ 42{,}920\ kJ/kg$

$$Required\ mass\ of\ waste\ oil\ =\ \frac{64{,}400kJ}{42{,}920\ kJ/kg} = 1.56kg$$

$\boldsymbol{\rho}_{oil} =\ 870\ kg/m^3$

$$Required\ amount\ of\ waste\ oil\ = \frac{1.56}{870} x1000\ l = 1.79\ l$$

$$Efficiency\ of\ the\ furnace, \quad \boldsymbol{\eta} = \frac{1.79\ l}{24.4} = 7.3\ \%$$

Results: The tilting furnace showed an efficiency of approximately 7.3%, underscoring the need for better heat management techniques.

4.3. Review of Combustion System Designs

4.3.1. Combustion Principles and Their Applications

As the CEB foundry exclusively utilizes crucible furnaces, the analysis of the combustion system design is specifically focused on this type of furnace.

4.3.1.1. Crucible Shape and Size

Crucible geometry and design are critical to the efficiency of combustion and temperature distribution in crucible furnaces. These factors directly influence the melting performance, fuel consumption, and operational safety of the furnace.

- Cylindrical Geometry: Cylindrical crucibles are commonly preferred due to their ability to promote even heat distribution around the molten material. The circular shape ensures uniform flame interaction and minimizes hot and cold spot[16], [37].
- Conical Bottoms: Crucible designs as shown in the figure 31 improve heat distribution and reduce the likelihood of unmelted residues at the bottom.

Figure 35-Rounded and Conical bottom crucibles

- Furnace to Crucible Diameter Ratio: The furnace height should account for optimal airflow and space for the crucible and combustion chamber, ensuring efficient heat transfer. For example, maintaining a gap of 1–2 inches between the crucible lip and furnace lid helps in better temperature control [9], [37]

- Material: Graphite and silicon carbide crucibles, while costly, offer durability and consistent thermal performance under repeated heating cycles[37], [38].

4.3.1.2. Airflow and Combustion Dynamics

- Tangential Airflow: Burner ports are positioned tangentially at the furnace base direct flames around the crucible, promoting uniform heating. This design prevents direct impingement of the flame on the crucible, reducing localized stress and prolonging crucible life[9], [37]. The figure 32 shows the air flow pattern around the crucible.

- Air-to-Fuel Ratio: An optimal air-to-fuel ratio (e.g., 400:1 as seen in several designs) ensures complete combustion and minimizes unburnt fuel, enhancing temperature uniformity and furnace efficiency[9], [16].

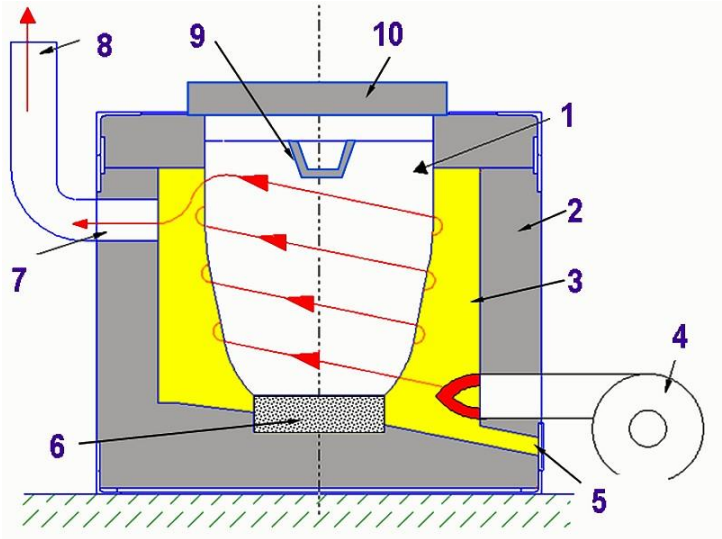

Figure 36-Fig. 1: Schematic diagram of a fuel-fired and tiltable crucible furnace. 1) Crucible, 2) Furnace lining (permanent lining), 3) Firing compartment, 4) Gas or oil burner, 5) Emergency tap (leading towards the emergency accumulation pit), 6) Refractory base, 7) Exhaust port, 8) Stack

- Material Choice: The use of refractory materials like silica, alumina, or mullite aids in heat retention and prevents heat losses. A thick refractory lining enhances thermal insulation but must not overly restrict the internal furnace volume[16], [38].
- Radial Flame Gap: Maintaining a radial gap between the crucible and refractory lining allows for effective combustion and heat circulation[16].

4.3.1.3. Chimney and Ventilation Design

- Proper venting through chimneys ensures that combustion gases are efficiently expelled, preventing back pressure and maintaining a steady flame.

These factors collectively influence the thermal efficiency, safety, and operational lifespan of crucible furnaces.

4.4. Modelling of Crucible Furnace and Study of Combustion Mechanism Using Ansys Fluent

The combustion pattern of the crucible furnace was studied using ANSYS Fluent, providing critical insights into the dynamics of the combustion processes within the furnace. The primary objective was to study how flame distribution, burner placement, temperature distribution and heat transfer within the furnace.

Combustion chamber geometry was designed using SolidWorks software, featuring a crucible with dimensions of 410 mm in height and 330 mm in diameter which is the size of the crucible used for the pit furnace at CEB foundry. This design was subsequently imported into ANSYS Fluent for combustion and flow analysis.

4.4.1. Simulation Simplifications Applied

Given the computational constraints and complexity of a real foundry furnace, the following simplifications were applied to reduce model size while retaining essential physical behavior:

- **Geometry Simplification**: Only the internal **air cavity** surrounding the crucible was modeled. External components like the outer steel shell and detailed refractory lining structure were excluded, assuming minimal impact on steady-state combustion behavior.
- **Material Merging**: The crucible base and lid, both made of refractory materials, were combined into a single domain to simplify meshing.
- **Neglecting Minor Heat Losses:** Small radiative and convective heat losses through minor gaps and seams were neglected.

4.4.2. Computational Model Setup

The simulation relied on the following physical and numerical models:

- **Solver Type**: Pressure-based solver.
- **Time** : Steady state
- **Flow Regime**: Turbulent, with the **standard k-ε model** selected for its stability and reliability in high-temperature combustion systems.
- **Combustion Modeling**: The **species transport model** was enabled to simulate chemical reactions and energy release during fuel-air combustion. Volumetric reactions and eddy dissipation turbulence chemistry interaction sub options were selected.
- **Energy Equation**: Activated to capture heat transfer throughout the domain.
- **Gravity**: Included to reflect buoyancy effects from hot gas flows.
- **Fluid**: Lubrication oil is not available in the materials database in the Ansys Fluent. However, the calorific value of diesel is approximately equal to waste lube oil. Therefore, the air body material was selected as a diesel air mixture.

4.4.3. Boundary Conditions and Inputs

The following boundary conditions were applied:

Boundary	Condition
Air inlet	Air inlet mass flow rate is 0.0505kg/s. The temperature of the stream is 35ºC. Species mass fraction is 0.23 for Oxygen. The air inlet pressure after the blower is 600Pa.
Fuel Inlet	Fuel inlet mass flow rate is 0.00296kg/s at 80ºC and 15bar pressure. The diesel mass fraction ($C_{10}H_{22}$) is 1.
Exhaust Outlet	Pressure outlet at atmospheric pressure. The backflow temperature is 600ºC. Carbon dioxide mass fraction is 0.192 and Oxygen mass fraction is 0.04 at the outlet.
Air body outside wall material and boundary conditions	Engineering brick from the list of materials were selected as the approximate material and, the thermal conductivity was adjusted to 0.05W/mK to meet the thermal conductivity of fire bricks. Thermal boundary condition for the wall: Convection heat transfer coefficient=10W/m^2.K, Free stream temperature = 35ºC, external emissivity = 0.8, External radiation temperature = 35ºC, Wall thickness = 150mm,
Air body inside wall material and boundary conditions	The inside of the air body is in contact with the crucible. The inside wall material was selected as graphite to represent the close approximation of crucible material. Thermal boundary condition for the wall: Convection heat transfer coefficient=30W/m^2.K, Free stream temperature = 308K, external emissivity = 0.9, External radiation temperature = 35ºC, Wall thickness = 30mm,

4.4.4. Mesh and Geometry

The crucible furnace geometry was created in SolidWorks and imported into ANSYS Fluent. Default mesh size was reduced p to 12mm and achieved the required level of mesh quality. The final mesh had ~0.4 million cells. Mesh quality was assessed using the Aspect Ratio Metrix, Skewness Matrix and Orthogonal Quality Matrix. Figure 33 below shows the mesh generated by the Ansys Fluent Mesh Generator.

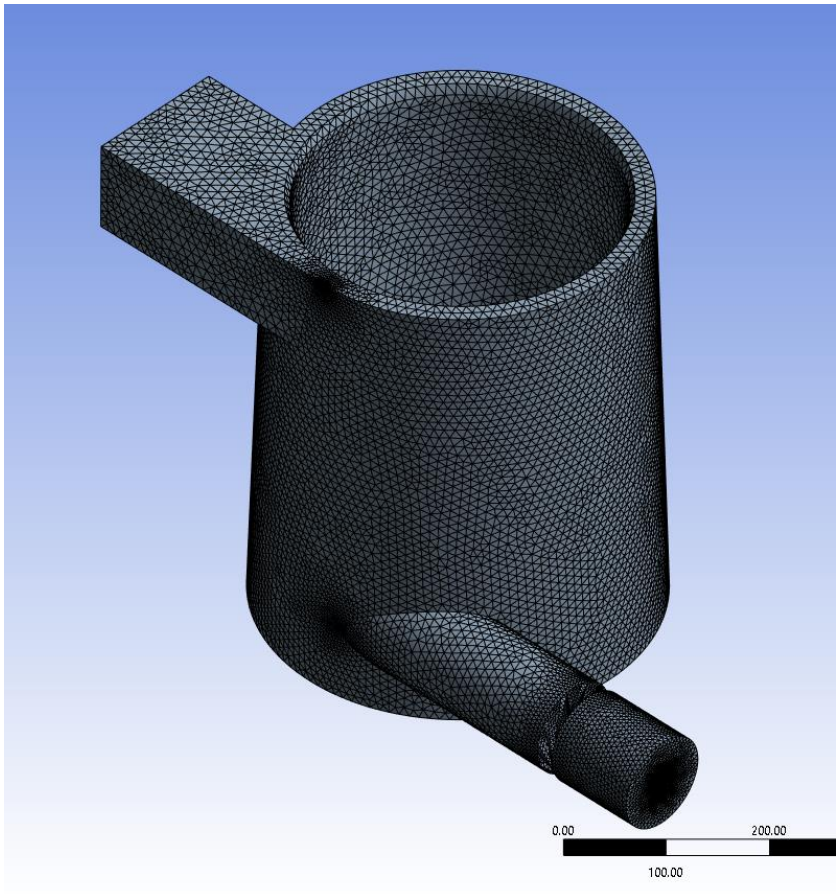

Figure 37: Air body geometry with mesh

4.4.5. Solution and Solution Controls

The simulation employed the Coupled pressure-velocity coupling scheme, which provides robust and efficient convergence for compressible and reacting flows. Initially, first-order upwind discretization was applied to the momentum, turbulent kinetic energy, and turbulent dissipation rate equations to ensure numerical stability during early iterations. After approximately 100 iterations, the solution was switched to second-order upwind schemes to enhance solution accuracy. Under solution controls, the pseudo-transient time scale factor was adjusted from 0.1 to 1 during the iteration process, which helped stabilize the solution. Relaxation factors for turbulent kinetic energy and turbulent dissipation rate were initially set to 0.4 and finally to default values, contributing to smoother residual convergence. The number of iterations was progressively increased from 50 to 500 in stages, allowing controlled convergence monitoring and ensuring numerical stability throughout the simulation process.

4.4.6. Key Findings from the Simulation

The simulation provided valuable insights into combustion dynamics.. Figure 33 illustrates the temperature distribution from the burner to the exhaust pipe. Notably, the results indicated that when the flame speed was not adequately maintained by the burner and the furnace geometry, combustion products tended to bypass the crucible, leading to uneven heating and reduced thermal efficiency. The figure 34 illustrates the velocity streamlines diagram which shows more clearly the flow behaviour inside the furnace air body. According to this diagram, most of the velocity streamline which are starting from the burner air and fuel inlet, flows towards the gas exit without travel around the crucible. Accordingly, the temperature distribution on the crucible surface as shown in the figure 35 is uneven and thermal performance of the furnace is affected.

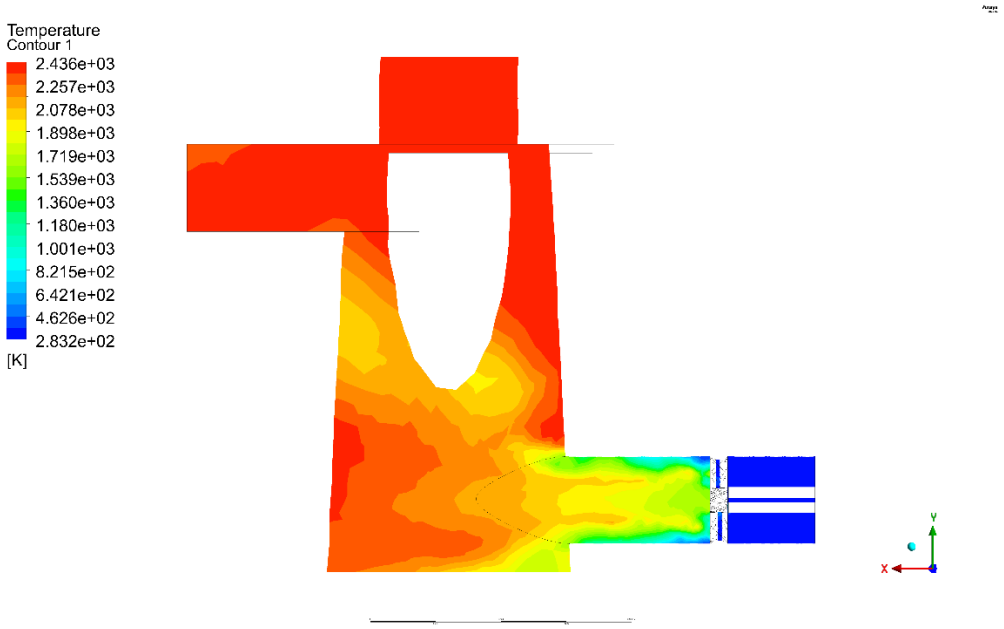

Figure 38-Temperature contour across the X-Y plane of the burner.

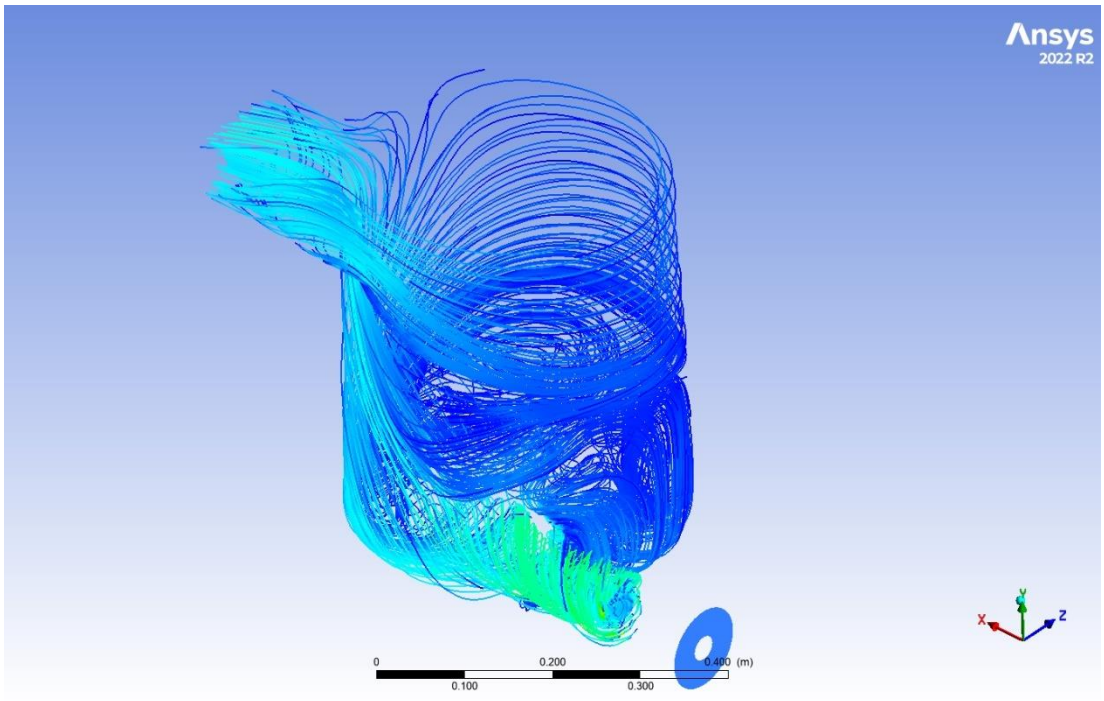

Figure 39-Velocity streamlines from burner inlet to furnace exhaust within the air body

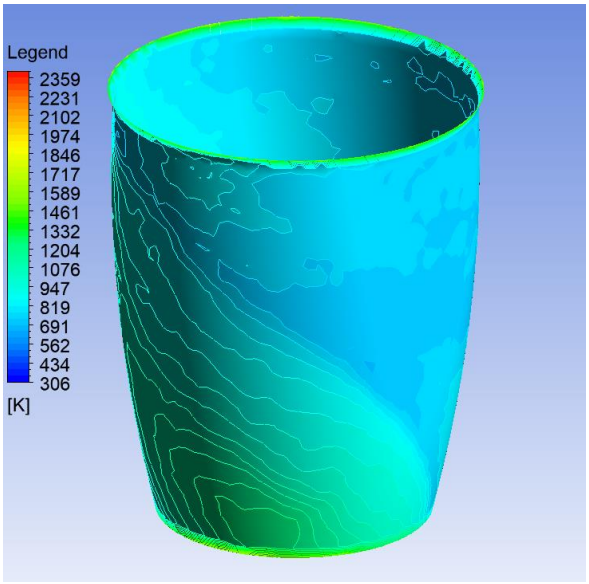

Figure 40: Surface Temperature Distribution Contour Diagram for Crucible Surface

Another study was conducted with reduced burner head diameter for the purpose of increasing the air flow velocity. In Figure 34, it is evident that when the burner is positioned horizontally, the combustion flame interacts with the airflow in a manner that causes it to recirculate within the furnace. This interaction leads to uneven flow patterns around the crucible. The flame trajectory fails to distribute heat uniformly, as the airflow is redirected backward rather than rising consistently around the furnace. This uneven heat distribution impacts the overall efficiency and thermal uniformity of the crucible heating process, highlighting the need for optimizing burner placement and flame direction.

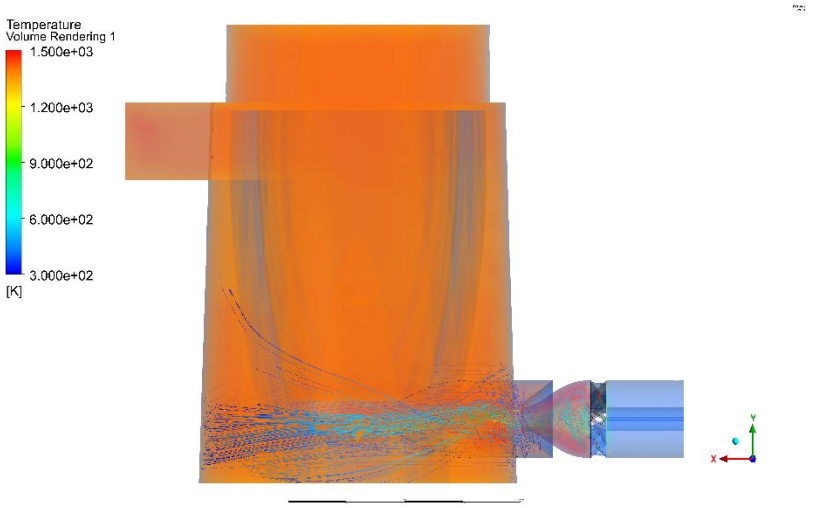

Figure 41-Velocity streamline of the flow inside the air body of crucible furnace in a burner designed for high air velocity

Another study on the effects of burner angle on temperature distribution was attempted using ANSYS simulation, as shown in Figure 35. This study utilized combustion modeling and particle tracking for the furnace geometry optimized for the silicon carbide crucible. The results, depicted in the figure below, illustrate that the flow pattern travels around the furnace and ascends, achieving a more uniform temperature distribution around the crucible. This uniformity is a result of positioning the burner at a five-degree angle relative to the horizontal axis, which enhances the interaction of the flame with the surrounding airflow, ensuring effective temperature distribution within the furnace.

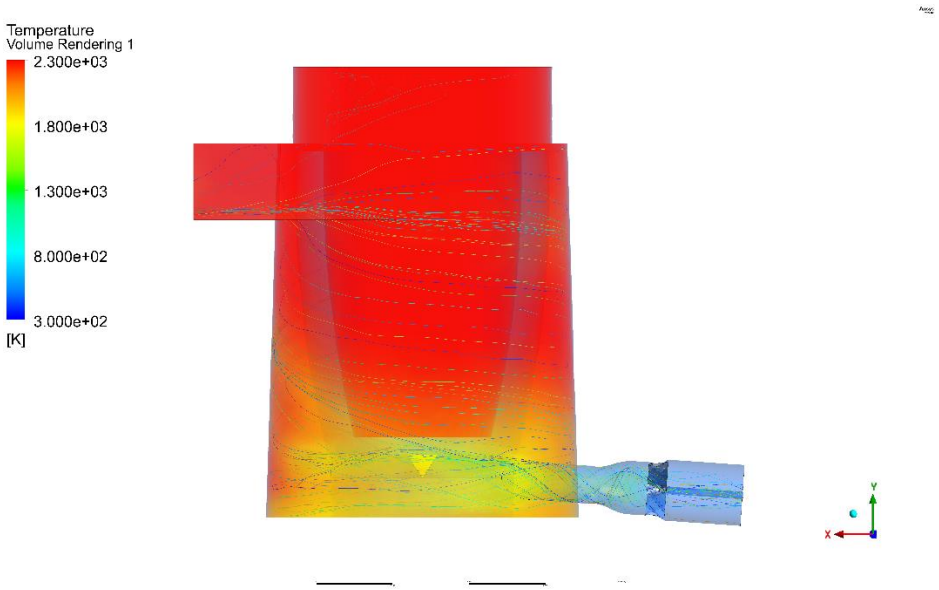

Figure 42-Study of the effects of burner angle for temperature distribution

Physical Path for Combustion Air Around the Crucible Furnace

The simulation figure 36 illustrates an attempt of a study for enhancing the thermal efficiency of crucible furnaces by designing a structured physical path for combustion air to circulate around the furnace. This approach focuses on guiding the combustion air in a controlled helical or spiral trajectory, maximizing the interaction between the hot air and the crucible surface. This concept can be used for a future research direction. Physical prototypes of the helical path design should be built and tested to validate the simulation results. Investigate high-temperature resistant materials for constructing the airflow path may be required.

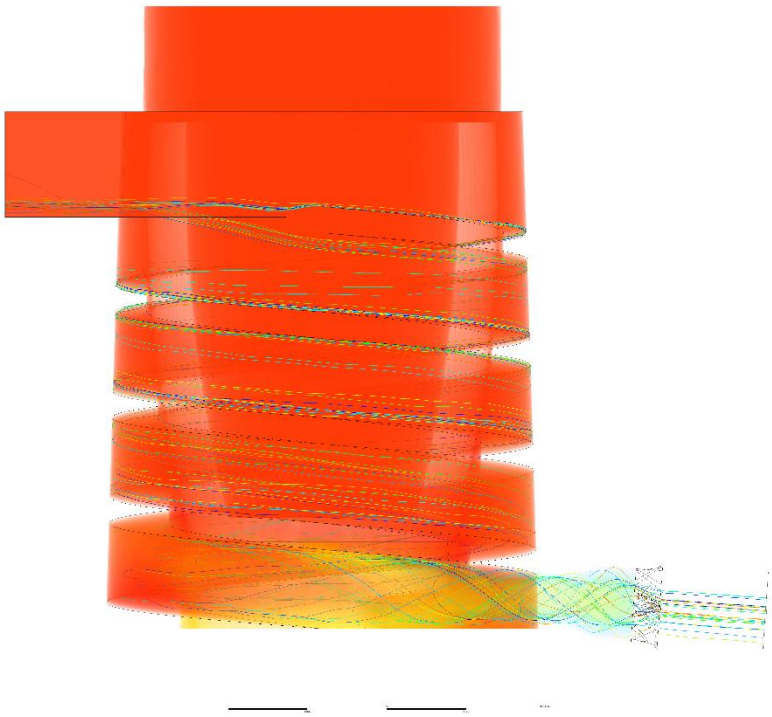

Figure 43-Designated path for flame travel around the crucible

The simulation revealed key operational factors influencing combustion performance:

- **Burner Position and Angle**: Adjustments to the burner angle significantly impacted flame propagation and temperature distribution around the crucible.
- **Flame Stability**: Maintaining an optimal flame speed ensured that heat was effectively transferred to the crucible, preventing bypass effects.
- **Heat Distribution**: Tangential airflow design improved the uniformity of heat around the crucible, minimizing localized hotspots or cold zones.

These findings emphasize the importance of precise furnace geometry, burner configuration and airflow control in optimizing furnace performance. The simulation results serve as a foundation for refining furnace designs and integrating advanced heat recovery techniques to enhance energy efficiency.

4.5. Development of the Combustion Air Preheating Methodology

4.5.1. Rationale for Combustion Air Preheating

In this study of improving the efficiency of crucible furnaces, several techniques were initially explored, including modifications to the combustion chamber and adjustments to flow patterns. While these methods provided some incremental enhancements, the overall impact on furnace efficiency will remain minimal, with recorded efficiency levels around 4% to 19% for crucible furnaces. Such low efficiency levels highlight the significant energy losses inherent in traditional crucible furnace designs, rendering these minor optimizations insufficient to achieve meaningful energy savings or operational improvements at the initial stage and will be beneficial for the continuous improvements. A significant portion of the energy supplied to the furnace is lost through exhaust gases, making energy recovery the primary opportunity for improving efficiency.

4.5.2. Proposed Methodology

The tilted furnace was taken for the study. The proposed methodology involves the following steps:

1. Baseline Assessment on current heat losses

   Data:

   Fuel flowrate - $\dot{m}_{fuel} = 0.00296$ kg/s

   $GCV_{oil} = 42{,}920\ kJ/kg$

   Exhaust gas temperature: 840°C

   Stoichiometric air to fuel ratio (AFR) = 14.5:1

$$Thermal\ energy\ input\ to\ the\ furnace = \dot{m}_{fuel}\ x\ GCV_{oil}$$

$$= 0.00296\ kg/s\ x\ 42{,}920\ kJ/kg$$

$$\underline{= 127kW}$$

$$Heat\ lost\ to\ the\ surrounding\ = \dot{m}_{flue\ gas}\ .\ c_p.\ \Delta T$$

$$m_{flue\ gas} = fuel\ flow\ +\ air\ flow$$

$$Total\ AFR\ =\ Stoichiometric\ AFR\ x\ (1\ +\ Excess\ air\ factor)$$

$$= 14.5\ x\ (1\ +\ 0.2)$$

$$= 17.4$$

$$\underline{Accordingly, Air\ mass\ flow\ rate\ =\ 17.4\ x\ Fuel\ Flow\ =\ 17.4\ x\ 0.00296\ kg/s}$$
$$\underline{=\ 0.0515\ kg/s}$$

$$\underline{m_{flue\ gas} =\ 0.00296 + 0.0515 = 0.0544 kg/s}$$

$$\underline{Heat\ lost\ to\ the\ surrounding\ with\ the\ exhaust\ gas}$$
$$\underline{=\ 0.0544\ x\ 1.069\ x\ (840 - 30) = 47.1 kW}$$

2. Heat Exchanger Design Parameters:

- Air mass flow rate: 0.0515 kg/s
- Flue gas mas flow rate: 0.0544kg/s
- Exhaust gas inlet temperature: 840°C
- Inlet air temperature :30 °C
- Target energy recovery rate = achieve 50% effectiveness or more using iterative design calculations and cost comparison
- Heat exchanger type-Welded plate heat exchanger
- Plate size = 600mm x 400mm;
  - Fits well into standard sheet steel dimensions (1200 mm×2400 mm) minimizing material waste.
  - Allows efficient handling and assembly, making it suitable for small and medium-scale foundry setups.
  - Facilitates local fabrication without requiring advanced or large-scale manufacturing facilities.

    - Ergonomic for testing and installation in local foundries, where labor and space constraints are common.
- Plate thickness-1mm - The plate thickness for the welded plate heat exchanger has been selected as 1 mm. This choice is based on several practical and performance-oriented considerations. The 1 mm thickness allows for easier fabrication using gas welding and arc welding, which are commonly employed techniques in small to medium-scale foundries. These methods are well-suited for handling thinner plates, reducing challenges such as warping during the welding process. Additionally, the lower plate thickness significantly enhances heat transfer efficiency by minimizing the thermal resistance (δ/k), thereby improving the overall performance of the heat exchanger. This choice also aligns with material economy, as thinner plates reduce material consumption, lowering costs while maintaining the structural integrity required for the operating conditions. Overall, the 1 mm plate thickness strikes an optimal balance between ease of fabrication, cost-effectiveness, and thermal performance, making it an ideal choice for the given application.

4.5.3. Design Objectives

The design of a welded plate heat exchanger involves a step-by-step process that ensures the final product meets performance and practical requirements. The approach combines calculations and design adjustments to achieve the desired balance between effectiveness and feasibility.

1. Initial Design Assumptions

The process begins with selecting a plate size and estimating the number of plates based on material availability, fabrication ease, and practical constraints. For example, a plate size of 600 mm×400 mm is chosen to minimize material waste and ensure easy handling during fabrication. Passage dimensions are defined based on these initial choices.

2. Performance Calculations

Key parameters, such as Reynolds numbers and heat transfer coefficients, are calculated using the initial dimensions. These values determine the overall heat transfer coefficient (U), which is used to estimate the heat exchanger's effectiveness and thermal performance.

3. Design Refinement

If the calculated performance does not meet the target effectiveness, adjustments are made to the number of plates, spacing, or other design aspects. Each change is followed by recalculations to confirm the improvements.

4. Simulation and Validation

The design is validated using simulation tools like SOLIDWORKS and ANSYS to ensure thermal and structural performance. These simulations provide insights into flow distribution, pressure drops, and heat transfer efficiency, allowing further refinements if necessary.

5. Practical Considerations

Fabrication and cost factors are evaluated alongside performance. Adjustments to the design are made to ensure the heat exchanger is efficient, economical, and suitable for the foundry environment.

4.6. Design of the Heat Exchanger

4.6.1. Design Calculations

The figure 37 shows a 3D model of the welded plate heat exchanger, designed for efficient thermal energy transfer between two fluids. The structure consists of a series of parallel plates welded together, creating alternating channels for the hot and cold fluids.

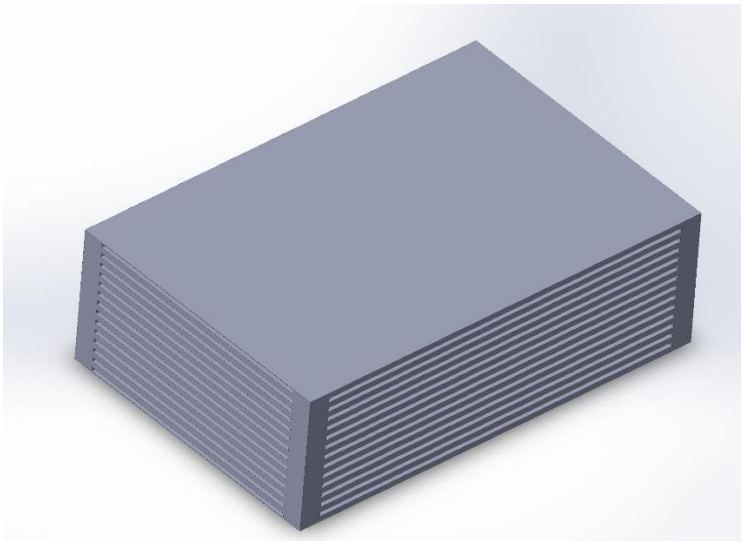

Figure 44-3D model of the Welded plate heat exchanger

$Cold\ air\ inlet\ temperature, Tc = 30\ C$

$Target\ air\ outlet\ temperature\ for\ cold\ air\ out;\ Tcold.out\ =\ 400\ C$

$No\ of\ cold\ air\ flow\ passages\ as\ per\ the\ original\ design\ =\ 14$

$Hot\ air\ inlet\ temperature, Thot.in = 840\ C$

$Target\ air\ outlet\ temperature\ for\ hot\ air\ our;\ Thot.out\ =\ 500\ C$

$No\ of\ cold\ air\ flow\ passages\ as\ per\ the\ original\ design\ =\ 13$

$Effective\ surface\ area\ per\ plate\ =\ 540mmx340mm$

$No\ of\ heat\ transfer\ surfaces\ =\ 26$

$Total\ Heat\ transfer\ surface\ area\ ;\ As\ =\ 540mmx340mmx26\ =\ 4.7736m^2$

Cold side convection heat transfer coefficient calculation

$Average\ cold\ air\ temperature\ =\ (30 + 400)/2\ =\ 215C$

$Air\ density\ at\ average\ cold\ side\ temperature\ =\ 0.722\ kg/m^2$

$Air\ volume\ flowrate\ \dot{V} = \frac{\dot{m}}{\rho} = \frac{0.0515}{0.722} = \frac{0.0713m^3}{s}$

$Air\ volume\ flow\ rate\ through\ a\ single\ passage\ = \frac{0.0713}{14} = 0.00509m^3/s$

$Flow\ velocity;\ volume\ flow\ rate\ =\ Cross\ section\ area\ x\ velocity$

$0.00509 = 0.006\ x\ 0.340\ x\ \ v$

$\underline{v =\ 2.495m/s}$

$$Renold\ number\ ;\ Re\ = \frac{Velocity\ x\ Hydraulic\ Diameter}{Kinematic\ Viscocity}$$

$$Hydraulic\ Diameter\ = 4\ x\ Cross\ Section\ Area/Perimeter$$

$$= 4\ x\ 6mm\ x\ 340mm\ /(6mm\ x\ 2\ +\ 340mm\ x\ 2)\ =\ 11.8\text{mm}$$

$$Kinematic\ viscosity\ at\ 215C\ = 3.633\ m^2/s\ x10^{-6}$$

$Re = 2.495\ x\ 0.0118/(36.33\ x\ 10^{-6})$ = 810. The flow is below Renod number of 2000. Therefore, the flow is laminar.

$For\ lamina\ \ flow, Nusselt\ number, Nu$ =8.24 (Table 8.1 of Heat & Mass Transfer [39])

$$Thermal\ conductivity\ of\ air\ at\ 215C\ \ =\ 0.03779W/m.K$$

$$Convection\ heat\ transfer\ coefficient;\ h_{c.cold}\ =\ k\ x\ Nu/Dh$$

$$=\ 0.03779\ x\ 8.24\ /0.0118$$

$\underline{= 26.38\ W/m^2.K}$

Hot side convection heat transfer coefficient calculation

$$Average\ air\ temperature\ =\ (840 + 500)/2\ =\ 670C$$

$$Air\ density\ at\ average\ hot\ side\ temperature\ =\ 0.3627\ kg/m3$$

$$Air\ volume\ flowrate\ \dot{V} = \frac{\dot{m}}{\rho} = \frac{0.0544}{0.3627} = \frac{0.15m^3}{s}$$

$$Air\ volume\ flow\ rate\ through\ a\ single\ passage\ \ = \frac{0.15}{13} = 0.0115m^3/s$$

$$Flow\ velocity;\ volume\ flow\ rate\ =\ Cross\ section\ area\ x\ velocity$$

$$0.0115 = 0.006\ x\ 0.540\ x\ \ v$$

$\underline{v =\ 3.54m/s}$

$$Renold\ number\ ;\ Re\ = \frac{Velocity\ x\ Hydraulic\ Diameter}{Kinematic\ Viscocity}$$

$$Hydraulic\ Diameter\ = 4\ x\ Cross\ Section\ Area/Perimeter$$

$= 4\ x\ 6mm\ x\ 540mm\ /(6mm\ x\ 2\ +\ 540mm\ x\ 2)\ =\ 11.8$

$Kinematic\ viscosity\ at\ 670C\ = 107.11\ m^2/s\ x10^{-6}$

$Re = 3.54\ x\ 0.0118/(107.1\ x\ 10^{-6})$ = 390, The flow is below Renod number of 2000. Therefore, the flow is laminar.

$Nu\ =\ 8.24$

$Thermal\ conductivity\ of\ air\ at\ 670C\ =\ 0.06581 W/m.K$

$$Convection\ heat\ transfer\ coefficient;\ h_{c.hot}\ =\ k\ x\ Nu/Dh$$

$$=\ 0.06581\ x\ 8.24\ /0.0118$$

$\underline{= 45.9\ W/m^2.K}$

Overall heat transfer coefficient

$$Overall\ heat\ transfer\ coefficient\ across\ plat\ thin\ plate;\ \frac{1}{U}$$

$$= \frac{1}{h_{c.hot}} + \frac{1}{h_{c.cold}}$$

$$\frac{1}{U} = \frac{1}{26.38} + \frac{1}{45.9}$$

$$\underline{\underline{U\ =\ 16.75\ \text{W/m}^2\text{.K}}}$$

$$Effectiveness,\qquad \varepsilon\ =\ \frac{Actual\ Heat\ Transfer\ Rate}{Maximum\ Possible\ Heat\ Transfer\ Rate}$$

$$NTU\ =\ \frac{U\ x\ As}{(m.Cp)min}$$

Since U and Cp values are constants, NTU is a measure of heat transfer surface area of the heat exchanger.

$$C\ =\ Cmin/Cmax\ =\ (m_{air}\ x\ C_{p.air})/(m_g\ x\ C_p\ gas\ )$$

$$=\ (0.0515\ x\ 1.023)/(0.0544\ x\ 1.1135)\ =\ 0.87$$

$NTU\ =\ \frac{16.75\ x\ 4.7736}{0.0515\ x\ 1023} =$ 1.517

The figure 38 shows the chart for Number of Transfer Units vs Effectiveness for both fluid unmixed type cross flow heat exchanger. The chart will be used to find the effectiveness value for the NTU=1.517.

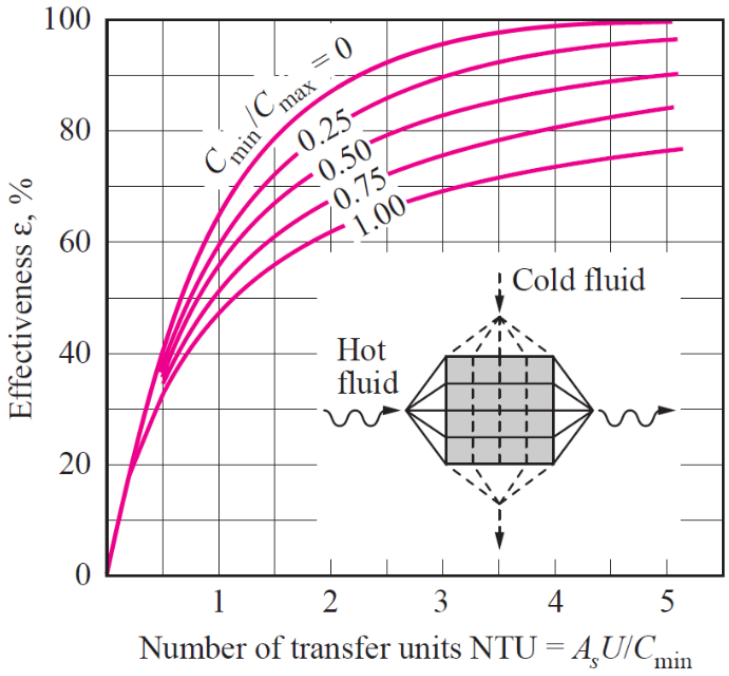

Figure 45-Effectiveness for Heat Exchangers [36]

Effectiveness = 0.6

Calculation of the hot gas outlet temperature and the cold air outlet temperature

$Q_{max} = C_{min}(T_{hot.in} - T_{cold.in})$

= 0.0515 x 1.023 x (840 – 30) = 42.67kW

$heat\ transfer\ rate\ from\ hot\ side\ to\ cold\ side, Q = \varepsilon\ x\ Q_{max}$

$Q = 0.6 * 42.67 = 25.6\ kW$

From energy balance

$Q = C_{hot}(T_{hot.in} - T_{hot.out}) = 25.6 = 0.0544\ x\ 1.1135\ x(840 - T_{hot.out})$

$T_{hot.out}\ from\ calculations;\ T_{hot.out} = 417.3$ C

$Q = C_{cold}(T_{cold.out} - T_{cold.in}) = 25.6 = 0.0515x\ 1.023\ x(T_{cold.out} - 30)$

$T_{cold.out}\ from\ calculations;\ T_{cold.out} = 515.9$ C

The proposed combustion air preheating methodology for crucible furnace efficiency improvement demonstrates the viability of utilizing a welded plate heat exchanger to recover energy from exhaust gases. The design and calculations confirm the feasibility of achieving a target effectiveness of 50% or more. The final results show a calculated heat exchanger effectiveness of 60%, translating to a recovered energy of 25.6 kW. This corresponds to significant energy savings and operational improvements.
The cold air outlet temperature ($T_{cold,out}$=515.9°C) and the hot gas outlet temperature ($T_{hot,out}$=417.3°C) were determined through calculations, maintaining energy balance and aligning with the heat exchanger's design parameters.

4.7. Modeling of Heat Exchanger and Study of Heat Transfer using ANSYS Fluent Simulations

To enhance the design process and gain deeper insights into the energy recovery potential of the welded plate heat exchanger, modeling and simulation tools were utilized. This section describes the SolidWorks modeling process and the ANSYS simulations performed to validate the design and predict its performance.

4.7.1. 3D Modeling

The plate heat exchanger was modeled as shown in figure 39 using SolidWorks to visualize the structure, optimize dimensions, and assess its practicality for fabrication.

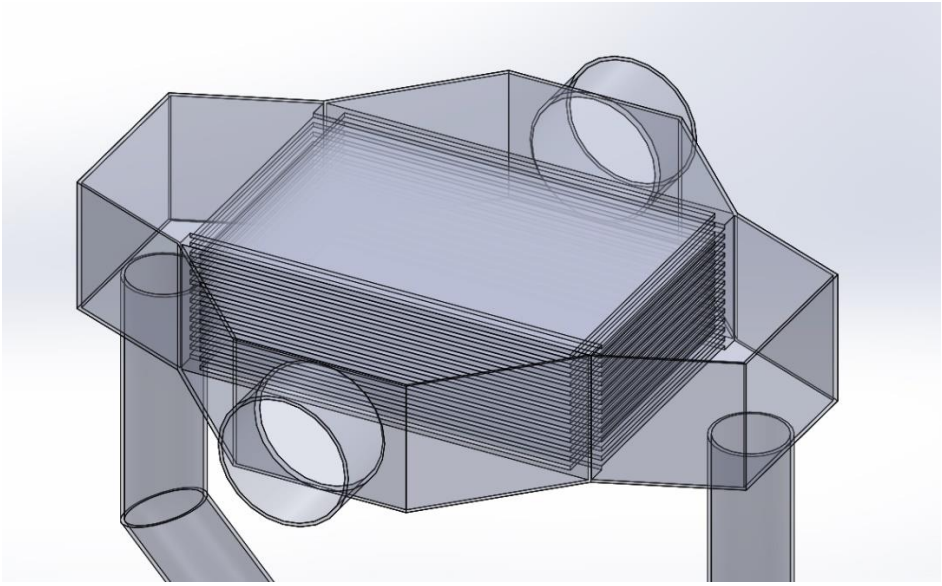

Figure 46-3D Wireframe model of welded plate heat exchanger assembly

4.7.2. Simplified Simulation Approach for Welded Plate Heat Exchanger

ANSYS software was employed to simulate the thermal and fluid flow performance of the heat exchanger. The welded plate heat exchanger in this study is used to recover waste heat from the crucible furnace exhaust. In the actual system, hot combustion gases exiting the furnace are directed into the heat exchanger, where they transfer heat to incoming fresh air supplied by a blower. This preheated air is then recirculated back into the furnace, improving overall thermal efficiency.

However, due to the high computational cost and geometric complexity of simulating the entire furnace–heat exchanger system as a coupled domain, a simplification was introduced. Instead of modeling the full system, the simulation was limited to the heat exchanger alone. The hot air outlet temperature of the furnace was measured experimentally and used as the inlet boundary condition for the hot side of the heat exchanger model. Similarly, blower-supplied air characteristics were used for the cold side inlet.

This approach allows for evaluating the thermal performance and effectiveness of the heat exchanger independently, while significantly reducing computational time and resource demands. The key assumption is that the thermal boundary conditions at the

heat exchanger inlets adequately represent real operating conditions of the coupled system.

It is noted that the full system, when simulated together, behaves as a transient system, as the hot air recirculated through the heat exchanger affects the pressure and temperature at the furnace inlet over time. However, in this simplified model, the system was assumed to be in steady-state, with fixed inlet temperatures and flow rates applied at both the hot and cold sides. This simplification is valid for assessing the standalone heat transfer characteristics of the welded plate heat exchanger, and it provides an accurate approximation of its performance under representative operating conditions.

4.7.3. Simulation Setup for Welded Plate Heat Exchanger:

The simulation relied on the following physical and numerical models:

- **Solver Type**: Pressure-based solver.
- **Time** : Steady state
- **Flow Regime**: The realizable k–ε turbulence model with scalable wall functions was selected to ensure accurate prediction of near-wall behavior in the narrow flow passages of the welded plate heat exchanger.
- **Energy Equation**: Activated to capture heat transfer throughout the domain.
- **Gravity**: Included to reflect buoyancy effects from hot gas flows.
- **Fluid Material**: The fluid material was selected as air
- **Heat Exchanger Material**: Steel was selected as the Heat Exchanger material.

4.7.4. Boundary Conditions

The following boundary conditions were applied:

Boundary	Condition
Cold Air inlet	Cold air inlet mass flow rate is 0.0515kg/s. The temperature of the stream is 35ºC.
Hot Air Outlet	Pressure outlet at atmospheric pressure. The backflow temperature is approximately selected as 300ºC.
Hot Gas Inlet	Hot air inlet mass flow rate is 0.0544kg/s. The temperature of the stream is 840ºC.
Cold Gas Outlet	Pressure outlet at atmospheric pressure. The backflow temperature is approximately selected as 400ºC.

4.7.5. Mesh and Geometry of the Welded Plate Heat Exchanger

The geometry of the welded plate heat exchanger was initially developed using SolidWorks and later imported into ANSYS Fluent via SpaceClaim, where the fluid domains were extracted. The heat exchanger comprises three distinct regions:

1. Hot air body (Figure 42),
2. Cold air body (Figure 43), and
3. Steel plate walls (Figure 44) that separate the two air streams.

These three domains were modeled explicitly to account for conjugate heat transfer between the hot and cold sides of the exchanger through the solid steel plates.

The plates separating the air streams have a thickness of 1 mm, which required a mesh element size of 0.5–1 mm in those regions to resolve the thermal gradients accurately. Due to the intricate layered structure and narrow passageways (approximately 5 mm wide and 600 mm long), the geometry presented significant challenges in meshing. The default mesh size was reduced to 6 mm, with finer refinement near wall boundaries and solid-fluid interfaces.

The final computational mesh as shown in figure 45 consisted of approximately 4.3 million cells, but full-domain simulations involving all three bodies in high resolution typically exceeded 5 million cells. Mesh quality was evaluated using Aspect Ratio, Skewness, and Orthogonal Quality metrics to ensure numerical accuracy and stability. The mesh was optimized to maintain:

- Skewness below 0.85,
- Orthogonal quality above 0.2, and
- Aspect ratios under 10, with exceptions in narrow duct regions

Given the fine meshing required, especially in the thin steel plates and boundary layers, the computational cost was significant. Each iteration consumed a substantial amount of processing time, and full simulations required extended runtimes due to the complexity and size of the model.

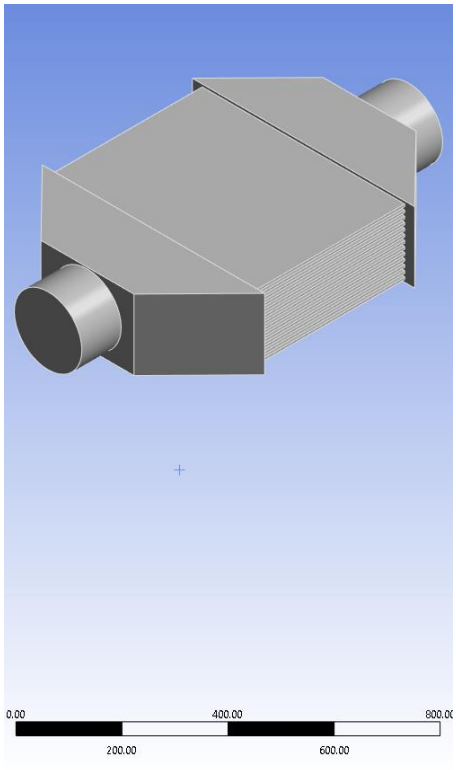

Figure 47: Hot Air Body

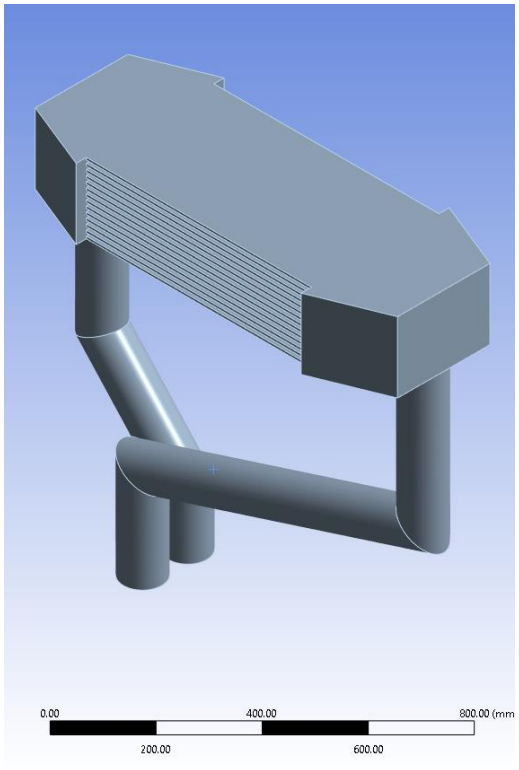

Figure 48: Cold Air Body

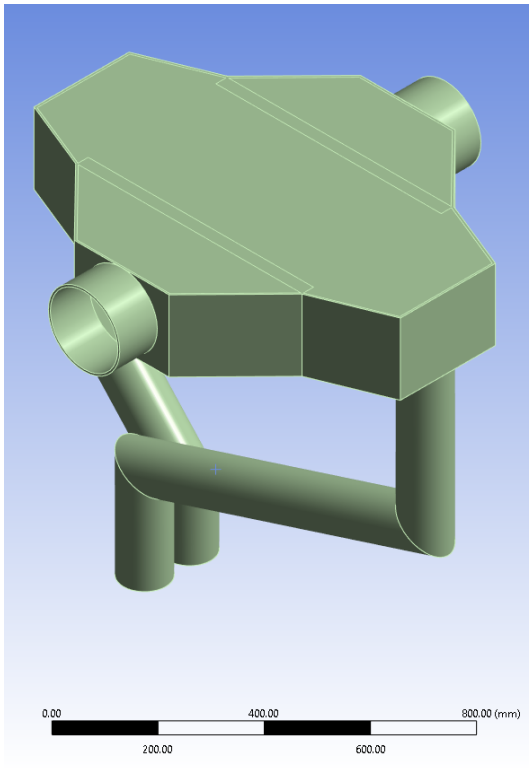

Figure 49: Steel Body

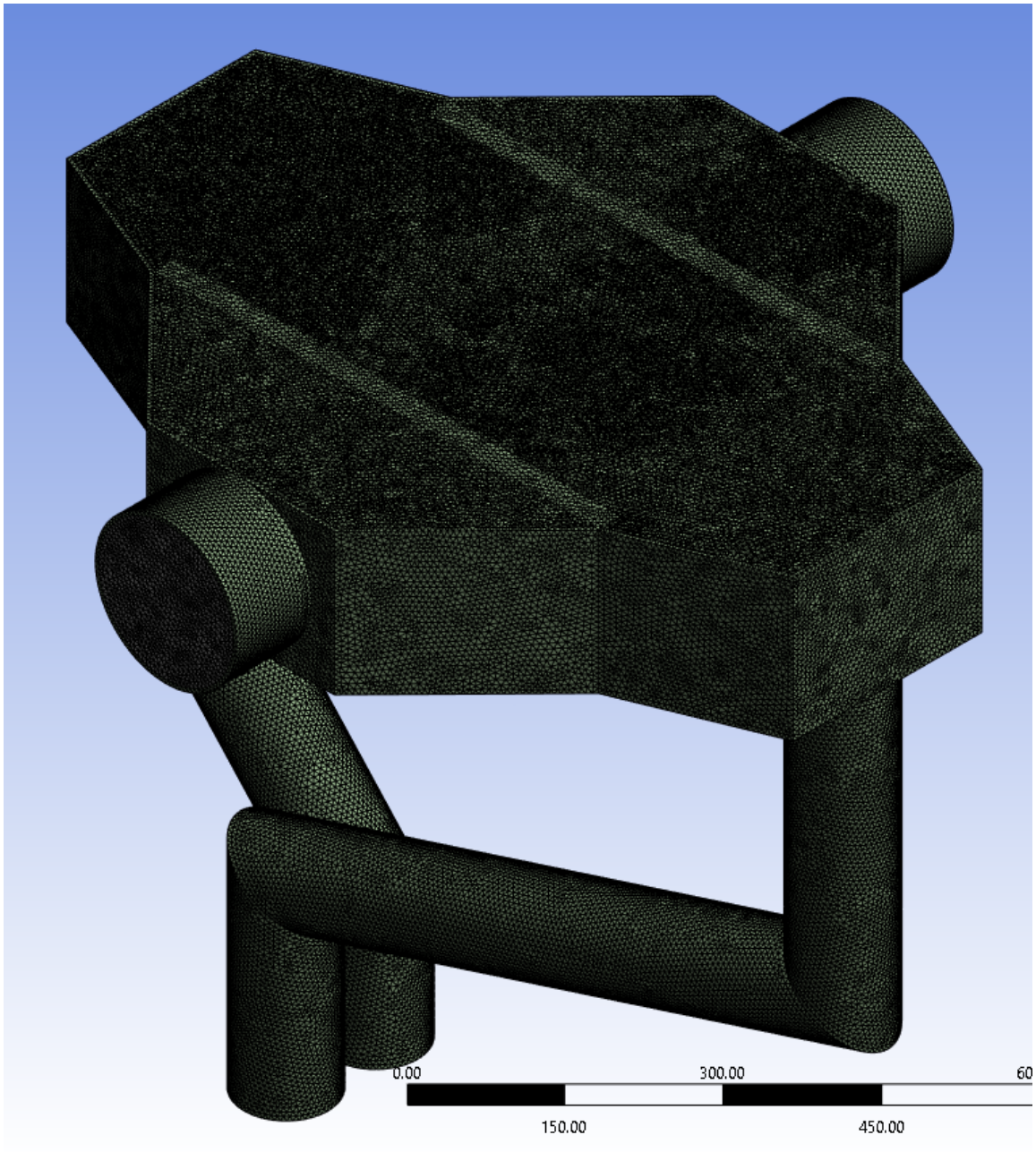

Figure 50: Welded Plate Heat Exchanger Mesh

4.7.6. Solution and Solution Controls

The welded plate heat exchanger simulation was performed using the Coupled pressure-velocity coupling scheme, and energy equations involving conjugate heat transfer.

To maintain solution convergence during the initial iterations, first-order upwind discretization was applied to the momentum and energy equations, as well as to the turbulence parameters (turbulent kinetic energy and turbulent dissipation rate). After approximately 100 iterations, the solution method was upgraded to second-order upwind schemes to improve solution accuracy.

The time scale factor was carefully adjusted between 0.1 and 1 during the iteration process. Relaxation factors for turbulent quantities were initially set to 0.4 to dampen fluctuations during the early solution phase, and were later returned to Fluent's default values to allow the simulation to converge smoothly.

Given the complexity of the geometry and the fine mesh required to resolve 1 mm-thick steel plates, the number of solver iterations was progressively increased from 50 up to 500, allowing convergence.

4.7.7. Key Findings from the Simulation

- The simulation provided valuable insights into heat transfer efficiency of the welded plate heat exchanger. **Temperature Distribution**:
    - The figure 40 shows the temperature distribution throughout the volume of the heat exchanger. The figures 41 and 42 shows the temperature contours along the cross sections of the heat exchanger. The cold air outlet temperature was reach to 473.8°C, aligning approximately with theoretical calculations.
    - Hot gas outlet temperature dropped to 373.5°C, confirming effective heat transfer.

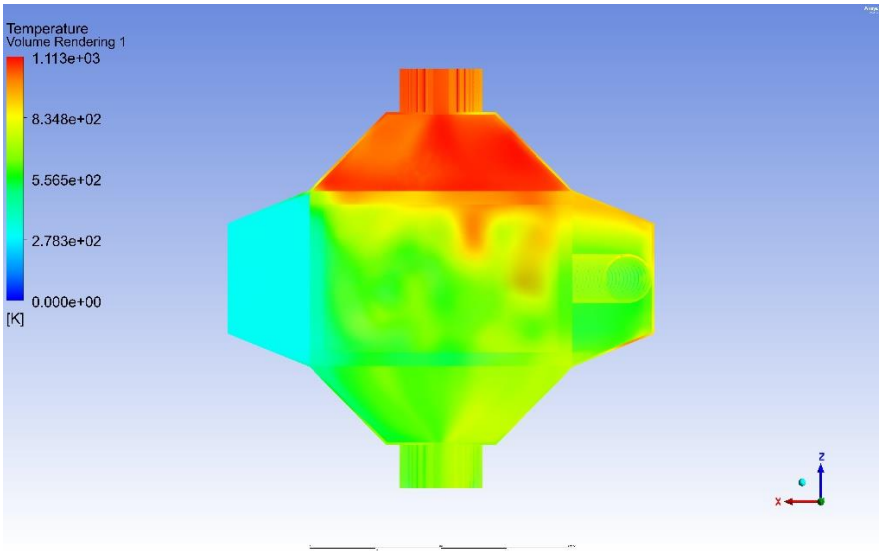

Figure 51-Temperature volume rendering diagram for plate heat exchanger

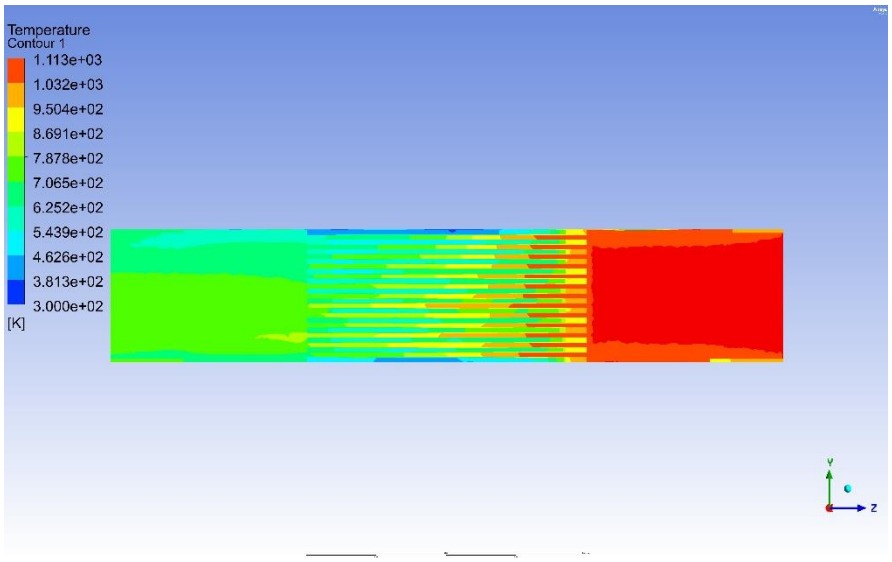

Figure 52- Temperature contours across the hot gas inlet to hot gas outlet

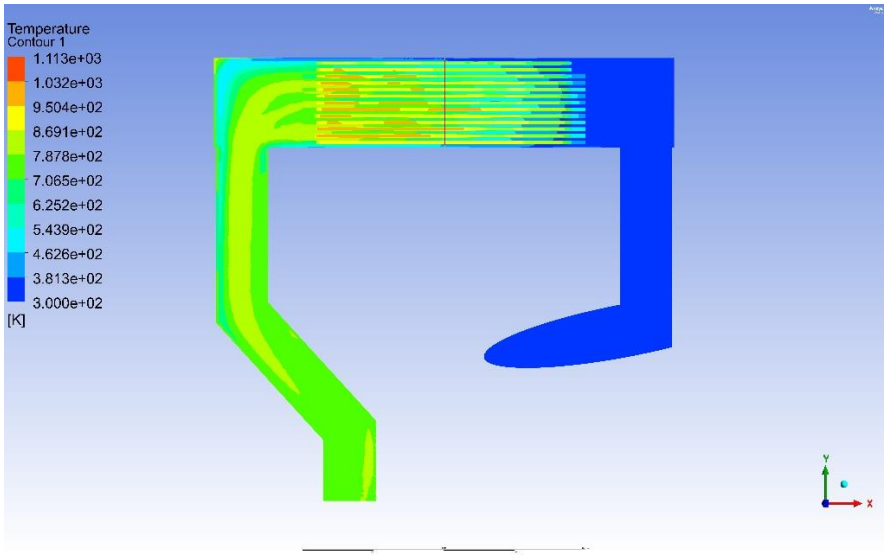

Figure 53-Temperature contour across the cold air inlet to hot air outlet

- **Pressure Drop**:
  - The pressure drops across the hot and cold passages were minimal, ensuring efficient flow without significant resistance.
- **Heat Recovery Potential**:
  - The heat recovery potential at the hot air outlet of the heat exchanger was reached to 23.2kW which is closely aligned with the calculated heat recovery rate of the plate heat exchanger.
- **Heat exchanger effectiveness**

  Hot gas inlet temperature =840

  Hot gas outlet temperature =373.5

  Cold air inlet temperature =26.85

  Cold air outlet temperature = 473.8

$$\varepsilon = \frac{\dot{Q}_{\text{actual}}}{\dot{Q}_{\text{max}}}$$

Where:

$$\dot{Q}_{\text{actual}} = \dot{m} \cdot c_p \cdot (T_{\text{outlet}} - T_{\text{inlet}})$$

$$\dot{Q}_{\text{max}} = \dot{m}_{\text{min}} \cdot c_p \cdot (T_{\text{hot, inlet}} - T_{\text{cold, inlet}})$$

$\dot{m}$: Mass flow rate of the working fluid

c_p: Specific heat capacity of the fluid

T_{outlet}: Outlet temperature of the fluid

T_{inlet}: Inlet temperature of the fluid

$\dot{m}_{min}$: Smaller mass flow rate between the hot and cold streams

$$\varepsilon = \frac{0.0515 \text{ x } 1.033 \text{ x } (473.8 - 26.85)}{0.0515 \text{ x } 1.033 \text{ x } (840 - 26.85)} = 0.55$$

2. **Insights from Simulation**:
    - The ANSYS results confirmed the effectiveness of the plate dimensions and spacing in achieving the desired energy recovery.
    - Temperature gradients across the plates highlighted areas of efficient and inefficient heat transfer, guiding future design improvements.

CHAPTER 5: FABRICATION AND EXPERIMENTAL SETUP

5.1. Fabrication of the Welded Plate Heat Exchanger

5.1.1. Material Selection and Construction Details

The welded plate heat exchanger was designed to recover heat from the exhaust gases of a crucible furnace. Materials were selected based on their thermal conductivity, structural integrity, and suitability for local fabrication.

- **Plate Material**: Mild steel sheets with a thickness of 1 mm were chosen for their high thermal conductivity. Stainless steel is much better but mild steel is sufficient for experimental setup.
- **Dimensions**: Each plate was cut to a size of 600 mm × 400 mm, optimizing material usage from standard sheet sizes (1200 mm × 2400 mm) to minimize waste.
- **Spacers**: Mild steel spacers were used to maintain uniform spacing between plates, ensuring consistent flow channels for hot gases and cold air.

5.1.2. Assembly Techniques and Equipment Used

The fabrication process involved precision cutting, welding, and assembly to ensure a robust and efficient design.

- **Cutting and Preparation**: Plates were cut using a shearing machine for high precision and smooth edges.
- **Welding**: Gas and arc welding techniques were employed to join the plates and spacers. Intermittent welds were made along the edges to secure the plates while allowing for thermal expansion during operation. The figures 44 below shows various stages of fabrication of the plate heat exchanger using in house labor.

Figure 54-Fabricaiton of the welded plate heat exchanger

- **Leak Testing**: After assembly, the heat exchanger was pressure-tested using compressed air to identify and leaks. Considerable amount leaks were noticed which would negatively affect the efficiency. However, since pressure inside the system is very low, this will not be significant at the testing. This can be completely arrested through proper welding.

- **Final Assembly**: Inlet and outlet ports were designed in sleeve design so that the pipes will run inside the other and facilitate for easy connection to the furnace system. The entire unit was inspected for structural integrity and alignment. The figure 45 below shows the final assembly with all the instrumentation for experiments.

Figure 55-Integrated assembly of welded plate heat exchanger and the tilted crucible furnace consisting all the instrumentation for testing

5.2. Experimental Setup

The experimental setup integrated the welded plate heat exchanger with a crucible furnace designed for aluminum melting. The system was configured to preheat combustion air using recovered exhaust heat.

The experimental process was particularly demanding due to the high-temperature and energy-intensive nature of the work. The furnace system operated at temperatures reaching 800°C to 900°C, with significant radiation heat impacting the environment. Despite these challenges, adjustments were made to improve the setup and ensure a safer and more controlled environment for conducting experiments.

- **Furnace Details**: The crucible furnace was fueled by waste lube oil and equipped with a non-premixed burner for efficient combustion. Exhaust gases exited through a duct that connected to the heat exchanger.
- **Heat Exchanger Integration**: Hot exhaust gases flowed through the hot-side passages of the heat exchanger, transferring heat to the cold air in the adjacent passages. Preheated air was routed back to the furnace for combustion, improving fuel efficiency.

5.3. Measurement and Instruments

1. **Temperature Measurement**:
    - K-type thermocouples were installed at the following locations:
        - Hot gas inlet and outlet.
        - Cold air inlet and outlet.
        - Molten aluminum. The figure 46 below shows measuring of molten aluminum temperature using a K-type thermocouple fitted to a steel pipe

Figure 56-Molten aluminum temperature measurement using a K-type thermocouple

- A digital temperature controller was used for reading temperature values. The figure 47 below shows the temperature of the heat exchanger inlet denoted by T3.

- 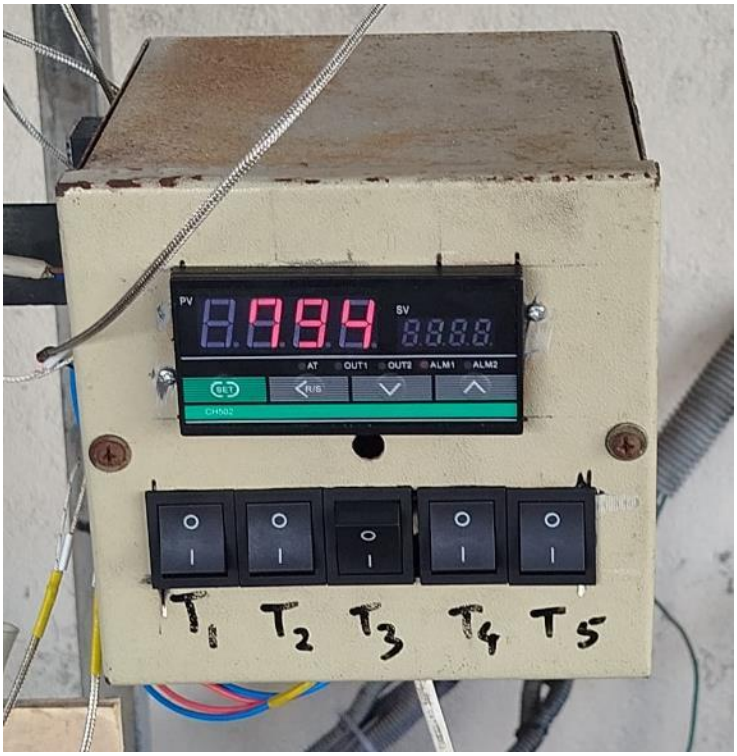

Figure 57-Digital temperature controller for temperature measurement, 1) T1-Cold air inlet, 2) Hot air outlet, 3) T3-Hot gas inlet, 4) T4-Hot gas outlet, 5) For temperature measurements inside the liquid aluminum

2. **Fuel Parameters**:

   - Fuel pressure and temperature were monitored using the available pressure gauges and temperature gauges. The figure 48 below shows the temperature gauge installed on the fuel preheater for temperature measurements. The figure 49 below shows the temperature controller setpoint adjustment for setting up the fuel preheating temperature. The figure 50 below shows the fuel pressure gauge installed at the fuel pump discharge point for measuring the fuel discharge pressure. Fuel discharge quantity is adjusted by the adjustment of the fuel pump pressure regulator until the desired discharge pressure is achieved.

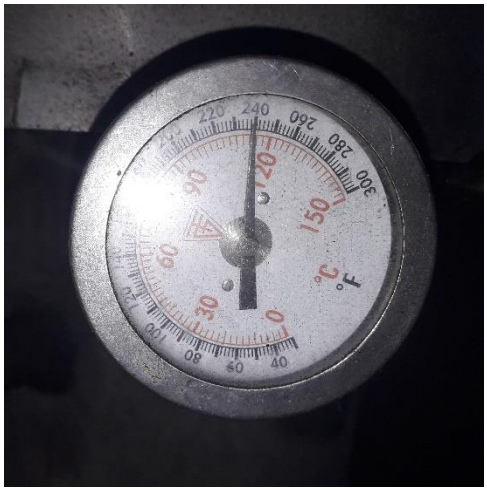

Figure 58-Gauge for fuel temperature measurement

Figure 59-Fuel temperature adjustment

Figure 60-Fuel pressure gauge

3. **Fuel Consumption Measurement**:

   - Fuel tank level was monitored by the dip stick marked in millimeters. The figure 51 shows the dipstick available in the fuel tank for level measurements.

Figure 61-Fuel tank dipstick

4. Air to fuel ratio adjustment

The figure 52 below shows the blower damper position indicator. In the absence of exhaust gas analysis equipment, combustion performance was assessed visually by monitoring exhaust gas flow, smoke, and observing the temperature variations while adjusting the damper.

Figure 62-Blower damper position indicator

5. Burner Power Output

- Burner discharge Pressure was monitored using a U-tube manometer. The burner characteristic curves are available in the burner catalogue as shown if figure 53. According to the catalogue, the burner operating range is from 120kW to 525kW. The fuel flow rate is 10kg/h to 45kg/h. According to this diagram, and the experiment fuel flow rate figures, the burner operates close to the lowest power area.

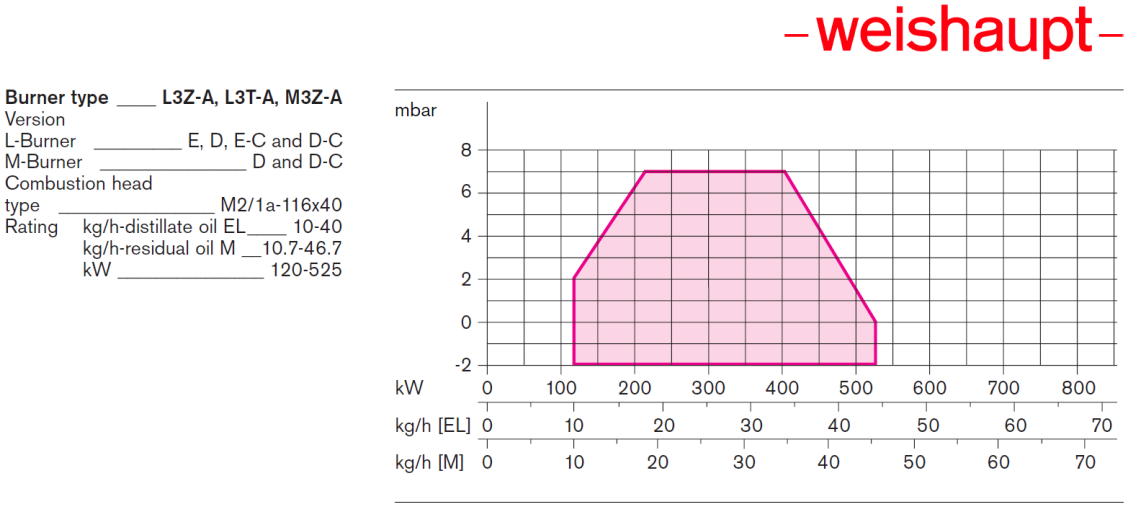

Figure 63-Burner characteristic curve

5.4. Procedure for Evaluating Heat Exchanger Performance

The performance of the heat exchanger was evaluated using the following steps:

1. **System Initialization**:
    - The furnace was started with an initial charge of 8 kg of aluminum.
    - Melting starts about 45min to 1 hour. Loading of aluminum charge is continued at this point until all the aluminum are loaded. were recorded.
2. **Data Collection**:
    - Temperature and fuel level measurements were recorded from start to over the melting period to evaluate performance. It was noted that the temperature readings continue to rise throughout the operation.
    - Meting time was calculated from the furnace start time and melting completion time
    - Energy recovery was calculated using the recorded temperature differences, fuel flow rates and theoretical air flowrates.
3. **Performance Metrics**:

1. Effectiveness

The effectiveness of the heat exchanger was calculated using the equation:

$$\varepsilon = \frac{\dot{Q}_{\text{actual}}}{\dot{Q}_{\text{max}}}$$

Where:

$$\dot{Q}_{\text{actual}} = \dot{m} \cdot c_p \cdot (T_{\text{outlet}} - T_{\text{inlet}})$$

$$\dot{Q}_{\text{max}} = \dot{m}_{\text{min}} \cdot c_p \cdot (T_{\text{hot, inlet}} - T_{\text{cold, inlet}})$$

- $\dot{m}$: Mass flow rate of the working fluid
- c_p: Specific heat capacity of the fluid
- T_{outlet}: Outlet temperature of the fluid
- T_{inlet}: Inlet temperature of the fluid
- $\dot{m}_{\text{min}}$: Smaller mass flow rate between the hot and cold streams

2. Energy Recovery $Q_{\text{recovered}}$

The energy recovery was calculated as:

$$Q_{\text{recovered}} = \dot{m}_{\text{air}} \cdot c_p \cdot \left(T_{\text{air, outlet}} - T_{\text{air, inlet}}\right)$$

Where:

- $\dot{m}_{\text{air}}$: Mass flow rate of combustion air
- c_p: Specific heat capacity of air
- $T_{\text{air, outlet}}$: Outlet temperature of air
- $T_{\text{air, inlet}}$: Inlet temperature of air

3. Pressure Drop (ΔP)

The pressure drops across the heat exchanger was determined using:

$$\Delta P = P_{\text{inlet}} - P_{\text{outlet}}$$

Where:

- P_{inlet}: Pressure at the inlet of the heat exchanger
- P_{outlet}: Pressure at the outlet of the heat exchanger

4. Fuel Savings (%)

The percentage fuel savings due to the heat exchanger was calculated using:

$$\text{Fuel Savings (\%)} = \frac{\text{Fuel consumption without HX} - \text{Fuel consumption with HX}}{\text{Fuel consumption without HX}} \times 100$$

Where:

- Fuel consumption without HX: Baseline fuel consumption without the heat exchanger
- Fuel consumption with HX: Fuel consumption with the heat exchanger installed

CHAPTER 6: RESULTS AND DISCUSSION

6.1. Overview

This chapter presents the iterative process and outcomes of the calculations, simulations conducted and experimental testing on the integrated furnace and welded plate heat exchanger system. The challenges faced during testing, modifications implemented, and final results are discussed in detail. Insights derived from the findings are contextualized with broader implications for foundry operations.

6.2. Experimental Challenges and Setup

The experimental setup involved multiple challenges, particularly due to the high-temperature and energy-intensive nature of the process. Testing conditions in the foundry exposed the team to extreme radiation and temperatures, often reaching up to 800-900°C. Initial tests revealed flue gas leaks and inconsistencies in the air-to-fuel ratio, leading to inefficient combustion and elevated fuel consumption.

Modifications were implemented to optimize the system:

- **Air-to-Fuel Ratio Adjustment**: Excess air initially introduced into the combustion chamber resulted in high fuel consumption. By observing exhaust gas flow and smoke characteristics, the fuel injection pressure was reduced from 30 bar, 22 bar and finally 14 bar, achieving a more efficient combustion process. Modifications to the damper facilitated easier airflow adjustments, enabling fine-tuning of the Air to Fuel ratio and maintaining combustion stability.
- **Safety and Environment Improvements**: Additional measures were taken to create a safer and more sustainable working environment, considering the extreme heat and radiation exposure.

6.3. Experimental Results before the integration of combustion air preheating system.

Table 5 below shows the tilted furnace performance analysis data before installation of the combustion air preheating system.

Table 5-Combustion air preheater performance evaluation test data

Date	Furnace Started at	Furnace Stopped at	time (min)	Weight of Al Charge	Dip stick level at start	Dip stick level at stop	Fuel Consumption (liters)	Specific Fuel Consumption (*l/kg*)
2024.11.08	8:45 AM	11:00 AM	135	83	733	610	24.1	0.290
2024.11.11	1:30 PM	4:00 PM	150	83	780	655	24.5	0.295
2024.11.19	8:45 AM	11:10 AM	145	83	655	535	23.5	0.283
2024.11.20	8:40 AM	11:20 AM	160	83	535	400	26.4	0.318
2024.11.21	8:40 AM	11:15 AM	155	83	660	527	26.1	0.313
2024.11.27	1:30 PM	4:05 PM	155	83	527	400	24.9	0.299
2024.11.28	1:20 PM	3:30 PM	130	83	830	715	22.5	0.271
2024.11.29	1:45 PM	3:55 PM	130	83	715	597	23.1	0.278

Performance parameters before the installation of combustion air preheating system

1. Average specific fuel consumption = 0.294 *l/kg*
2. Average melting time = 145 minutes
3. Average thermal efficiency = 7.3%

6.4. Experimental results after integration of combustion air preheating system

The fabricated heat exchanger was tested under actual operating conditions to evaluate its thermal performance and energy recovery capabilities. The chart 01 below shows the temperature variation of the four measuring points on the plate heat exchanger. It can be seen that; the temperature readings continuously increasing and reach steady state after 45 to 50 minutes.

Table 6-Operating Conditions and System Parameters for the Combustion Air Preheating Test

Date	21.01.2025
Furnace started at	10:58 AM
Furnace stopped at	12:55 PM
Fuel pressure	14bar

Air Damper position	3.7
Waste oil level	473mm
Waste oil level	372mm
Aluminum Charge	80kg

Table 7-Temperature Variation at Measuring Points on the Plate Heat Exchanger

	HX Cold air in	HX Hot air out	HX hot gas in	HX hot gas out
	T1	T2	T3	T4
Time				
11:05	37	139	510	148
11:15	40	189	565	164
11:25	42	228	600	183
11:35	43	259	644	197
11:45	58	282	671	209
11:55	46	293	687	212
12:05	48	305	689	215
12:15	57	308	702	218
12:25	50	310	672	213
12:35	48	311	688	221
12:45	50	310	652	218

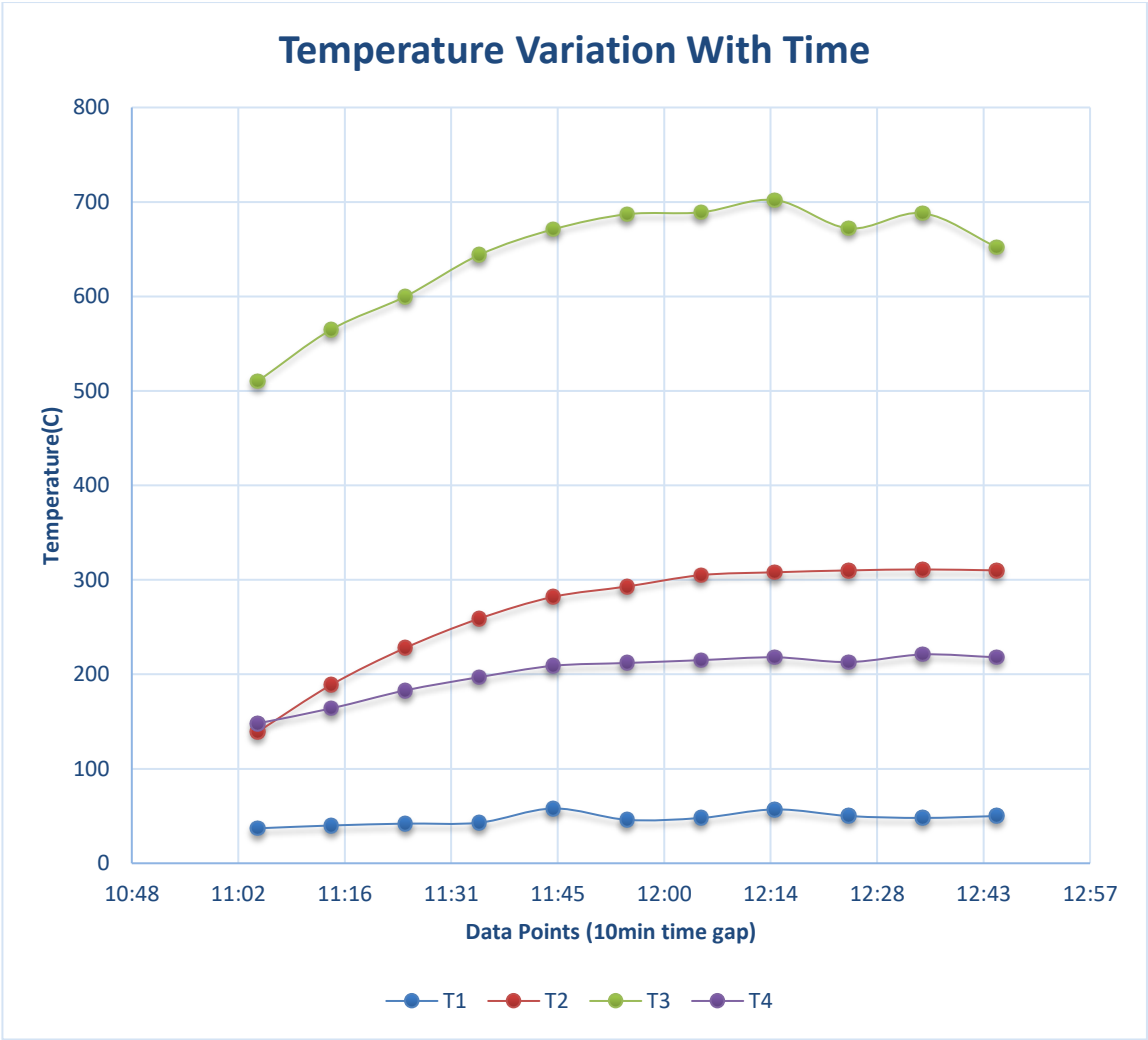

The Table 8 below shows the tilted furnace performance analysis data after installation of the combustion air preheating system.

Table 8- Performance Analysis of Tilting Furnace with Combustion Air Preheating System

Date	Furnace Started at	Furnace Stopped at	time (min)	Weight of Al Charge	Dip stick level at start	Dip stick level at stop	Fuel Consumption (liters)	Specific Fuel Consumption (l/Kg)
2025.01.09	11:00 AM	12:33 PM	93	83	597	500	19.0	0.228
2025.01.21	10:58 AM	12:55 PM	117	83	473	372	19.8	0.238
2025.01.23	09:10 AM	11:00 AM	120	83	486	395	17.8	0.214

Performance parameters after the installation of combustion air preheating system

1. Average specific fuel consumption = 0.227 *l/kg*
2. Average melting time = 110 minutes
3. Average thermal efficiency = 9.6%

6.5. Comparative Analysis: Experimental Results Before and After Heat Exchanger Integration.

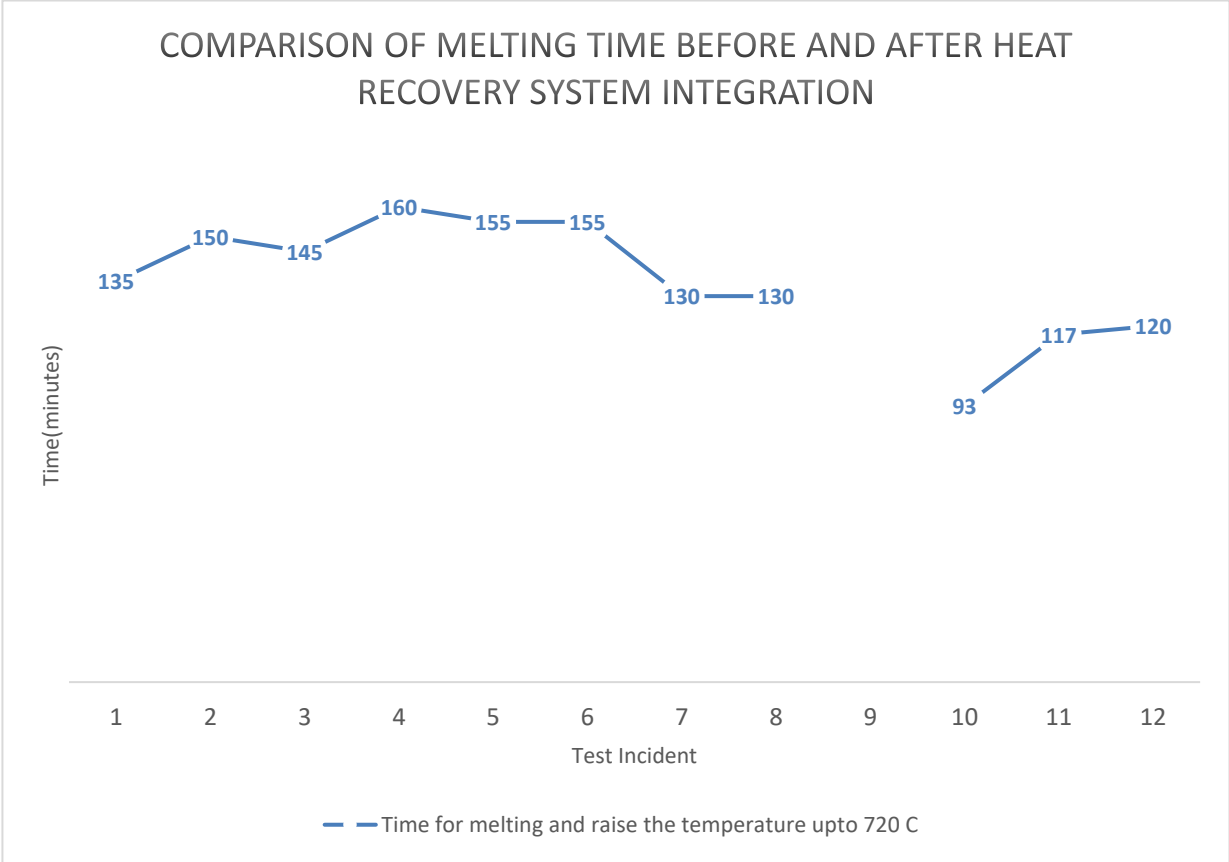

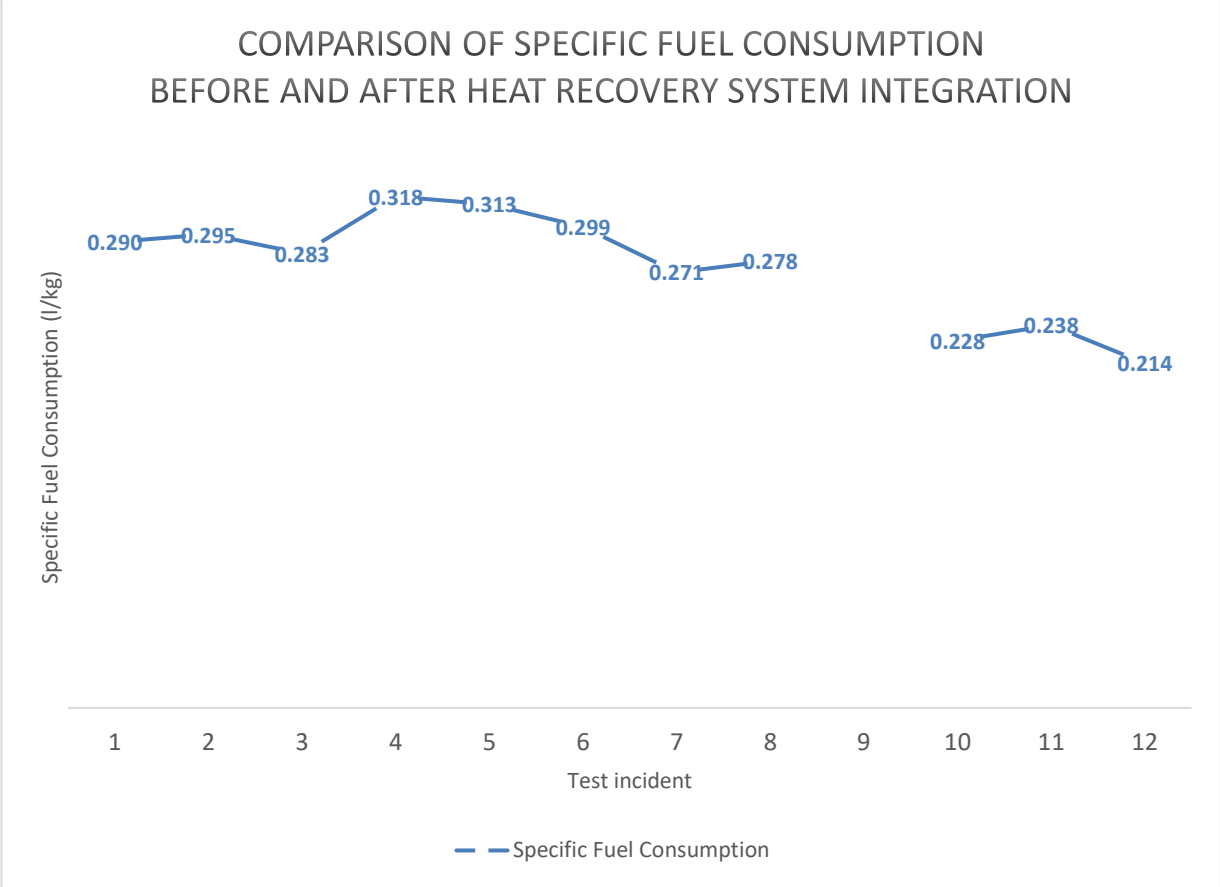

The analysis of the combustion air preheating system is based on the steady state measurements.

1. **Temperature Data**:
    - **Hot Gas Side**:
        - Inlet temperature: 700°C
        - Outlet temperature: 270°C
    - **Cold Air Side**:
        - Inlet temperature: 50°C
        - Outlet temperature: 300°C

2. **Heat Recovery**: Using the measured temperatures and flow rates, the recovered heat was calculated as:
    - Mass flow rate of cold air: 0.0515 kg/s

- Specific heat capacity at average temperature; Cp: 1.019 kJ/kg.K
- Maximum recovered energy:

$\dot{Q}_{\text{actual}} = \dot{m} \cdot c_p \cdot (T_{\text{outlet}} - T_{\text{inlet}})$=0.0515 x 1.019 x (300-50) = 13.11kW

3. **Heat Exchange Effectiveness**

$$\varepsilon = \frac{\dot{Q}_{\text{actual}}}{\dot{Q}_{\text{max}}}$$

Where:

$\dot{Q}_{\text{max}} = \dot{m}c_{p_{\text{min}}} \cdot (T_{\text{hot, inlet}} - T_{\text{cold, inlet}})$ = 0.0515 x 1.019 x (700-50) = 34.11kW

$$c_p \; at \; average \; hot \; air \; temperature = 1.019 \; kJ/kg$$

$$\varepsilon = \frac{13.85}{34.11} = 0.4$$

4. **Fuel Consumption**:
   - Initial waste oil level: 473 mm
   - Final waste oil level: 372 mm
   - Fuel used: (473 - 372) mm × 0.195 l/mm= 19.7 L
   - Fuel efficiency was optimized by reducing pressure from 28 bar to 14 bar and adjusting the air flowrate accordingly.

Fuel Savings (%)

The percentage fuel savings due to the heat exchanger was calculated using:

Fuel Savings (%)

$$= \frac{\text{Fuel consumption without HX} - \text{Fuel consumption with HX}}{\text{Fuel consumption without HX}} \times 100$$

The fuel saving was calculated based on the specific fuel consumption before and after installation of combustion air preheating system.

$$\text{Fuel Savings (\%)} = \frac{294 - 227}{227} \times 100 = 29.5\%$$

5. **Pressure Drop**:
    - Burner discharge pressure is at 6mbar.
    - This value is within acceptable limits of the burner blower as per the blower characteristic curve, ensuring efficient operation without significant resistance (Appendix 03-Burner data sheet).

Specific Fuel Consumption (SFC):

Before the integration of the welded plate heat exchanger, the average SFC was recorded at **0.294 L/kg** of aluminum melted. After implementation, this value dropped to **0.227 L/kg**, yielding a **reduction of 29.5%** in fuel consumption. This result signifies a meaningful improvement in energy efficiency through combustion air preheating. The experimental SFC reduction confirms theoretical expectations and validates the design of the heat recovery system.

Melting Time:

The average melting time of 145 minutes was shortened to 98 minutes post heat exchanger integration—a **32.2% reduction**. This enhancement aligns with the expected rise in initial combustion temperature due to air preheating, which accelerates the heat transfer to the aluminum charge.

Thermal Efficiency:

Thermal efficiency improved from **7.3% to 9.6%**, demonstrating how better utilization of exhaust heat can elevate the overall furnace performance. Though modest in absolute value, this increment represents a **31.5% relative improvement**, and offers a valuable precedent for small-scale foundries using similar furnace technologies.

6.6. Simulation Results Intepretation

- .

Crucible Furnace (Air Body) Simulation:

ANSYS Fluent simulations revealed that the flame trajectory within the combustion chamber tended to bypass the crucible when burner orientation and flow velocity were not optimized. The temperature contours confirmed thermal non-uniformity, with hot zones concentrated along direct flame paths and cold spots near the base and back walls of the crucible.

- **Burner Angle Optimization:** A 5-degree downward angle resulted in improved flame wrapping and upward convection, enhancing circumferential heating and reducing temperature gradients.
- **Velocity Streamlines:** The introduction of tangential airflow and reduced burner diameter led to improved residence time and mixing.

These findings align well with experimental results showing uneven aluminum melting before design correction. This validates the simulation's predictive capability and supports its use in future burner configuration optimization.

2. Welded Plate Heat Exchanger Simulation:

The ANSYS model accurately replicated the temperature profiles across the hot and cold air paths. The cold air was preheated from **26.85°C to 473.8°C**, while the hot gas cooled from **840°C to 373.5°C**, leading to an effectiveness (ε) of **55%**, close to the **theoretically calculated value of 60%**.

- **Heat Recovery Rate:** The simulation predicted an energy recovery of **23.2 kW**, which closely matches the actual measured energy gain of **13.1 kW** under real operating conditions, considering unmodeled losses such as external convection and radiation.
- **Pressure Drops:** Simulated flow resistance was minimal, validating the spacing and geometry of the welded plate design.

6.7. Correlation Between Simulation and Experimental Findings

Despite the simplification in the simulation, especially isolating the heat exchanger and using fixed temperature inlets instead of modeling the full transient coupling with the furnace, the trends observed are consistent with experimental data.

- **Temperature Gain in Preheated Air:** Measured rise from ambient to ~310°C matched simulation results, supporting the validity of the inlet boundary approximations.
- **Fuel Efficiency Improvement:** The simulated thermal gains directly translated to reduced SFC in field tests, confirming the model's usefulness in performance prediction.
- **Limitations Identified:** While simulation assumes convection and radiation losses under steady flow, the real system suffered from uninsulated ducts and flame misalignment under transient conditions. This explains slight discrepancies in temperature values.

6.8. Economic Analysis of the welded plate heat exchanger

6.8.1. Payback Associated with the Fuel Saving.

The welded plate heat exchanger is designed using 29 stainless steel plates, each measuring 600mm x 400mm x 1mm, optimized for efficient waste heat recovery. The plates are arranged to minimize material usage, with the cutting plan allowing the use of only three standard 2400mm x 1200mm stainless steel sheets. This approach ensures minimal material wastage while accommodating the required dimensions. The design also incorporates additional plates for ducting and piping to enable seamless integration into the furnace system.

Material costs have been estimated based on the dimensions of stainless steel, amounting to USD 300. Anticipated costs for consumables, such as welding rods and cutting wheels, are projected at 20% of the material cost. Labor costs, approximated at 50% of the material cost, bring the total estimated production cost to USD 510.

The system is expected to achieve significant fuel savings, with a projected reduction of 4.4 liters of fuel per cycle. Over 250 working days, this corresponds to annual

savings of 1100 liters, valued at USD 1100. These savings highlight the potential of the system to improve furnace thermal efficiency while substantially reducing operational costs. The payback period, calculated as the ratio of the production cost to annual savings, is estimated at 0.46 years (approximately 169 days), demonstrating a rapid return on investment.

This design provides a scalable and cost-effective solution for integrating waste heat recovery systems into foundry operations. Once fabricated and tested, the welded plate heat exchanger is expected to significantly enhance energy efficiency and sustainability, particularly in small- to medium-scale foundries seeking to optimize energy use and reduce operating expenses.

6.8.2. Time Saving and Associated Labor Cost Benefit

In addition to energy savings, the introduction of the welded plate heat exchanger and improved combustion design yielded significant **reduction in melting time,** a benefit that translates directly to labor productivity and cost efficiency.

Time Saved per Melting Cycle

Experimental trials showed that the **average melting time was reduced from 145 minutes to 98 minutes**, yielding a **time saving of 47 minutes per batch**. On a daily basis, assuming one melting cycle per day:

- **Time saved per day**: 47 minutes = **0.783 hours**
- **Labor cost rate**: Rs. 695 per hour
- **Number of personnel involved**: 4

Daily Labor Cost Saving

Daily saving=0.783 hr×695 Rs/hr×4 employees=Rs. 2,174.34

Annual Saving Over 250 of Working Days

Annual labor cost saving=2,174.34×250=Rs. 543,585.00

Operational Value of Time Saving

This saving becomes especially meaningful when the time saved is **allocated to other productive tasks**, such as mold preparation, equipment maintenance, or handling multiple melts per day. Thus, the time saved does not simply reduce idle labor hours but potentially increases foundry throughput and efficiency

6.9. Deviations, Limitations and Future Scope

1. **Deviations:**
    - One significant deviation was caused by the lack of insulation on the heat exchanger outer surface. Due to the absence of insulation, substantial heat was lost from the outer surface of the heat exchanger, leading to lower overall thermal efficiency.
    - Additionally, the exhaust pipe from the furnace exhaust to the heat exchanger inlet was not insulated. This resulted in a rapid temperature drop during this segment due to high radiation losses.
    - Furnace geometry and flame entry design presented significant issues. The current design places the flame entry point approximately eight inches higher than the furnace bottom, deviating the recommended parting plane of the crucible bottom and crucible base. As a result, the furnace bottom does not get heated effectively, increase the melting time efficiency and heat transfer area. This geometric flaw creates a barrier to performance improvements, even with substantial energy recovery from the combustion air preheating system.

2. Limitations:

- The absence of an exhaust gas analyzer further restricted the ability to evaluate combustion performance accurately, leading to potential discrepancies between simulated and experimental results.

3. Future Directions:

- Incorporation of insulation on the heat exchanger and the exhaust pipe to minimize heat losses.

- Redesigning the furnace geometry to align the flame entry point with the recommended parting plane of the furnace bottom and base for optimal heat transfer and performance.
- Installation of exhaust gas analyzers for detailed combustion studies.
- Scaling the system for larger foundries to extend its applicability.
- Development of a commercially optimized furnace design integrated with a combustion air preheater, tailored for the small to medium-scale foundry industry in Sri Lanka.

CHAPTER 7: CONCLUSIONS AND RECOMMENDATIONS

7.1. Conclusion

This

The research demonstrated how combustion air preheating, enabled via a welded plate heat exchanger, can substantially improve the thermal performance and fuel efficiency of crucible furnaces used in aluminum casting.

Key conclusions are as follows:

1. **Energy Efficiency Improved:**
    - Fuel consumption reduced by 29.5%, from 0.294 to 0.227 L/kg.
    - Thermal efficiency increased from 7.3% to 9.6%.
    - Melting time was shortened by 32.2%, improving productivity.
2. **Heat Exchanger Effectiveness:**
    - Simulation and experimental studies indicated effectiveness values between 50% and 60%.
    - Temperature and pressure data validated the suitability of the selected plate dimensions, spacing, and flow design.
3. **Validated Simulation Techniques:**
    - Simulation outcomes correlated strongly with measured values, despite simplifications, justifying the use of steady-state models for heat exchanger-only analysis.
4. **Design Implications for Industry:**
    - The integrated system presents a cost-effective retrofit for existing foundries.
    - Simulation-led design optimization enables burner placement refinement, airflow improvement, and radiation loss minimization, yielding a better energy-saving furnace designs.

5. **Recommendations for Future Work:**
    - Full transient simulations including the furnace and heat exchanger should be considered.
    - Use of exhaust gas analyzers and improved insulation can further reduce performance deviations.
    - Alternative materials like stainless steel or ceramic composites should be explored for long-term operation.

This research provides a replicable model for enhancing thermal performance in small- to medium-scale industrial aluminum melting operations across Sri Lanka and similar contexts.

While this study was conducted using a specific crucible furnace setup at the CEB foundry, the engineering principles, simulation techniques, and practical outcomes are applicable to a wide range of thermal systems and heat recovery applications across industrial sectors.

1. Combustion Air Preheating for Fuel-Fired Furnaces

The principle of preheating combustion air to improve thermal efficiency is not unique to crucible furnaces. It is broadly applicable to:

- Reverberatory and rotary furnaces used in aluminum recycling,
- Billet and ingot heating in steel rolling mills,
- Boilers and kilns in ceramics, cement, and food processing industries.

In all these systems, combustion efficiency can be enhanced by using exhaust heat to raise the temperature of incoming air, thereby:

- Reducing fuel consumption,
- Improving flame temperature and stability, and
- Accelerating process heat-up times.

2. Welded Plate Heat Exchanger Applications

The welded plate heat exchanger design studied in this research offers several

general-use advantages:

- High heat transfer surface area in a compact volume,
- Compatibility with dirty or particle rich gas streams (e.g., furnace exhaust),
- Easy integration into retrofit systems for heat recovery.

3. Numerical Simulation Techniques for Complex Heat Systems

The simplified modeling approach used, where the furnace and heat exchanger were simulated separately using experimentally validated boundary conditions, demonstrates a scalable method for simulating large and computationally intensive systems. This strategy is especially useful for:

- **Process design and optimization**
- **Feasibility studies** of retrofitting existing plants with energy recovery devices,

4. Industrial Implications

Key general findings that can be applied across sectors:

- Specific fuel consumption can be reduced by 25–35% through heat recovery and combustion air preheating.
- **Heat transfer simulations with appropriate simplifications** can yield reliable design insights.

APPENDICES

Appendix 1-Production Data of Manufactured Components at CEB Foundry

S/No.	Item	Quantity (Nos)	Unit Cost (Rs.)	Branch of CEB	Total Cost
1	T clamps-Lynx - Lynx	30	3,520.00	CE-S.C&M-PHMDD4	105,600.00
2	T clamps-Lynx - Lynx	12	3,520.00	CE-DM-WPS-2	42,239.94
3	T clamps-Lynx - Lynx	9	3,520.00	CE-DM-WPS-2	31,679.99
4	132kVA CT cable holding clamp	1	135,000.00	EE-Tr. O&M-Colombo Region	135,000.00
5	Bus bar earth clamps-G/S Badulla	18	18,600.00	CE-tr.O&M	334,800.00
6	T clamp Lynx - Lynx	50	3,800.00	CE-HLC&M-DD3)	190,000.00
7	132kV Aluminum clamps	2	26,800.00	EE-Tr.O&M-CR	53,600.00
8	T clamps Lynx - Lynx	6	4,285.49	CE-DM-WPS2	25,712.95
9	T clamps-Lynx - Racon	50	4,285.49	DGM-P&DDD2	214,274.55
10	T clamps-Lynx - Lynx	100	4,285.49	CE-HLC&M-DD3	428,549.10
11	T clamps-Lynx - Lynx	30	4,285.49	CE-HLC&M-DD3	128,564.73
12	T clamps	50	6,654.85	DGM(P&HM)-DD2	332,742.71
13	T clamps	50	6,654.85	DGM(P&HM-DD2	332,742.71
14	T clamps Lynx - Lynx-04 th batch	50	6,654.85	DGM(P&HM)-DD2-Kandy	332,742.71
15	T clamps Lynx - Lynx -Batch 05	50	6,808.67	DGM(P&HM)-DD2	340,433.63
16	T clamps Lynx - Lynx-Batch 06	50	6,808.67	DGM(P&HM)-DD2	340,433.63
17	Al -T Connectors	18	9,301.43	CE-GSCP-Transmission	167,425.65
18	T clamps(Lynx to Racon)	50	6,844.06	CE-Commercial-WPS2	342,202.88
19	T connectors	40	11,215.00	CE (MM)-Tr.AM&CM	448,599.90
20	Stud-Duplex coupler-Type-1	60	16,207.03	CE (MM)-Tr.AM&CM	972,421.80
21	Stud-Duplex coupler-Type-2	60	16,537.91	CE (MM)-Tr.AM&CM	992,274.68
22	Stud T Connector	40	11,215.00	CE (MM)-Tr.AM&CM	448,599.90
23	single-duplex T connector Type-3	60	20,989.02	CE (MM)-Tr.AM&CM	1,259,341.13
24	single-duplex T connector Type-2	60	20,989.02	CE (MM)-Tr.AM&CM	1,259,341.13
25	single-duplex T connector Type-1	60	20,811.44	CE (MM)-Tr.AM&CM	1,248,686.25

26	T clamps-Lunx to Racon -03nos., Lunx -Lynx -03nos	6	6,859.04	CE(DM-WPS2)	41,154.23
27	T clamps(L/L)-batch -07	50	6,924.17	DGM(P&HM)DD2-Kandy	346,208.63
28	T clamps(L/L)-batch -08	50	6,924.17	DGM(P&HM)DD2-Kandy	346,208.63
29	L/L T clamps	6	6,859.04	CE-DM-WPS2	41,154.23
30	T clamps L/L	100	6,893.36	CE-SC&M-DD1	689,335.50
31	Al Clamp 132kV Disconnector to twin MOOSE conductors	1	147,961.80	Chief Engineer (Tr, O&M - Southern)	147,961.80
32	T Connector Clamp (LYNX to LYNX)	200	7,814.20	Chief Engineer (SC&M)DD1	1,562,839.69
33	T connector clamp (ELM to ELM)	40	7,720.85	EE (Construction) Vavunia	308,833.88
34	Zebra conductor clamp (4 Nut & Bolt)-CT connection plate	30	9,971.36	CE(Transmission Asset Management & Condition Monitoring)	299,140.80
35	Zebra conductor clamp (4 Nut & Bolt)-Conductor clamp (4 Nut & Bolt)	30	15,395.73	CE(Transmission Asset Management & Condition Monitoring)	461,871.90
36	Lynx to Zebra T Connector clamps	3	18,657.10	CE (HLC&M)-P&HM-DD3	55,971.30
37	Clamp for NCT type II stud 30mm,	12	21,194.64	CE(Transmission asset management & condition monitoring)	254,335.73
38	HV Clamp type I conductor 26mm to stud 40mm	6	22,522.24	CE(Transmission asset management & condition monitoring)	135,133.43
39	LV clamp type I conductor 26mm	6	20,683.43	CE(Transmission asset management & condition monitoring)	124,100.50
40	Clamp for NCT type I conductor 22.68mm stud 30mm	6	22,522.24	CE(Transmission asset management & condition monitoring)	135,133.43
41	HV clamp type II conductor 32.6mm to stud 40mm	6	22,522.24	CE(Transmission asset management & condition monitoring)	135,133.43
42	LV Clamps type II conductor 22.68mm	6	20,683.43	CE(Transmission asset management & condition monitoring)	124,100.55
43	Lynx to Lynx T connector clamps	150	8,181.04	CE(SC&M)-DD3	1,227,156.00
44	Zebra to Lynx T connector clamps	6	18,004.35	CE(Tr. Line Construction Projects)	108,026.10
45	Aluminum jumper sockets for Lynx Conductor	12	5,089.92	CE(Tr. Line Construction Projects)	61,079.03

46	H-Clamps for Lynx conductor	40	3,447.70	CE- Laxapana Power Station	137,908.05
47	Clamps for surge arrester	20	11,807.25	CE-Laxapana Power Station	236,145.00
48	VT Clamps	12	6,367.38	CE(MM) Transmission Asset	76,408.50
49	PG Clamp Conductor 26mm-22.68mm	12	17,217.81	CE(MM) Transmission Asset	206,613.75
50	Clamps for transformer bushing	16	12,288.28	CE(MM) Transmission Asset	196,612.50
51	T clamps (Without Bimetallic sleeve)	40	8,079.09	CE(Laxapana Power Station)	323,163.75
52	Clamps for CVT's (Without Bimetallic sleeve)	40	10,599.68	CE(Laxapana Power Station)	423,987.38
53	T clamps Lynx to Lynx - Batch 01	50	8,651.73	CE (Commercial) - WPS II	432,586.70
54	T clamps Lynx to Lynx - Batch 02	50	8,651.73	CE (Commercial) - WPS II	432,586.70
55	T clamps Lynx to Lynx 50 - Batch 03	50	8,651.73	CE (Commercial) - WPS II	432,586.70
56	T clamps Lynx to Lynx - Batch 04	50	8,651.73	CE (Commercial) - WPS II	432,586.70
57	T clamps Lynx to Lynx - Batch 05	50	8,651.73	CE (Commercial) - WPS II	432,586.70
58	T clamps Lynx to Lynx- Batch 06	50	8,651.73	CE (Commercial) - WPS II	432,586.70
59	T clamps Lynx to Racon - Batch 01	50	8,651.73	CE (Commercial) - WPS II	432,586.70
60	T clamps Lynx to Racon - Batch 02	50	8,651.73	CE (Commercial) - WPS II	432,586.70
61	T clamps Lynx to Racon - Batch 03	50	8,651.73	CE (Commercial) - WPS II	432,586.70
62	T clamps Lynx to Racon - Batch 04	50	8,651.73	CE (Commercial) - WPS II	432,586.70
63	T clamps Lynx to Racon- Batch 05	50	8,651.73	CE (Commercial) - WPS II	432,586.70
64	T clamps Lynx to Racon - Batch 06	50	8,651.73	CE (Commercial) - WPS II	432,586.70
65	Casting of Al clamps "connecting down dropper to ceiling head' (as per sample)	10	7,255.40	CE(Tr. O&M)- Western South	72,553.95
66	T clamps Lynx to Lynx	60	7,219.96	CE(HLC&M)-P&HM-DD3	433,197.45
67	T clamps Lynx to Racoon	60	7,219.96	CE(HLC&M)-P&HM-DD3	433,197.45
68	T clamp Zebra to Lynx conductor	3	22,377.25	CE-Laxapana Power Station	67,131.75
69	T clamp Lynx to Lynx	100	8,192.55	DGM (P&HM)-DD2	819,255.15

70	T clamp Lynx to Lynx	100	9,152.24	CE(HLC&M)	915,224.10
71	Copper Compression type 'C' clamp (Using csrap copper from electrical section)	150	3,063.65	DGM(P&HM)-DD2	459,547.20
72	Copper 'C' connector 150sqm (Using scrap copper from electrical section)	150	3,063.65	DGM(P&HM)-DD2	459,547.20
73	Production of Zn Anodes 80mm x 80mm	9	11,723.53	CE(Barge Mounted Power Plant)	105,511.77
74	Production Aluminum Cable Brackets 2.5" (ZD1508)	50	8,982.71	DGM(P&HM) DD2	449,135.40
75	Production 75mmx450mm AL shaft	3	3,657.15	Priciple (Training Center-Piliyandala)	10,971.45
76	T clamp Lynx to Lynx	100	8,695.29	CE(HLC&M)-P&HM-DD3	869,529.15
77	T clamp Lynx to Racoon	50	8,842.34	CE(HLC&M)-P&HM-DD3	442,117.20
78	Production of Lugs for 7/4.0 counterpoise Earth Wire	100	1,275.68	CE(TLCP)	127,567.65
79	Production of Zn Anodes 6"x4"x1x"	40	11,246.71	CE KCCP	449,868.30
80	T Clamp Lynx to Lynx (12 Bolt Type)	50	19,692.98	CE (Asset Management & Condition Monotoring)	984,649.05
81	T Clamp Lynx to Lynx -08 Bolt Type	80	11,733.04	CE (Distribution & Maintanance)	938,643.30
82	T Clamp Lynx to Lynx - 12 bolt Type)	132	18,951.90	CE (Substation Construction & Maintanance) - DD1	2,501,651.25
83	Production of Jumper sockets for Zebra Conductor	12	22,728.30	CE (Transmission line construction projects)	272,739.60
84	Fabricating of pump end cover for sea water pump	3	71,766.10	CE (Barge Mounted Power Plant)	215,298.30
85	Production of T clamp Lynx to Lynx (08 Bolt type)	60	10,200.52	CE(Substation construction &maintanance p&hm-dd2)	612,031.35
86	Production of T clamp zebra to lynx (12 bolt type)	40	19,951.00	CE(Substation construction &maintanance p&hm-dd2)	798,039.90

87	Production of T clamp Lynex to Lynex (08 Bolt Type)	1050	10,994.18	CE- Substation Construction and maintranance - DD1	11,543,885.35
88	Production of earth clamps (Without Bolts)	500	4,091.86	CE (Transmission Line Construction Projects)	2,045,930.25
89	Production of Aluminum Anode	10	83,722.80	CE (Barge)	837,228.00
90	Production of T clamps Lynex to lynx (08 Bolt) type	75	10,785.33	CE (Mat. Mgt. Tr AM & CM)	808,900.05

Appendix 2-Waste oil calorific value test report

... Continuation Sheet

TEST REPORT
Report No. SS 2500578

Customer : Ceylon Electricity Board, Central Workshop & Garage Unit.	**Test Item :** Oil **Service Requested :** Customer's letter dated 2025-01-09
Description : One (01) test item. Approximately 750ml . Following information was given in the customer's letter. Sample : Used Engine oil	**Identification of Test Item :** Test item was not labelled . **Date of Receipt of Test Item :** 2025-01-10
Test Dates : 2024-01-16	

TEST RESULTS:

Test/Unit	Test Method	Result
Gross Calorific value/ kcal/kg	ASTM D 240-19	10752

.....
Authorized Signatory

2025-01-17
-/AR

A. A. M. T. Adikari
Senior Deputy Director
Materials Laboratory
Industrial Technology Institute

.....
Gihan Bandara
Assistant Research Technologist

Page 03 of 03 pages

Appendix 3- Weishaupt burner data sheet

Description

–weishaupt–

Weishaupt Monarch oil burners are of the fully automatic pressure atomising type. Their design has been carefully considered down to the smallest detail and has been proved successful over and over again. They meet all the demands for safety, reliability and low cost servicing. Weishaupt oil burners are type tested to EN 267.

The burners are distinguished by a variety of interesting features:

- Range of application 6 - 65 kg/h (71 - 775 kW)
- Automatic sequence of operations
- Stable fan characteristics – good combustion results
- Air regulation on pressure side
- Air damper closed on burner shut-down
- Quiet operation
- Complete pre-wired integral switch-gear
- Hinged burner casing
- Combustion head can be withdrawn when the burner is hinged open
- The design of the burner makes installation, adjustment and servicing easy

Construction
All the components are assembled in one unit. The motor drives the fan and the fuel pump. All the equipment used for the regulation of fuel and air is clearly arranged and easily accessible. The burners can be hinged to the left or right, which simplifies service work on the combustion head, diffuser, nozzles and ignition electrodes.

Application
The burners can be used on hot water boilers, steam boilers, air heaters and for certain heating processes. The burners are used in particular on modern, high rated boilers, as they are capable of overcoming high combustion chamber pressures. RL burners are preferably used where there is a continually changing heat demand.

Fuels
Distillate oil and medium oil to DIN 51 603 can be fired.
Viscosity:
Types Monarch L and RL -
< 6 mm^2/s at 20°C
Type Monarch M -
≤ 75 mm^2/s at 50°C

Regulation
On L and M type burners, the regulation of oil and air takes place as follows:
- two stage, nozzle head with two nozzles and a motor controlled, quickly opening air damper.
- three stage, with three nozzles and a motor controlled, slowly opening air damper.

The RL burner alters its capacity slowly (sliding). Fuel and air are controlled in compound. The burner can, depending on the controller and servomotor, be either:
- sliding two stage (20 s running time) or
- modulating (42 s running time)

With sliding two stage regulation, the partial and full load positions are fixed within the burner operating range. The burner slides to one position or the other, depending on the appliance demand, and there are no rapid changes of fuel throughput .

By fitting a suitable controller into the control panel, the burner can be altered to modulating operation. Modulating burners operate at any point within the capacity range, depending on the heat demand.

On sliding two stage burners and modulating burners, the slow capacity alteration ensures a particularly good matching to the heating appliance.

Flame supervision
The burner controller automatically sequences the operations and monitors the flame optically via the flame sensor.

The controller is mounted on the burner on all standard L and M burners, but can be supplied loose if requested. Together with the control panel, each burner forms one complete unit. On the RL burner, the burner controller is supplied loose for fitting into the control panel.

There is no interference with radio and television reception, as radio interference created during ignition is below the permitted limits specified by the relevant EMC standards and regulations.

Quiet operation
Weishaupt burners operate quietly. All air handling burner parts have been aerodynamically designed, the fuel / air mixing noise is reduced to a minimum and rotors and fan wheels are dynamically balanced. For installations where special emphasis is placed on burners with low noise levels, sound absorbers which reduce burner noise by approximately 70% are available (please ask for details).

Oil temperature regulation
Residual oil burners are fitted with an oil preheater. The oil is quickly heated to the required atomising temperature, due to the large heat exchange surface combined with a relatively small oil volume. Fast, even heat distribution prevents local overheating and carbonisation of the oil.

Heated nozzle head and nozzle recirculation system on residual oil burners
All residual oil burners are fitted with a heated nozzle head system. After the oil temperature in the nozzle head has been reached, the burner starts by means of a release thermostat. During prepurge, heated oil flows through the nozzle head and oil line system. This ensures that evenly heated oil is available for flame establishment.

Burner type _____ **RL3-A**
Version _____ ZME and ZMD
Combustion head type__ M2/1a-116x40
Rating kg/h _____ 10-44
kW _____ 120-525

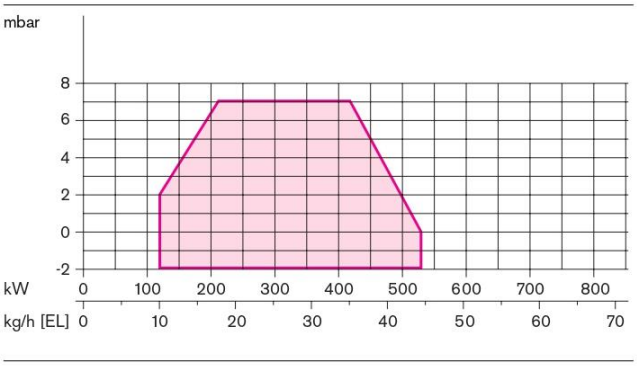

Burner type _____ **RL3-A**
Version _____ ZME and ZMD
Combustion head type _ M5/2a-116x40
Rating kg/h _____ 16-65
kW _____ 190-775

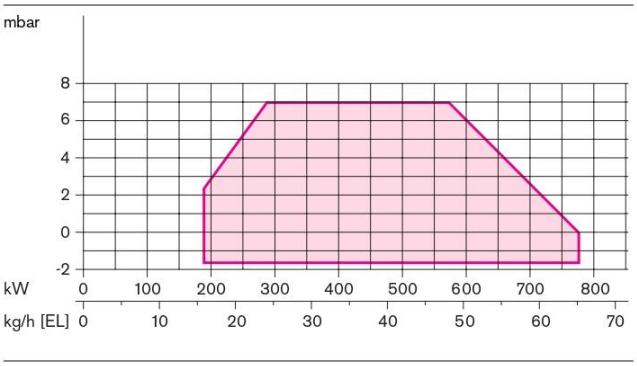

The capacities in relation to combustion chamber resistances are maximum values, which were measured to EN 267 on idealised test flame tubes.

All ratings data given relate to an air temperature of 20°C and an installation height above sea level of 500 m.

The oil throughput information refers to a calorific value of
11.91 kWh/kg for distillate oil EL
11.24 kWh/kg for residual oil M

Shut off devices
All burners with an oil throughput > 30 kg/h are equipped with a second solenoid valve (safety valve) as standard.

Voltages and frequencies
The burners are supplied with single phase 230 V, 50 Hz supply (E), or three phase 400 V, 50 Hz supply (D) as standard. Please indicate other voltages and frequencies required (no extra price).

Burner motor standard version
Btrop class insulation, to IP54. Motors can also be supplied to F class insulation (additional price on request).

Residual oil burners
The burner type M3Z-A is not type tested and may only be used outside the Federal Republic of Germany.

Modulating burners
The modulating RL3-A burner is based on the sliding two stage burner. The modulating feature is obtained by fitting a suitable electrical controller into the panel (for price see accessories list).

Reference

[1] V. A. Gnatush and V. S. Doroshenko, “The growth of aluminum casting production at the beginning of the XXI century,” *Metal and Casting of Ukraine*, vol. 310–311, no. 3–4, pp. 25–33, Jul. 2019, doi: 10.15407/pmach2019.03.025.

[2] R. G. N. De. S. Munasinghe and G. I. P. De Silva, “Quality Enhancement of Foundry Products - A Case Study of Foundry Industry of Sri Lanka,” *Engineer: Journal of the Institution of Engineers, Sri Lanka*, vol. 38, no. 1, p. 46, Jan. 2005, doi: 10.4038/engineer.v38i1.7207.

[3] I. De Silva, *Foundry Industry in Sri Lanka*. 2020. [Online]. Available: https://www.researchgate.net/publication/343049504

[4] S. P. Guluwita, R. G. N. De. S. Munasinghe, and W. L. W. Fernando, “Review Study of Historical Iron and Steel making in Sri Lanka and its Future Trends,” *Engineer: Journal of the Institution of Engineers, Sri Lanka*, vol. 44, no. 1, p. 43, Jan. 2011, doi: 10.4038/engineer.v44i1.7016.

[5] “Foundry Development and Services Institute - SriLanka.” Accessed: Jan. 11, 2025. [Online]. Available: https://www.fdsi.lk/

[6] Serope. Kalpakjian and S. R. . Schmid, *Manufacturing engineering and technology*. Pearson, 2020.

[7] J. G. . Kaufman and E. L. . Rooy, *Aluminum alloy castings : properties, processes, and applications*. ASM International, 2004.

[8] S. R. Tittagala and N. P. N. M. Navarathna, “DESIGN & CONSTRUCTION OF AN ENERGY-EFFICIENT FURNACE FOR MELTING NON-FERROUS ALLOYS IN THE LOCAL FOUNDRY INDUSTRY.”

[9] A. Adefemi, “Development of a 30Kg Aluminium Oil-Fired Crucible Furnace Using Locally Sourced Materials,” *American Journal of Mechanics and Applications*, vol. 5, no. 3, p. 15, 2017, doi: 10.11648/j.ajma.20170503.11.

[10] J. Haraldsson and M. T. Johansson, “Barriers to and drivers for improved energy efficiency in the Swedish aluminium industry and aluminium casting foundries,” *Sustainability (Switzerland)*, vol. 11, no. 7, Apr. 2019, doi: 10.3390/su11072043.

[11] M. Neri, A. M. Lezzi, G. P. Beretta, and M. Pilotelli, “Energy- and Exergy-Based Analysis for Reducing Energy Demand in Heat Processes for Aluminum Casting,” *Journal of Energy Resources Technology, Transactions of the ASME*, vol. 141, no. 10, Oct. 2019, doi: 10.1115/1.4043389.

[12] Olivier. Martin, *Light metals 2018*. Springer, 2018.

[13] S. S. Bhandari, S. B. Badadal, V. G. Kinagi, H. S. Tuljapurkar, and Prof. S. H. Bansode, “Design and Fabrication of Crucible Furnaces by using Black Smithy Setup,” *International Journal of Engineering and Management Research*, vol. 8, no. 4, Aug. 2018, doi: 10.31033/ijemr.8.4.16.

[14] M. B. Ndaliman, M. B. Ndaliman, and A. P. Pius, “Behavior of Aluminum Alloy Castings under Different Pouring Temperatures and Speeds Leonardo Electronic Journal of Practices and Technologies Behavior of Aluminum Alloy Castings under Different Pouring Temperatures and Speeds,” 2007, [Online]. Available: https://www.researchgate.net/publication/26492966

[15] “Diecaster is Rebranding and Investing | Fall River Die Cast | Foundry Management & Technology.” Accessed: Jan. 12, 2025. [Online]. Available: https://www.foundrymag.com/melt-pour/article/21931728/optimal-air-to-fuel-ratio-for-optimal-results

[16] “Design and Construction of A 50kg Capacity Furnace,” *Innovative Systems Design and Engineering*, Apr. 2021, doi: 10.7176/isde/12-2-03.

[17] I. Bonefačić, I. Wolf, and P. Blecich, “Improvement of fuel oil spray combustion inside a 7 MW industrial furnace: A numerical study,” *Appl Therm Eng*, vol. 110, pp. 795–804, Jan. 2017, doi: 10.1016/j.applthermaleng.2016.08.218.

[18] L. Wang, S. Sunden, and R.M. Manglik, “Plate Heat Exchangers,” 2007. [Online]. Available: http://library.witpress.comwww.witpress.comWITPRESS

[19] O. Arsenyeva, L. Tovazhnyanskyy, P. Kapustenko, J. J. Klemeš, and P. S. Varbanov, “Review of Developments in Plate Heat Exchanger Heat Transfer Enhancement for Single-Phase Applications in Process Industries,” Jul. 01, 2023, *Multidisciplinary Digital Publishing Institute (MDPI)*. doi: 10.3390/en16134976.

[20] B. R. Lamb, “Plate heat exchangers—a low-cost route to heat recovery,” *Journal of Heat Recovery Systems*, vol. 2, no. 3, pp. 247–255, Jan. 1982, doi: 10.1016/0198-7593(82)90018-2.

[21] L. XUE, G. MA, F. ZHOU, and L. WANG, “Operation characteristics of air–air heat pipe inserted plate heat exchanger for heat recovery,” *Energy Build*, vol. 185, pp. 66–75, Feb. 2019, doi: 10.1016/j.enbuild.2018.12.036.

[22] R. Brogan, “SHELL AND TUBE HEAT EXCHANGERS,” in *A-to-Z Guide to Thermodynamics, Heat and Mass Transfer, and Fluids Engineering*, Begellhouse. doi: 10.1615/AtoZ.s.shell_and_tube_heat_exchangers.

[23] M. Picón-Núñez and J. E. Rumbo-Arias, “Improving thermal energy recovery systems using welded plate heat exchangers,” *Energy*, vol. 235, Nov. 2021, doi: 10.1016/j.energy.2021.121373.

[24] P. Zhang, T. Ma, W. D. Li, G. Y. Ma, and Q. W. Wang, “Design and optimization of a novel high temperature heat exchanger for waste heat cascade recovery from exhaust flue gases,” *Energy*, vol. 160, pp. 3–18, Oct. 2018, doi: 10.1016/j.energy.2018.06.216.

[25] B. Egilegor *et al.*, “ETEKINA: Analysis of the potential for waste heat recovery in three sectors: Aluminium low pressure die casting, steel sector and ceramic tiles manufacturing sector,” *International Journal of Thermofluids*, vol. 1–2, Feb. 2020, doi: 10.1016/j.ijft.2019.100002.

[26] C. Zeng, S. Liu, and A. Shukla, “A review on the air-to-air heat and mass exchanger technologies for building applications,” 2017, *Elsevier Ltd*. doi: 10.1016/j.rser.2016.11.052.

[27] H. N. Chaudhry, B. R. Hughes, and S. A. Ghani, “A review of heat pipe systems for heat recovery and renewable energy applications,” 2012, *Elsevier Ltd*. doi: 10.1016/j.rser.2012.01.038.

[28] “Self-Powered Thermoelectric Waste Oil Burner,” 2019. [Online]. Available: https://www.engineeringtoolbox.com/fuel-oil

[29] A. K. Goßmann *et al.*, “A Low-power Liquid-fuelled Burner Using a Novel Atomization Concept,” *Combustion Science and Technology*, vol. 191, no. 9, pp. 1711–1723, Sep. 2019, doi: 10.1080/00102202.2019.1639683.

[30] I. A. Ibrahim, T. M. Farag, M. E. Abdel-baky, A. K. Abd El-samed, and H. M. Gad, “Experimental study of spray combustion characteristics of air-blast atomizer,” *Energy Reports*, vol. 6, pp. 209–215, Nov. 2020, doi: 10.1016/j.egyr.2019.12.014.

[31] I. A. Ibrahim, T. M. Farag, M. E. Abdel-baky, A. K. Abd El-samed, and H. M. Gad, “Experimental study of spray combustion characteristics of air-blast atomizer,” *Energy Reports*, vol. 6, pp. 209–215, Nov. 2020, doi: 10.1016/j.egyr.2019.12.014.

[32] I. S. Anufriev, E. P. Kopyev, I. S. Sadkin, and M. A. Mukhina, “Diesel and waste oil combustion in a new steam burner with low NOX emission,” *Fuel*, vol. 290, Apr. 2021, doi: 10.1016/j.fuel.2020.120100.

[33] C. T. Chong *et al.*, “Dual-fuel operation of biodiesel and natural gas in a model gas turbine combustor,” *Energy and Fuels*, vol. 34, no. 3, pp. 3788–3796, 2020, doi: 10.1021/acs.energyfuels.9b04371.

[34] “PROPERTY TABLES AND CHARTS (SI UNITS)-HEAT and MASS TRANSFER.”

[35] M. Leitner, T. Leitner, A. Schmon, K. Aziz, and G. Pottlacher, “Thermophysical Properties of Liquid Aluminum,” *Metall Mater Trans A Phys Metall Mater Sci*, vol. 48, no. 6, pp. 3036–3045, Jun. 2017, doi: 10.1007/s11661-017-4053-6.

[36] A. Sharma, K. Rathod, S. Gupta, and S. Prakash, “Energy-Efficient Melting Technologies in Foundry Industry,” 2016. [Online]. Available: https://www.researchgate.net/publication/311303999

[37] “Crucibles and their Furnaces.”

[38] D. J. Gingery, “BUILDING A GAS FIRED CRUCIBLE FURNACE.”

[39] Yunus A., Cengel, Afshin J., and Ghajar, “Heat and Mass Transfer,” 2017.